Inaugural dissertation

for

obtaining the doctoral degree

of the

Combined Faculty of Mathematics, Engineering and Natural Sciences

of the

Ruprecht - Karls - University Heidelberg

Presented by

M.Sc. Sophia Flad

born in: Waiblingen, DE

Oral examination: 10.10.2024

tRNA modification landscape shaping protein synthesis and energy production in early ectodermal differentiation

Referees:

Prof. Dr. Michaela Frye

Prof. Dr. F. Nina Papavasiliou

Abstract

Gene expression is a multi-layered process, tightly regulated by several transcriptional and post-transcriptional mechanisms. While transcription is regulated for example by DNA methylations and chromatin modifications, the fate of RNA post-transcriptionally is modulated by RNA modifications on coding and non-coding RNAs. The accurate control of gene expression is essential to ensure proper cellular function and normal development. Its disruption can lead to diseases. The aberrant deposition of tRNA modifications has been closely linked to neuro-developmental disorders and mitochondrial-linked disorders.

However, the precise underlying molecular mechanisms how tRNA modifications contribute to human neuro-developmental processes are still largely unknown. In my study, I focused on elucidating the influence of tRNA modifications in human early ectodermal differentiation which defines the origin of central nervous system development.

I differentiated human embryonic stem cells into the major ectodermal cell types neuroectoderm, neural crest, cranial placode and non-neural ectoderm. To determine the landscape of tRNA modifications, including expression of tRNA modifying enzymes and tRNA anticodon pools, I performed mass spectrometry, RNA sequencing, tRNA pool sequencing and proteomics analysis. I observed, that while tRNA modifications and tRNA anticodon pools remained largely stable throughout differentiation, the tRNA modifying enzymes were strongly downregulated in ectodermal cells compared to pluripotent stem cells. This downregulation of tRNA modifiers was accompanied by reduced global and mitochondrial protein synthesis in differentiated cells.

By performing a knockdown screen of 47 tRNA modifiers, I observed that mitochondrial tRNA modifying enzymes affected not only mitochondrial protein synthesis but also strongly affected global protein synthesis. The reduction in mitochondrial protein synthesis in ectodermal cells led to reduced mitochondrial metabolic and OXPHOS activity. Since protein synthesis requires high amounts of energy, reduction of mitochondrial activity and therefore, reduced energy production affected also global protein synthesis.

In summary, I showed that human early ectodermal cell types are in a more quiescent state compared to pluripotent stem cells and downregulate tRNA modifying enzymes, protein synthesis and mitochondrial activity.

Zusammenfassung

Die Genexpression ist ein vielschichtiger Prozess, der streng reguliert wird durch verschiedene transkriptionelle und posttranskriptionelle Mechanismen. Während die Transkription zum Beispiel durch DNA-Methylierungen und Chromatin-Modifikationen reguliert wird, wird das Schicksal der RNA nach der Transkription durch RNA-Modifikationen auf kodierenden und nichtkodierenden RNAs bestimmt. Eine genaue Kontrolle der Genexpression ist essenziell um die Zellfunktion zu erhalten und eine normale Entwicklung sicherzustellen. Wird diese gestört, kann das in Erkrankungen resultieren. So wurden Fehler in der Modifizierung von tRNAs in engen Zusammenhang mit neurologischen Entwicklungsstörungen und Mitochondriopathien gebracht.

Die genauen zugrunde liegenden molekularen Mechanismen, wie tRNA-Modifikationen zur menschlichen neurologischen Entwicklung beitragen, sind allerdings noch weitgehend unbekannt. In meiner Studie fokussierte ich mich auf die Aufklärung des Einflusses von tRNA-Modifikationen auf die frühe Entstehung des Ektoderms im Menschen, welches den Ursprung für das zentrale Nervensystem bildet.

Hierfür habe ich menschliche embryonale Stammzellen in die wichtigsten ektodermalen Zelltypen differenziert: in Neuroektoderm, in die Neuralleiste, in kraniale Plakode und in Oberflächenektoderm. Um die Landschaft der tRNA-Modifikationen, einschließlich der Expression der tRNA modifizierenden Enzyme und der Zusammensetzung des tRNA-Anticodon-Pools, zu bestimmen nutze ich Massenspektrometrie, RNA-Sequenzierung, tRNA-Pool-Sequenzierung und Proteomik Analyse. Ich konnte beobachten, dass die tRNA-Modifikationen und tRNA-Anticodon-Pools während der Differenzierung größtenteils stabil blieben, jedoch die tRNA modifizierenden Enzyme in ektodermalen Zellen stark herunterreguliert wurden im Vergleich zu pluripotenten Stammzellen. Damit gingen in differenzierten Zellen eine verringerte globale und auch eine verringerte mitochondriale Proteinsynthese einher.

Mithilfe eines Knockdown-Screenings von 47 tRNA modifizierenden Enzymen konnte ich zeigen, dass Enzyme, die mitochondriale tRNAs modifizieren, nicht nur die mitochondriale Proteinsynthese, sondern auch die globale Proteinsynthese stark beeinflussten. In den ektodermalen Zellen konnte ich sehen, dass die reduzierte mitochondriale Proteinsynthese zu einer verringerten mitochondrialen metabolischen

Aktivität und verringerten oxidativen Phosphorylierung führte. Da die Synthese von Proteinen große Mengen an Energie erfordert, wirkte sich die verringerte mitochondriale Aktivität, und die damit einhergehende verringerte Energieproduktion, auch auf die globale Proteinsynthese aus.

Zusammenfassend habe ich gezeigt, dass sich die frühen ektodermalen Zelltypen im Menschen in einem ruhenden Zustand befinden und dass tRNA modifizierende Enzyme, Proteinsynthese und mitochondriale Aktivität nach der Differenzierung herunterreguliert sind.

Acknowledgements/Danksagung

First and foremost, I would like to thank Ela, my supervisor of more than the last five years. I am really grateful that you offered me the opportunity to do my PhD in your lab. You always believed in me and encouraged me when it was necessary. Thank you!

Next, I would like to thank my TAC committee: Nina, Moritz and Carsten. Thank you for following and guiding my project through the years.

I would also like to give a big thank you to Mark Helm who invited me to his lab to do the tRNA pool sequencing there and to Marc Lander, who helped me during the library preparation and who jazzed up all the incubation times with interesting and funny stories.

Another big thank you goes to Anna Falk, who offered me the opportunity to visit her lab in Lund and to teach me more about the culture of iPSCs and NES cells. And I would also like to thank Alice, who was a great supervisor and who made my stay in Lund especially great.

My next big thank you goes to Sabrina and Anke, who greatly supported me throughout my project. Without them it wouldn't have been possible. Thank you girls!

And a huge thank you goes to the whole Frye lab: Mika, Becky, Sylvain, Leona, Milica, Shafagh, Fu, Tim, Beatrice, Cornelius, Veronica, former lab members Dany and Alex, and to all our former students: Liana, Mark, Leonie and Katrin. Thank you all for making these last years a memorable time and for making the lab a nice and welcoming place!

Und last but not least, möchte ich meiner Familie danken. Vielen vielen Dank für eure Liebe und Unterstützung. Ohne euch hätte ich das nicht geschafft.

Contents

List of Figures

List of Tables

1 Introduction

1.1 Gene expression

1.1.1 An overview

Gene expression describes the process of translating the information in the deoxyribonucleic acid, short DNA, into functional molecules (Figure 1.1). Genes, which are the basic unit of inheritance, contain the information that define physical and biological features of an organism. Humans have approximately 20,000 protein coding genes which are encoded by only 1.5% of the entire genome. The rest of the genome is considered noncoding DNA, which contains many types of regulatory elements and genes for ribonucleic acid (RNA) species, e.g. transfer RNAs (tRNAs) and ribosomal RNAs (rRNAs) (International Human Genome Sequencing Consortium, 2004).

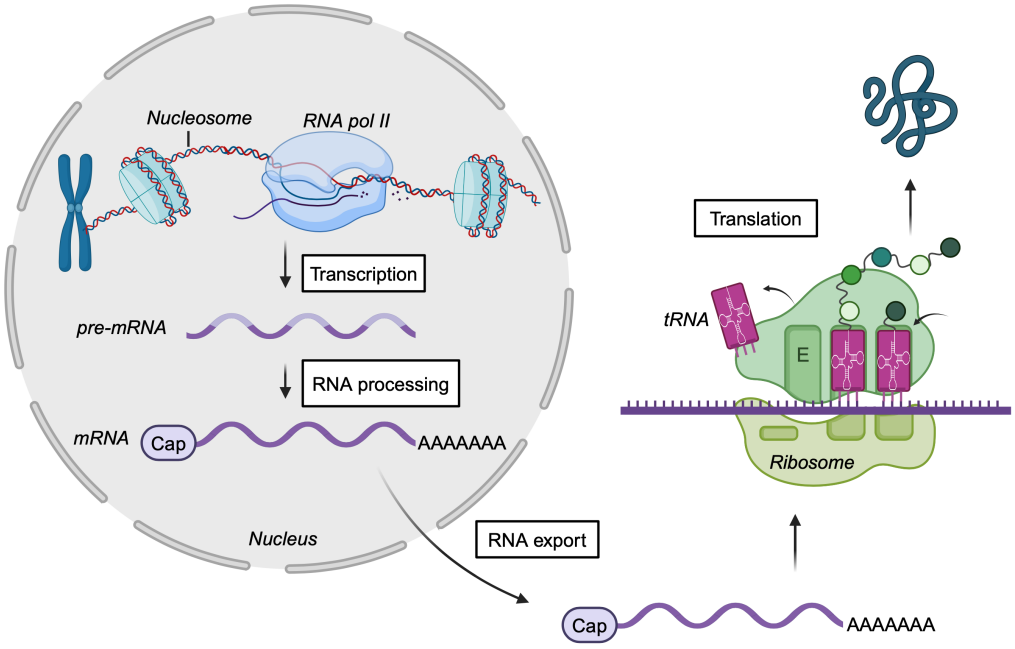

Figure 1.1: ***Overview of nuclear gene expression.***
Nuclear gene expression consists of four major steps: Transcription of DNA into mRNA, mRNA processing, mRNA export into the cytoplasm and translation of mRNA into a protein. This figure was generated using Biorender.

The DNA is the molecule that carries the genetic information in our cells. It is made out of two linked strands forming a double helix (Watson and Crick, 1953). Each strand is composed of a backbone, made from the sugar deoxyribose and phosphate groups, and four nucleobases: adenine (A), thymine (T), cytosine (C) and guanine (G). These bases can pair with each other through the formation of hydrogen bonds, where A pairs with T and C pairs with G (Watson and Crick, 1953). The DNA is stored in the nucleus and compactly packed by being wrapped around histone octamers and further condensed into chromosomes (Berg et al., 2013). Each cell has 22 pairs of autosomes and one pair of sex chromosomes (Adkison, 2012).

The process of gene expression is divided in transcription of DNA into messenger RNA (mRNA), mRNA processing, mRNA export and translation. Transcription is the first step in gene expression. A piece of DNA is transcribed into RNA which contains the base uracil (U) instead of thymine. An RNA polymerase binds to a promoter on the antisense DNA strand and transcribes in 3' to 5' direction. The resulting RNA matches the sense strand, also called coding strand (Alberts et al., 2014). RNA polymerase II produces mRNA which can be further translated into proteins. Other RNA species are produced by either RNA polymerase I (rRNAs) or III (tRNAs and other non-coding RNAs) (Roeder and Rutter, 1969, Roeder and Rutter, 1970).

The processing of the produced primary transcript (pre-mRNA) starts already during transcription elongation. The pre-mRNA molecule undergoes splicing, where intronic non-coding regions are excised by the spliceosome (Alberts et al., 2014). Alternative splicing allows for the production of several different proteins from the same gene, generating proteomic diversity (M. Chen and Manley, 2009). Furthermore, the pre-mRNA molecule is modified by the addition of a 5' 7-methylguanosine (m^7G) cap (Ramanathan et al., 2016) and a 3' poly(A) tail (Passmore and Coller, 2022). The final structure of the mRNA molecule is: 5' m^7G cap – 5' untranslated region (UTR) – coding sequence – 3' UTR – poly(A) tail. Since protein synthesis takes place in the cytoplasm, the mRNA molecule is transported into the cytoplasm through the nuclear pore complex, which recognizes and transports only completely processed mRNAs (Soheilypour and Mofrad, 2018).

During protein synthesis, the nucleotides of the mRNA are translated into amino acids,

which are the building blocks for proteins. The connection between nucleic acid sequence and amino acid sequence is described by the genetic code. It contains 64 codons, each composed of three bases, which decode 20 amino acids and three stop codons (Brenner et al., 1967). The genetic code is almost universal (Koonin and Novozhilov, 2009).

Protein synthesis, also called translation, happens at the ribosomes. The ribosome is a complex molecular machinery build of 80 ribosomal proteins and four ribosomal RNA molecules: 28S rRNA, 5S rRNA, 5.8S rRNA in the 60S subunit and the 18S rRNA in the 40S subunit of the ribosome (Rodnina et al., 2017). The ribosome is not only catalyzing the peptide bond formation but also ensures a correct reading frame and accuracy (Djumagulov et al., 2021, Milicevic et al., 2024). Actively translated mRNAs are not only translated by one ribosome but many, which are called polysomes.

Translation can be split into three parts: initiation, elongation and termination. During initiation, the small 40S ribosome subunit binds to the mRNA together with several initiation factors and a special initiator tRNA, $tRNA_i(Met)$ (Kolitz and Lorsch, 2010), and scans the mRNA in 5' to 3' direction until it finds the start codon AUG. The initiator tRNA, which is bound in the peptidyl site (P site) of the ribosome, pairs with the start codon and provides the first peptide building block. The initiation factors leave the complex and the large 60S subunit joins, assembling the 80S ribosome. Elongation of the peptide chain occurs by the entering of a new aminoacyl-tRNA into the aminoacyl site (A site), formation of a peptide bond, release of the now deacylated P site tRNA through the exit site (E site) and the move of the newly formed peptidyl-tRNA from the A site to the P site (Dever et al., 2018). Once a stop codon is reached, release factors bind to the A site and a H_2O molecule is added to the peptide. The polypeptide chain is released and the ribosome falls off (Nakamura et al., 1996). The emerging peptide starts folding into a protein while being synthesized. The folding process is controlled by chaperones (Kim et al., 2013).

Mitochondrial gene expression

Gene expression in mitochondria differs from the nuclear one, which is described above (Figure 1.2). Mitochondria contain their own mitochondrial DNA (mtDNA) and gene expression machinery. In addition, the genetic code used in mitochondria is different: the codon AUA is used for methionine (Met), the codon UGA for tryptophan (Trp) and the

codon AGR (R = A and G) for stop codons (Gonzalez et al., 2012). In total there are 60 sense codons which are decoded by 22 mt-tRNAs.

The inheritance of the mtDNA is asexual and maternal (Luo et al., 2018). The DNA is circular and double stranded. It is packaged into a compact nucleoid structure, composed of a single copy of the DNA plus mitochondrial transcription factor A (TFAM) protein (Brown et al., 2011). Mitochondria have their own 37 genes: 13 genes for essential subunits of the respiratory chain complexes, 22 mt-tRNA genes and 2 mt-rRNA genes. Each DNA strand contains a main promoter for transcription, which is executed by the polymerase POLRMT. The two generated transcripts are first processed into tRNAs, rRNAs and mRNAs (Ojala et al., 1981). Another difference from nuclear gene expression is, that mt-mRNAs do not have the m^7G cap modification and they have only short poly(A) tails (Ojala et al., 1981).

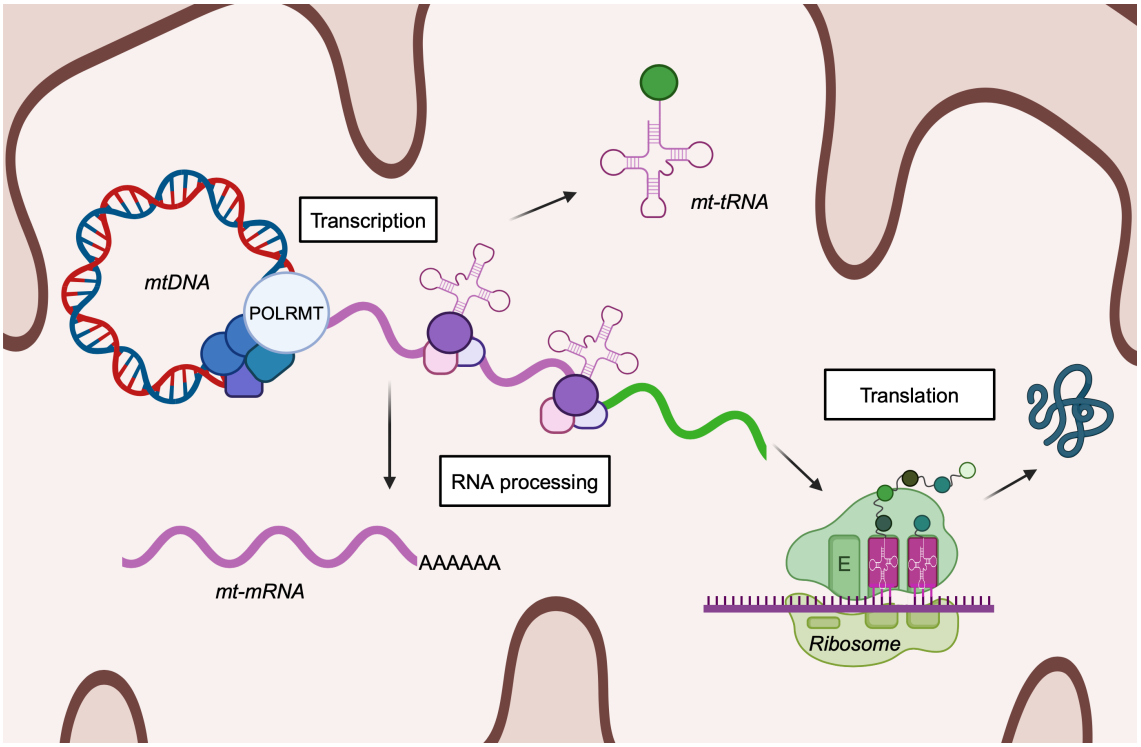

Figure 1.2: ***Overview of mitochondrial gene expression.***
Mitochondrial DNA is transcribed into two big transcripts, which are further processed into rRNAs, tRNAs and mRNAs. The mRNAs are then translated into proteins.This figure was generated using Biorender.

Mitoribosomes contain 80 ribosomal proteins, 2 mt-rRNA molecules (16S and 12S) and a mitochondrial tRNA(Val), which substitutes the 5.8S rRNA of the ribosome (Amunts

et al., 2015, Greber et al., 2015). Ribosomal proteins, translational factors, the aminoacyl-tRNA synthetases, processing and modifying enzymes are encoded in the nucleus. The principal of translation in mitochondria is similar to cytoplasmic translation, except for the usage of distinct initiation, elongation and termination factors (Rackham and Filipovska, 2022).

1.1.2 Transfer RNAs

Transfer RNAs are the most abundant small non-coding RNAs in the cell, constituting 4-10% of all cellular RNA. Their unique structure is well conserved throughout all three domains of life. Consisting of 76 to 93 nucleotides, tRNAs fold into a cloverleaf-like secondary structure with four arms, the acceptor stem, the dihydrouridine (D) arm, the anti-codon arm and the TΨC-arm. Any additional nucleotides beyond the 76^{th} are incorporated in a variable loop which bulges out from the back of the structure to avoid internal steric conflicts. The tertiary structure of a tRNA forms an L shape (Giegé, 2008). Their structure and high density of nucleotide modifications (discussed in Chapter 1.2 in more detail) makes them extremely stable with a half-life of about 100 hours (Choe and Taylor, 1972). At the 3'-end, the tRNAs contain a CCA trinucleotide which provides the site of amino-acylation. Acylation is performed by 20 different aminoacyl tRNA synthetases (aaRSs) that are specific for each of the 20 canonical amino acids, discriminating the tRNAs by the anticodon loop and the discriminator base located before the 3' CCA tail (Ibba and Soll, 2000). The specificity of the amino-acylation is critical since the ribosome itself does not control if the correct amino acid is inserted.

In humans, 429 high-confidence nuclear-encoded tRNA genes exist, coding for only 21 different isoacceptor families (P. P. Chan and Lowe, 2016). Isoacceptor tRNAs are carrying the same amino acid. Isodecoder tRNAs describe tRNAs sharing the same anticodon but differ in the rest of the sequence. tRNA genes are transcribed by RNA polymerase III and transcription factors IIIB and IIIC into around 100 nucleotide long precursors (pre-tRNAs) (Jarrous et al., 2022). Pre-tRNAs are then processed by addition of preliminary modifications and the removal of the 5' leader sequence by RNase P and 3' trailer sequence by RNase Z (Deutscher, 1984). Next, pre-tRNA splicing is performed by the tRNA splicing endonuclease (TSEN) complex and HSPC117. After the addition of the 3'-CCA

tail and further modifications, the pre-tRNAs are exported from the nucleus into the cytoplasm, where they are modified into mature tRNAs. Correct tRNA biogenesis is controlled by TRAMP complex, which targets hypomodified pre-tRNAs for degradation (Kewu et al., 2015) and the rapid tRNA decay pathway (RTD), which leads to degradation of hypomodified and unstable mature tRNAs (Alexandrov et al., 2006, Guy et al., 2014).

The genetic code contains 61 amino acid encoding codons plus three stop codons. The discrepancy between the number of available tRNAs and the 61 codons is compensated by some of the tRNAs which tolerate a mismatch between their first anticodon and the third mRNA codon base (wobble basepairing) allowing the translation of multiple codons by a single tRNA (Crick, 1966).

Beyond their canonical role as adapter molecules in protein synthesis, tRNAs are involved in many other cellular processes. Uncharged tRNAs regulate gene expression upon amino acid starvation by activating a protein kinase that phosphorylates the eukaryotic translation initiation factor 2 (eIF2). This inhibits binding of Met-tRNA$_i$(Met) and thereby lowering translation initiation (Wek et al., 1995). Additionally, tRNAs are involved in cell wall biogenesis in bacteria (Lloyd et al., 2008), in regulation of cell death (Mei et al., 2010) and in stress response (Thompson et al., 2008, Saikia et al., 2014, Oberbauer and Schaefer, 2018).

1.1.3 Regulation of gene expression

Gene expression is a highly complex process that is carefully regulated to determine if a gene is expressed and how much protein is synthesized. Being able to steer and adapt gene expression is necessary for cells to respond to changes in their environment and to either gain or keep a specific cell identity and cell type. Dynamic regulation is therefore essential for proper cellular function and normal development (reviewed in T. I. Lee and Young, 2013).

Epigenetic mechanisms build the first layer of regulation on DNA level. The structure and density of chromatin determines if a gene is accessible for the transcription machinery. Histone acetylation and phosphorylation lead to chromatin remodeling and higher accessibility (Z. Wang et al., 2008) while histone methylation affects binding of chromatin

factors (Bannister and Kouzarides, 2011). Methylation is also present on the DNA itself. Here it recruits gene repressor proteins or inhibits binding of transcription factors and therefore is a mechanism of gene repression (Holliday and Pugh, 1975, Schulz et al., 2006).

As mentioned in Chapter 1.1.1, most of the genome consists of noncoding DNA containing e.g. cis regulatory elements (CREs). CREs comprise promoters, enhancers and transcription factor binding sites (Ong and Corces, 2011). Enhancer sequences are binding sites for regulatory proteins that enhance transcription and are located up- or downstream of a gene, in introns or even far away of the gene they regulate (Kleinjan and van Heyningen, 2005). Transcription factors are proteins that bind DNA at promoters or enhancers and interact with RNA polymerase II. Besides the general transcription factors that assemble on promoters of all genes, thousands of transcription factors are expressed specifically in certain cell types or stages of development. They play an important role in initiating patterns of gene expression and giving a cell its unique characteristics (Alberts et al., 2014).

Not only transcription needs to be tightly regulated but also processing and translation of mRNAs. The cell uses alternative splicing to produce several proteins from one gene, called isoforms, to create more proteomic diversity (M. Chen and Manley, 2009). The poly(A) tail, which is added to mRNAs after transcription, stabilizes the mRNAs and is important for translation (Gallie, 1991). Interestingly, the poly(A) tail is not static but dynamic and a shortening can repress translation and lead to mRNA decay, which can be rescued by subsequent poly(A) extension. Other regulatory sequences in an mRNA molecule are the 5' UTR and the 3' UTR. A 5' UTR can contain upstream open reading frames (uORFs) which decrease translation by trapping a scanning ribosome initiation complex, causing it to translate the uORF instead of the downstream gene. It can contain internal ribosome entry sites (IRES) which allows translation of two distinct protein coding sequences on one mRNA. And the 5' UTR can also contain micro RNA (miRNA) binding sites (Ryczek et al., 2023). Micro RNAs are involved in gene silencing through binding their target mRNAs and initiating their degradation (Filipowicz et al., 2008). The 3' UTR of an mRNA regulates its localization, stability and translation (Mayr, 2019).

Another big part in regulating gene expression is done by the epitranscriptome, which summarizes modifications on RNA. These are chemical modifications of RNA nucleotides, e.g. methylation, which affect RNA-RNA and RNA-protein interactions.

They are present in all types of RNA, coding and non-coding, and offer a quick way to adjust protein synthesis to changes in environment. They will be discussed in more detail in Chapter 1.2. And finally, synthesized proteins are also subjected to modifications. There are 400 different types of amino acid side chain modifications, e.g. acetylation, phosphorylation, glycosylation and methylation. These modifications affect the structure and dynamics of proteins (Mann and Jensen, 2003, Xu and Chou, 2016).

Taken together, all steps during gene expression are tightly regulated and can be adjusted depending on the cells need.

1.2 RNA modifications

Since their first discovery around 1960 (Amos and Korn, 1958, Cohn, 1960) over 300 types of RNA modifications across all species have been described until today (Boccaletto et al., 2022) including 180 nucleotide, 152 nucleoside modifications and three base modifications. Their importance gained more and more attention in the last years due to improved sequencing and detection technologies.

About ten types of modifications have been reported in eukaryotic mRNAs (Delaunay et al., 2024), e.g. the m^7G modification in the 5' cap of the mRNA, inosine (I), 6-methyladenosine (m^6A), 5-methylcytosine (m^5C) and pseudouridine (Ψ). Inosine is generated by deamination of adenosine. This reaction, which is called A-to-I RNA editing, is performed by ADAR enzymes (adenosine deaminases acting on RNA) (Savva et al., 2012). Inosine can pair with cytidine and therefore allows recoding of amino acid codons, start and stop codons and it has been shown to affect splicing (Nishikura, 2016). The m^6A and pseudouridine modifications are installed co-transcriptionally. The m^6A writer complex consists of methyltransferases METTL3 and METTL14 while pseudouridine is introduced by pseudouridine synthaseses (PUS). The m^5C modification in mRNA is mediated by NOP/Sun RNA methyltransferases (NSUNs). Most mRNA modifications ensure correct transcription (J.-H. Lee et al., 2021), processing (N. M. Martinez et al., 2022), subcellular localization, stability (Mauer et al., 2017, X. Chen et al., 2019) and translation of transcripts.

RNA modifications are also present in non-coding RNAs, like miRNAs, long noncoding RNAs (lncRNAs) and ribosomal RNAs. In rRNA, modifications stabilize the complex

structure and facilitate RNA-RNA and RNA-protein contacts during translation (Polikanov et al., 2015).

1.2.1 tRNA modifications

Transfer RNAs are highly modified, with a modification density of 10% to 20% in one tRNA molecule. Over 80 different types of modifications have been found in tRNAs across all species (Boccaletto et al., 2022). In humans, 39 modification types have been described in cytoplasmic tRNAs (Suzuki, 2021) (Figure 1.3A) and 18 types in mt-tRNAs (Suzuki et al., 2020) (Figure 1.3B).

Depending on their chemical nature and position within the tRNA molecule, modifications exert different functions. Modifications located in the anticodon loop mostly affect translation, while modifications in the body of the tRNA can affect the secondary and tertiary structure and stability of the tRNA. However, the exact role of many modifications is still not known and might also change depending on the context. A large number of diverse tRNA modifications are located at positions 34, the wobble position, and 37 in the anticodon loop, e.g. inosine at position 34 and 1-methylguanosine (m^1G) at position 37, contributing to increased translational accuracy and efficiency (Agris et al., 2007), accurate decoding and reading frame maintenance (Björk et al., 1989, L. Han and Phizicky, 2018). I34 is produced by deamination of adenosine catalyzed by heterodimeric adenosine deaminase acting on tRNAs (hetADAT), a complex consisting of the catalytic subunit ADAT2 and ADAT3 (Torres et al., 2015). Whereas A34 can only pair with U-ending codons, inosine expands the decoding capacity by pairing with U-, C- and A-ending codons and therefore reduces the required number of tRNA species for codon-anticodon recognition (Crick, 1966).

The *N*6-threonylcarbamoyladenosine (t^6A) modification is another modification found at position 37 and is present in almost all ANN-decoding tRNAs (Thiaville et al., 2014). It is deposited by YRDC and the KEOPS complex in cytoplasmic tRNAs / OSGEPL1 in mitochondrial tRNAs and has been shown to stabilize codon-anticodon pairing (Rozov et al., 2015). Modifications at position 38 in the anticodon loop have been also found to enhance translation accuracy, e.g. m^5C by DNMT2 (Tuorto et al., 2015). This modification fulfills an additional role, together with NSUN2 mediated m^5C modifications in the variable loop (Blanco et al., 2011). They have been shown to stabilize

the tRNA structure and protect tRNAs against endonucleolytic cleavage. A lack of these modifications allows tRNA cleavage by angiogenin and the derived 5' tRNA fragments (tRFs) inhibit cap-dependent translation (Tuorto et al., 2012, Blanco et al., 2014) and can lead to activation of cap-independent stress-response pathways (Ivanov et al., 2011). Besides their important role in translation and involvement in oxidative stress (Yoluç et al., 2021), tRNA modifications have been linked to cell cylce (Lin et al., 2018, Chang et al., 2019) and immunity (Koh and Sarin, 2018, Rak et al., 2021) as well.

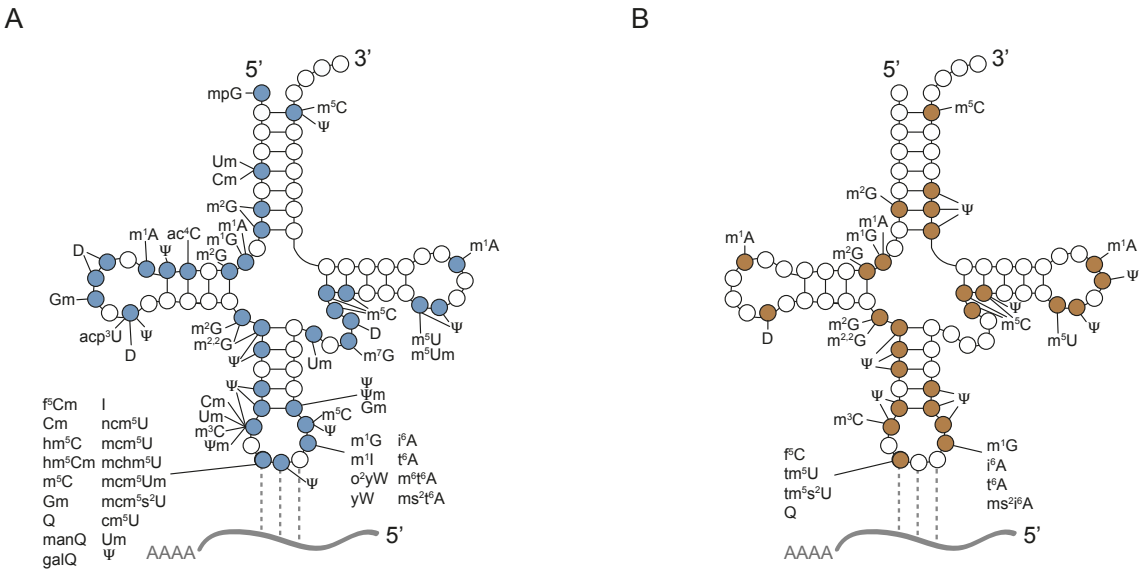

Figure 1.3: ***tRNA modifications in human.***
(A) *cytosolic tRNA modifications.* ***(B)*** *mitochondrial tRNA modifications. tRNA modifying enzymes listed in Suppl. Table 5.1.*

While mitochondria contain the genes for their own tRNAs, the mt-tRNA modifying enzymes are all nuclear encoded and have to be transported into the mitochondria. Some enzymes modify both, cytoplasmic and mitochondrial tRNAs, but there are also several enzymes that exclusively modify mitochondrial tRNAs. An important modification in mt-tRNAs for decoding is the 5-formylcytidine (f^5C) modification at position 34 of mt-tRNA(Met). This modification is made by a first methylation of cytosine to m^5C by NSUN3 and further modification by ALKBH1 to form f^5C. It enables the decoding of AUA codons (Takemoto et al., 2009) and has been shown to be essential for normal mitochondrial translation and therefore, for a normal mitochondrial activity and function (Delaunay et al., 2022).

1.3 Mitochondria - the powerhouse of the cell

1.3.1 Structure and morphology

Mitochondria are semi-autonomous cell organelles that contain their own DNA, but they still require nuclear-encoded proteins for their function. They have two membranes, the outer membrane and a strongly folded inner membrane that forms cristae. The space between both membranes is called the intermembrane space and the inner space is called matrix. The matrix is the place where the citric acid cycle (TCA cycle) and the fatty acid oxidation take place. Oxidative phosphorylation (OXPHOS) happens in the inner membrane. Mitochondria are typically 2 µm long. They are associated with microtubules and they can for example move long distances along these microtubules as in neurons or they can have a fixed position at points of high energy demand as in muscle cells (Berg et al., 2013, Alberts et al., 2014).

Although mitochondria are usually depicted as round organelles, they are highly dynamic and can change their shape. They can exist in a fragmented, round state or they can build long connected networks. In general, fragmented mitochondria correlate with low OXPHOS and higher reactive oxygen species (ROS) production and longer fused mitochondria correlate with high OXPHOS and increased adenosine triphosphate (ATP) levels (Molina et al., 2009). These shaping processes are called fission and fusion and are used as quality control mechanisms. Fusion of mitochondria is used to dilute dysfunctional proteins and mutated mtDNA (D. C. Chan, 2006). It is mediated by OPA1, MFN1 and MFN2. Fission describes the fragmentation of mitochondria. The mitochondria can get rid of damaged components or even whole mitochondria through mitophagy (Youle and van der Bliek, 2012). Fission is mediated by DRP1, FIS1, MFF and MiD49 and MiD51 (Fonseca et al., 2019). Mitophagy describes the removal of dysfunctional mitochondria by autophagy. PINK1 accumulates in damaged mitochondria, recruits parkin and induces the degradation of mitochondria by lysosomes (Lazarou et al., 2015).

1.3.2 Mitochondrial functions

Mitochondria are the main place for energy production in the cell. They are involved in many metabolic pathways, including the glucose, amino acid and lipid metabolism. In the TCA cycle, acetyl-CoA, which derived from either pyruvate from glycolysis or fatty acids from fatty acid beta oxidation, is metabolized into CO_2, NADH and $FADH_2$ and thereby produces a lot of ATP. The electrons in NADH and $FADH_2$ are further used in the electron transport chain (ETC) and OXPHOS to produce even more ATP. They are transported through the ETC complexes I to IV into the intermembrane space and there transferred onto oxygen (Kühlbrandt, 2015). This builds a proton gradient which is used by the ATP synthase to phosphorylate ADP to ATP (MITCHELL, 1961).

Additionally, mitochondria are also involved in two steps of the urea cycle (Haskins et al., 2020), biosynthesis of heme groups (Piel et al., 2019), calcium buffering/homeostasis (Duchen, 2000), ROS production (Palma et al., 2024) and apoptosis (Renault and Chipuk, 2014).

1.4 RNA modifications in disease

The importance of tRNA modifications for correct gene expression and a functional cell is highlighted by the many diseases that have been linked to disruptions of tRNA modifiers and modifications, summarized under the term 'RNA modopathies'. Mutations in modifying enzymes and aberrant deposition of modifications can result in cancer, diabetes (Vangaveti et al., 2022), mitochondrial diseases (Bykhovskaya et al., 2004), encephalopathies and neurodevelopmental diseases.

tRNA modifications in cancer

Several modifications and modifying enzymes have not only been linked to cancer development but also to therapy resistance. These modifiers are mostly overexpressed in cancer and usually correlate with poor survival. Therefore, more and more research is toggled towards targeting them in therapy.

The METTL1/WDR4 mediated m^7G46 modification was found to be enriched in intrahepatic cholangiocarcinoma (ICC). The increased level of modification is needed by the cancer cell to ensure proper decoding of oncogenic mRNAs, which have a

higher frequency of m^7G-related codons (Dai et al., 2021). Additionally, m^7G was linked to radiotherapy resistance in hepatocellular carcinoma (HCC) (Liao et al., 2023). PUS7, which modifies uridine to pseudouridine in tRNA at position 13 and 35, is high expressed in glioblastoma multiforme (GBM) and associates with poor prognosis. It was shown, that this modification affects codon specific translation and regulates glioblastoma stem cell growth by downregulation of the TYK2-STAT1 pathway (Cui et al., 2021). Another modification involved in cancer development and progression is the mcm^5s^2U34 modification by the Elongator complex and CTU1/2, which was shown to be essential for invasion and metastasis of breast cancer (Delaunay et al., 2016). The mitochondrial m^5C34 modification by NSUN3 is essential for metastasis as well. Delaunay et al. have shown, that a lack of this modification results in reduced OXPHOS and drastically decreases the cancer cells ability to metastasize (Delaunay et al., 2022). This makes tRNA modifier an interesting target for future therapy.

tRNA modifications in neurological diseases

The fact that several neurological impairments are connected to tRNA modifications shows, that especially the brain is really sensitive to disruptions in the epitranscriptome (Table 1.1).

Intellectual Disability (ID) is a neurodevelopmental disorder that manifests during childhood. It is concomitant with cognitive deficits (an IQ below 70), deficits in functional and adaptive skills and difficulties in conceptual and social areas of living. Usually in RNA modopathies, it comes along with many more symptoms, as for example microcephaly and growth retardation (K. Lee et al., 2024).

The 2'-O-methyltransferase FTSJ1 is primarily expressed in the fetal brain (Freude et al., 2004). A loss of this enzyme and its modifications leads to a decrease of the tRNA(Phe)GAA, which affects the decoding of UUU codons which are enriched in genes associated with brain and nervous system (Li et al., 2020). Loss-of-function of NSUN2, which methylates cytosines at position 34 and in the variable loop, results in microcephaly (Abbasi-Moheb et al., 2012). In mouse, NSUN2 is highest expressed in the cerebral cortex, hippocampus and striatum. Flores et al. could show, that repression of NSUN2 inhibits neural migration and therefore impairs neural lineage commitment and growth of the brain (Flores et al., 2017).

Table 1.1: *Neurological diseases linked to tRNA modifications*

Neurological disease	**tRNA modification**	**Enzyme**	**Literature**
Intellectual disability, microcephaly, growth retardation, metabolic disorder	2'-O-methylribose	FTSJ1	Freude et al., 2004
	$m^2{}_2G$	TRMT1	Blaesius et al., 2018
	m^5C	NSUN2, NSUN3	F. J. Martinez et al., 2012, Van Haute et al., 2016
	m^7G	WDR4	Shaheen et al., 2015
	A-to-I editing	ADAT3	Alazami et al., 2013
	$mchm^5U$	ALKBH8	Monies et al., 2019
	s^2U, mcm^5s^2U	CTU2	Shaheen et al., 2016
	m^1A	FTO	Daoud et al., 2016
	Ψ	PUS3	Shaheen et al., 2016
	ac^4C	THUMPD1	Broly et al., 2022
	m^1G	TRMT10A, TRMT10C	Yew et al., 2016
Galloway-Mowat syndrome	t^6A	GON7, OSGEP, YRDC	Arrondel et al., 2019
Familial dysautonomia	mcm^5s^2U	IKBKAP	Slaugenhaupt et al., 2001
Amyotrophic lateral sclerosis, motor neuron degeneration	mcm^5s^2U	ELP3	Simpson et al., 2009, Bento-Abreu et al., 2018
Rolandic epilepsy	mcm^5s^2U	ELP4	Strug et al., 2009
Encephalopathy	tm^5U	GTPBP3	Kopajtich et al., 2014
Optic neuropathy, cognitive disability	tm^5U	MTO1	Charif et al., 2015
Autism spectrum disorder	Ψ	PUS7	S. T. Han et al., 2022

1.5 Ectodermal differentiation

1.5.1 The potential of embryonic stem cells

One of the first arising cell types in development are embryonic stem cells (ESCs). They originate from the inner cell mass of the early embryo and build the starting material for the development of the whole organism. ESCs are pluripotent, which means they have the ability to differentiate into almost all cell types, except extraembryonic tissue as the placenta. Another special feature of ESCs is, that in suitable culture conditions they have an indefinitely proliferation capacity due to high expression levels of active telomerase (Alberts et al., 2014).

In 2006, Nobel Prize winner Yamanaka and his colleague Takahashi reported a way to reprogram adult cells into pluripotent stem cells (iPSCs). By overexpressing OCT4, SOX2, KLF4 and MYC (OSKM), adult cells started to mimic embryonic stem cells and could now be used in research of pluripotency and development (Takahashi and Yamanaka, 2006). The reprogramming efficiency could be more and more improved by manipulating the activity of chromatin remodelers, histone and DNA modifiers and non-coding RNA expression (Alberts et al., 2014).

Both, ESCs and iPSCs, offer the opportunity of differentiation into various cell types or even into small organs. Therefore, they are an excellent model to study development and related diseases. Since iPSCs derive from adult cells, they can be obtained directly from patients helping to understand how the disease occurs and to study the effect of drugs. Additionally, they overcome the problem of immune rejection in stem cell therapy (Alberts et al., 2014).

1.5.2 Overview of brain development

The development of the central nervous system starts very early at day 16 post fertilization (in human) with the event of gastrulation. During gastrulation, the three germ layers are formed: mesoderm, endoderm and ectoderm, which will give rise to the nervous system and epidermis (Ghimire et al., 2021) (Figure 1.4A). The next important event in brain development is called primary neurulation. It starts with the formation of the notochord, which is a cylinder of mesodermal cells directly under the ectoderm. The notochord sends

inductive signals to the ectoderm in its close proximity which induces a neural fate and the formation of the so called neuroectoderm. The neuroectoderm thickens and forms the neural plate, which will fold inwards and forms the neural tube (Danzer et al., 2017). The neural tube is the origin structure for the brain (Figure 1.4B).

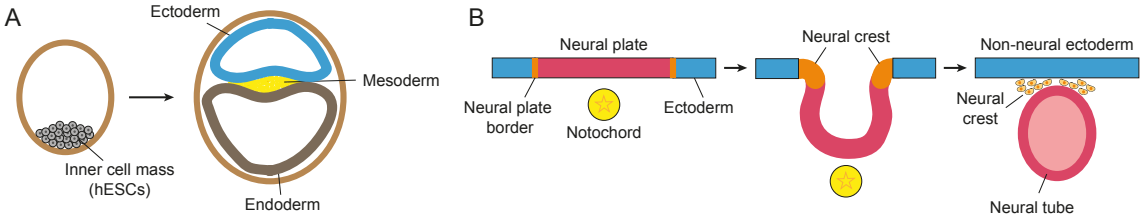

Figure 1.4: ***Gastrulation and Neurulation.***
(A) *Embryonic state after gastrulation.* ***(B)*** *Neural tube formation.*

At about the fourth and fifth week of gestation, brain vesicle formation starts. Initially three vesicles are formed: the prosencephalon (forebrain), the mesencephalon (midbrain) and the rhombencephalon (hindbrain). The prosencephalon/forebrain then further divides into the telencephalon and diencephalon, while the rhombencephalon/hindbrain divides into the metencephalon and myelencephalon (Figure 1.5).

The walls of the neural tube in these vesicles contain neuroepithelial cells (NEC). They sit in the ventricular zone (VZ) and divide rapidly, with each cycle driving the growth of the early brain. At the onset of neurogenesis, neuroepithelial cells give rise to apical radial glial cells (aRG) which are the major neuronal progenitors. These aRG cells can either self-renew or differentiate into neurons via intermediate progenitors (IPs), which reside in the subventricular zone (SVZ), or even directly into neurons (Paridaen and Huttner, 2014). The emerging neurons then migrate to their final location using special adhesion molecules on a temporary framework of supporting glial cells and differentiate into their predestined cell type (Figure 1.6). Distinct regions of similar cell types are formed. The layers of the cortex are built from the inside to the outside, so later originated neurons have to travel through all previously settled neurons. Once the migration stage is completed, some of the supporting glial cells will degrade but the rest will build the white matter of the brain. The final events of brain development start prenatal but continue for years after birth (Ackerman, 1992). Neurons will form innumerable connections within and across regions. At the age of 18 months, no more neurons are added, which marks the time of maximum connections. However, these connections compete among each other

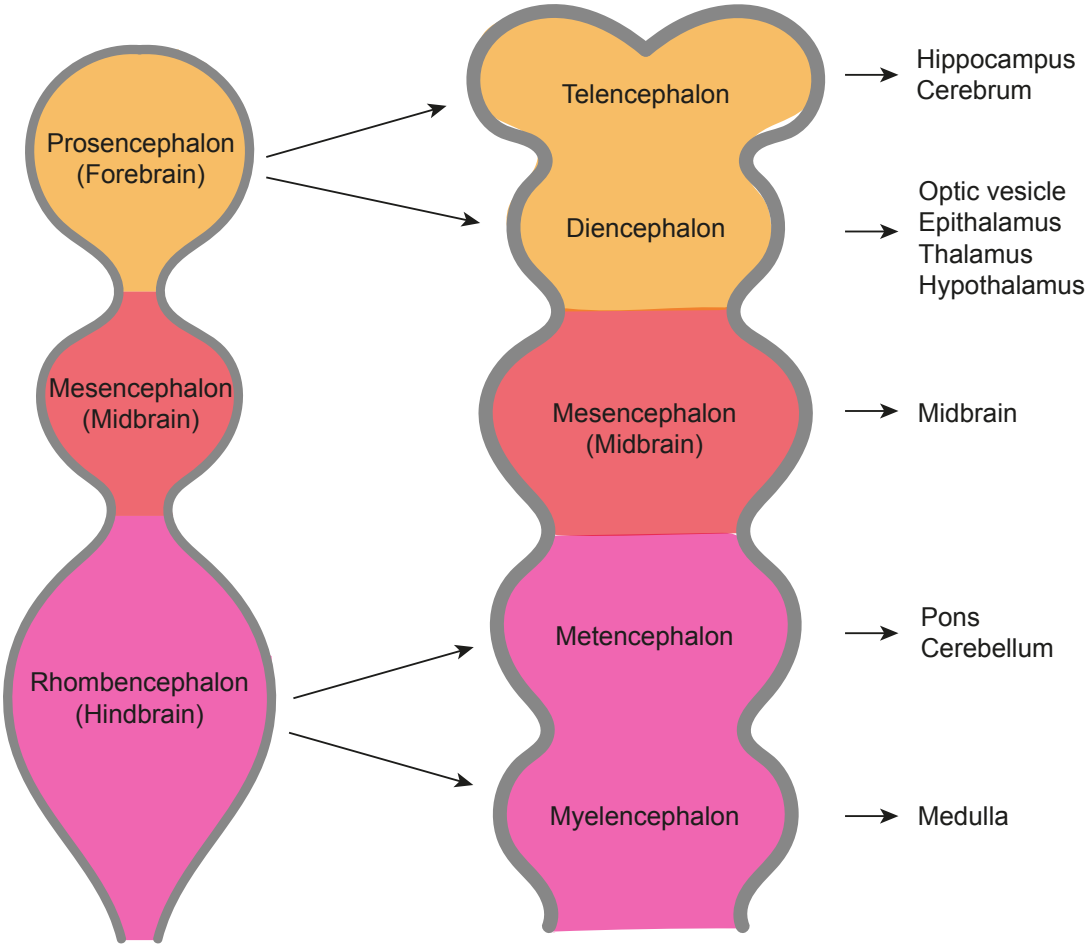

Figure 1.5: ***Human brain vesicles during development.***

and are selectively eliminated until around 100 trillion are stabilized.

Ethical reasons limit *in vivo* brain research in humans. Therefore, most findings in this field were made in animals, e.g. in mouse. However, brain development in humans differs in various ways which already appears in the first stages of development. Human embryonic stem cells (hESCs) do not resemble mouse embryonic stem cells (mESCs) but rather mouse epiblast-derived stem cells (Brons et al., 2007, Kojima et al., 2014). And while the developmental events from fertilization to the blastocyst are basically similar between mouse and human, the timing and molecular details, as e.g. transcriptional environments, are different (Rossant and Tam, 2017). An obvious difference between mouse brain and human brain is the size. The subventricular zone is substantially enlarged compared to rodents (Lui et al., 2011) and contains additionally outer radial glial cells (oRG)-like cells which are not observed in mouse (Haldipur et al., 2019).

Due to these differences, many human genomic and developmental features still remain

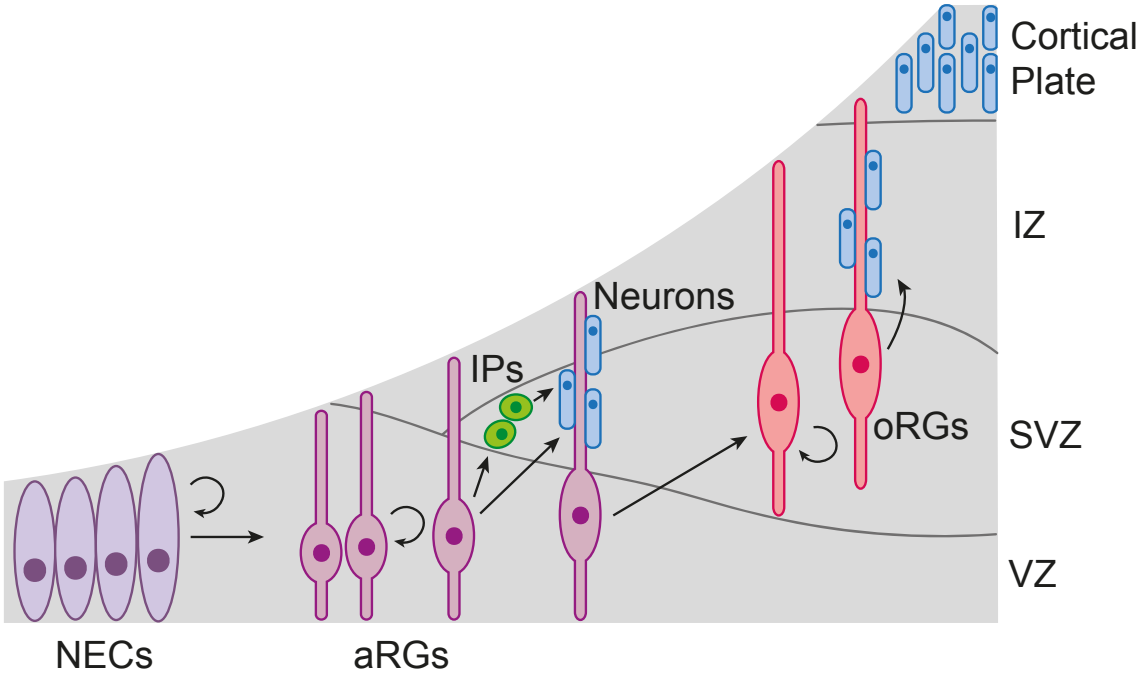

Figure 1.6: ***Overview of human brain development.***
NECs = neuroepithelial cells; aRGs = apical radial glial cells; IPs = intermediate progenitors; oRGs = outer radial glial cells; VZ = ventricular zone; SVZ = subventricular zone; IZ = intermediate zone

largely elusive and research using human pluripotent stem cell models is an important tool to uncover those.

1.5.3 Early ectodermal cell types

Besides the above described neuroectodermal cells (NE or NES), which are induced through notochord signaling and will form the central nervous system, there are three other early ectodermal cell types evolving during ectodermal differentiation.

Neural crest cells

Neural crest cells (NCs) are a migratory stem cell population that arises during neurulation (neural tube formation). They form at the edges of the infolding neuroectoderm between neural and non-neural ectoderm (neural plate border) and start delaminating via epithelial-to-mesenchymal transition (EMT) and migrate towards their appropriate destinations in the embryo. More than 30 distinct cell types arise from neural crest cells, e.g. melanocytes (pigment cells), neurons of the peripheral nervous system, facial bones and cartilage, smooth muscle cells, adipocytes and endocrine cells (Le Lièvre and

Le Douarin, 1975, Noden, 1983, Bronner and Simões-Costa, 2016).

Cranial placode

Cranial placodes (CP) are specialized regions of the non-neural ectoderm. They form as local thickenings after neural tube closure in the cranial part of the embryo. The special features of the placodes are an increased proliferation compared to the epidermis (Saka and Smith, 2001), morphogenetic movements such as migration and invagination, and the ability for neuronal differentiation. There are six types of cranial placodes present in the human embryo (Schlosser, 2006):

- the adenohypophyseal, which will form the anterior lobe of the pituitary gland
- the olfactory, which will form the olfactory epithelium of the nose
- the lens placode, which will form the transparent lens of the eye
- the trigeminal, which will form the sensory neurons of the V$^{\text{th}}$ cranial nerve
- epibranchial placodes, which will form the sensory neurons of the VII$^{\text{th}}$, IX$^{\text{th}}$ and X$^{\text{th}}$ cranial nerves
- the otic placode, which will form precursors for sensory epithelia of the inner ear and neurons of the VIII$^{\text{th}}$ cranial nerve

Cranial placodes build important parts of the sensory organs and ganglia and defects in placode development can result in blindness, deafness, loss of smell or hormone imbalance (Baker and Bronner-Fraser, 2001).

Non-neural ectoderm

All of the ectoderm, that is not exposed to notochord signaling and is not committed to a neural fate, is called non-neural ectoderm (NNE) or surface ectoderm. It will give rise to the skin, hair and nails. Development of the skin starts by the formation of the embryonic epidermal basal layer which gives rise to all structures of the future epidermis, including hair follicles and sweat glands, as well as the basement membrane (Mikkola, 2007), which separates the epidermis from the dermis and additionally provides growth factors for basal cells (S. Liu et al., 2013).

1.5.4 Mitochondrial function in neurodevelopment

In the last years it became more and more prominent that development and metabolism are closely connected (Khacho et al., 2019). The balance between aerobic glycolysis and oxidative phosphorylation is important for regulating cell state transitions. In general, the main energy resource during differentiation shifts from glycolysis in stem cells (Gu et al., 2016) to OXPHOS in differentiated cells. Nevertheless, mitochondrial respiration and oxidative phosphorylation are still active in hESCs (H. Zhang et al., 2016). The change in metabolism during differentiation is accompanied by a change in mitochondrial morphology. In mouse, Khacho et al. observed elongated mitochondria in uncommitted neural stem cells (NSCs) in the ventricular zone, fragmented mitochondria once NSCs commit and again elongated mitochondria during differentiation into neurons (Khacho et al., 2016).

Neural crest cells also undergo metabolic changes during their differentiation. Before delaminating from neural plate borders, they have a basal metabolism which changes into upregulated glycolysis in for migration primed NCs. During migration, neural crest cells use the Warburg effect to generate energy (Bhattacharya et al., 2020). Upon reaching their final destination and differentiation, they decrease their glycolysis and switch to OXPHOS (Bhattacharya et al., 2021).

Disruption of mitochondrial function during development causes encephalopathies, resulting in cognitive dysfunctions, as e.g. behavioral abnormalities (Fattal et al., 2006), epilepsy, hearing loss and progressive dementia (Kartsounis et al., 1992, Turconi et al., 1999). Examples of disorders are MELAS syndrome and Wolfram syndrome, both caused by mutations in mtDNA, Leigh syndrome and COX deficiency, both caused by mutations affecting mitochondrial respiration and OXPHOS. Mutations affecting mitochondrial morphology have been linked to encephalopathies as well (Kimmel et al., 2000, Waterham et al., 2007, Fang et al., 2016, Spiegel et al., 2016).

1.6 Aims of this thesis

Gene expression is a multi-layered process, tightly regulated by several transcriptional and post-transcriptional mechanisms. While transcription is regulated for example by DNA methylations and chromatin modifications, the fate of RNA post-transcriptionally is modulated by RNA modifications on coding and non-coding RNAs. The accurate control of the gene expression is essential to ensure proper cellular function and normal development and its disruption can lead to diseases. Aberrant deposition of tRNA modifications has been linked to cancer, type 2 diabetes, neuro-developmental disorders and mitochondrial-linked disorders.

However, the precise underlying molecular mechanisms how tRNA modifications contribute to developmental processes are still largely unknown. In this study, I focused on elucidating the influence of tRNA modifications in human early ectodermal differentiation which defines the origin of central nervous system development. I was using human pluripotent stem cells (hPSCs) and their differentiation into five early ectodermal cell types as a model system. I aimed to address the following by using multiple methods (Figure 1.7):

1. Landscape of tRNA modifications and modifying enzymes in early ectodermal differentiation.

2. Whether the tRNA anticodon pool changes during early ectodermal differentiation.

3. Effect of tRNA modifications on global translation.

4. Impact of mitochondrial tRNA modifications on mitochondrial function in early ectodermal differentiation.

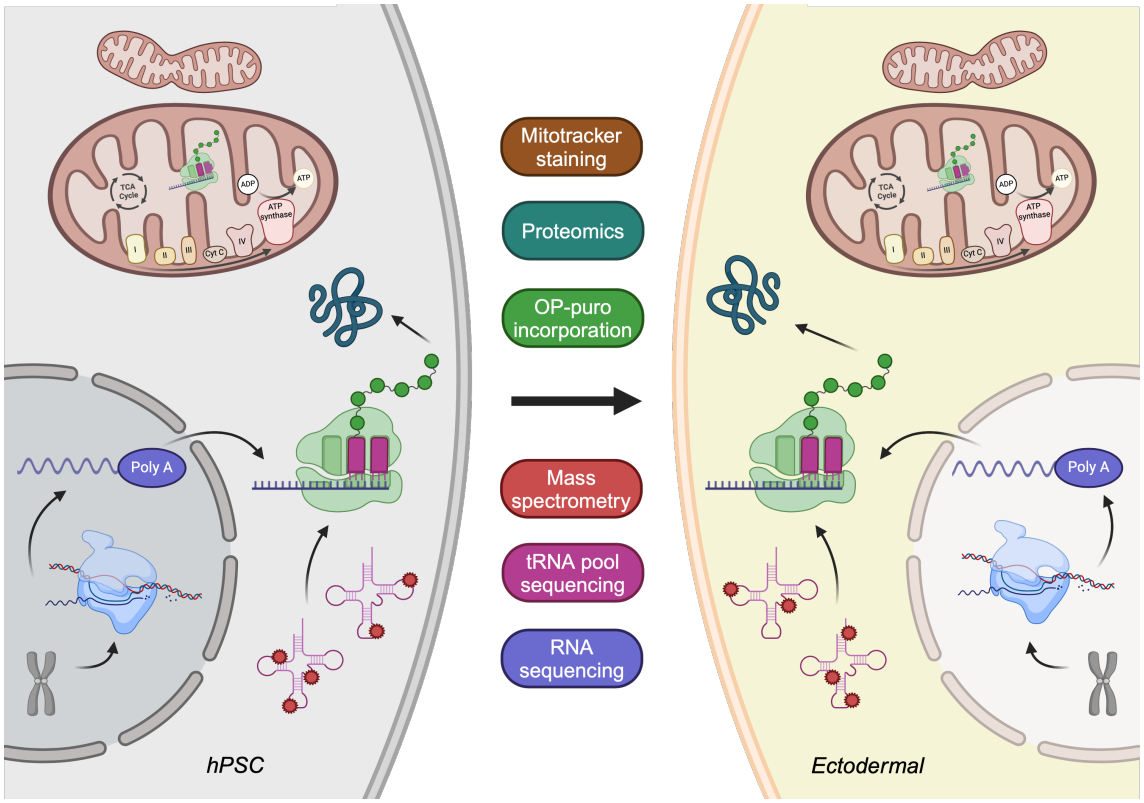

Figure 1.7: ***Methodical concept to address the aims of this thesis.*** *Mitotracker staining to analyze morphology, number and activity of mitochondria. Proteomics analysis to determine the change in proteomes. Incorporation of OP-puromycin the measure translation. Mass spectrometry to measure levels of tRNA modifications. Sequencing of tRNA pools to determine if tRNA anticodon pools change during differentiation. RNA sequencing to validate cell type identity and measure changes in transcriptomes. hPSC = human pluripotent stem cells. This figure was generated using Biorender.*

2 Materials and Methods

2.1 Cell Culture

2.1.1 Cell lines

The following cell lines were used in this thesis:

The pharyngeal carcinoma cell line "FaDu" was purchased from ATCC (ATCC-HTB-43).

The "Cal-33" cell line was obtained from the German Collection of Microorganisms (DSMZ). Experiments with this line were performed by Marc Krontal. Cells were cultured in Dulbecco's Modified Eagle Medium (DMEM) with high glucose + pyruvate (41966029, Life Technologies), supplemented with 10% FBS (16140071, Life Technologies) and 1% Penicillin-Streptomycin (15140122, Life Technologies).

The human embryonic stem cell line "H1" (WA01) was purchased from WiCell. A licence by the Robert-Koch-Institute for import and application of human embryonic stem cells is on hand (AZ 3.04.02/0143).

Induced pluripotent stem cells (iPSCs) and neuroepithelial stem cells (NES) were provided by Prof. Dr. Anna Falk from Lund University. iPSCs were induced from healthy donors and further differentiated into stable NES lines (Figure 2.1). In this thesis, five lines were used: control 7 (male), control 9 (male), control 10 (male), control 11 (female) and control 14 (female).

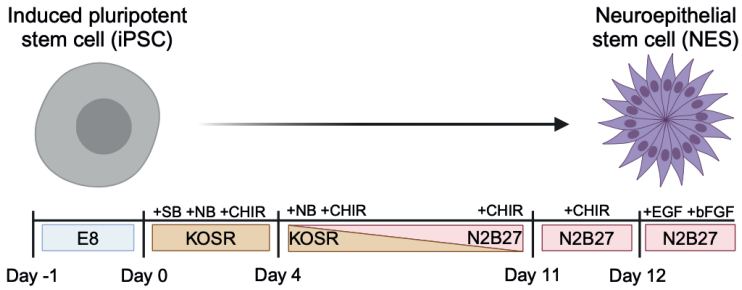

Figure 2.1: ***Protocol for NES generation.***
NES cells were generated by the Anna Falk group. Figure made using Biorender.

SAI1 cells, another hindbrain NES cell line, were originally obtained from Austin Smith (Tailor et al., 2013).

2.1.2 Culture of FaDu cells

FaDu cells were cultured in Eagle's minimum essential medium (EMEM) (30-2003, ATCC) supplemented with 10% FBS (16140071, Life Technologies) and 1% Penicillin-Streptomycin (15140122, Life Technologies). Cells were passaged twice a week. For passaging, cells were washed with PBS (14190250, Life Technologies) and then detached using Trypsin/EDTA (25200056, Life Technologies) for 5 minutes at 37°C. The Trypsin was inactivated by culture medium and cells were transferred into a new flask in the desired density.
To freeze, cells were pelleted after detachment at 400xg for 5 minutes and resuspended in culture medium with 10% DMSO (D2650-5x5ml, Sigma Aldrich) and stored in liquid nitrogen.

2.1.3 Culture of hESCs

Preparation of Matrigel coated plates

An aliquot of Corning® Matrigel® hESC-qualified matrix (11573560, Fisher Scientific) was thawed on ice and then added to ice cold DMEM/F-12 (11320033, Life Technologies). One 6-well was coated with 1 ml Matrigel® and incubated at room temperature for 1 hour before storing at 4°C for up to one week. Before use, plates were warmed up at 37°C for 30 minutes.

Culture of H1 cells

H1 cells were cultured in mTeSR™ Plus medium (100-0276, Stemcell Technologies) in Matrigel coated 6-well plates. Medium change was performed daily. Cells were passaged every 3 - 4 days or once the colonies started touching each other. First, cells were washed with PBS (14190250, Life Technologies). Then, 1 ml of ReLeSR™ (05872, Stemcell Technologies) was added per well and directly aspirated again. Cells were incubated at 37°C for 3 - 5 minutes and then carefully resuspended in medium, keeping them in small aggregates. Cells were splitted in a ratio of 1:4 to 1:10, depending on the experimental need.

For freezing, detached cell aggregates were spun down at 200xg for 3 minutes and resuspended in 500 µl CryoStor® CS10 (07930, Stemcell Technologies). Cells were stored at liquid nitrogen.

2.1.4 Ectodermal differentiation of hESCs

The ectodermal differentiation of H1 cells into neuroectoderm (NE), neural crest (NC), cranial placode (CP) and non-neural ectoderm (NNE) was performed according to the protocol of Tchieu et al., 2017.

Previous to the differentiation, H1 cells were cultured in TeSR™-E8™ medium (05990, Stemcell Technologies) for one passage. Cells were detached using ReLeSR™ (05872, Stemcell Technologies) for 10 minutes at 37°C and gently dissociated from the plate. Cells were seeded in the ratio of 1:2 per 6-well in TeSR™-E8™ medium supplemented with 10 µM ROCK inhibitor Y-27632 (72302, Stemcell Technologies). The next day, cells were washed once with PBS and further cultured in TeSR™-E6 medium (05946, Stemcell Technologies) containing different supplements for each line (Table 2.1).

	Day 0	**Day 1**	**Day 2**	**Day 3/5/7/9/11**	**Day 4/6/8/10/12**	**Day13**
NE	E6 + 500nM LDN + 10µM SB	E6 + 500nM LDN + 10µM SB		E6 + 500nM LDN + 10µM SB		Harvest cells
NC	E6 + 1ng/ml BMP4 + 10µM SB + 600nM CHIR	E6 + 1ng/ml BMP4 + 10µM SB + 600nM CHIR	E6 + 1ng/ml BMP4 + 10µM SB + 600nM CHIR	E6 + 10µM SB + 1.5µM CHIR		Harvest cells
CP	E6 + 5ng/ml BMP4 + 10µM SB	E6 + 5ng/ml BMP4 + 10µM SB	E6 + 5ng/ml BMP4 + 10µM SB	E6 + 10µM SB + 50ng/ml FGF2	E6 + 10µM SB + 50ng/ml FGF2	Harvest cells
NNE	E6 + 10ng/ml BMP4 + 10µM SB + 10µM SU	E6 + 10ng/ml BMP4 + 10µM SB + 10µM SU	E6 + 5ng/ml BMP4 + 10µM SB		E6 + 5ng/ml BMP4 + 10µM SB	Harvest cells

Table 2.1: *Protocol for ectodermal differentiation of hESCs*

At day 13, cells were harvested for RNA isolation. Briefly, cells were washed with PBS

and detached using 0.5 ml StemPro^{TM} Accutase^{TM} (A1110501, Thermo Fisher) per well for 10 minutes at 37°C. Accutase was inactivated by the addition of 1.5 ml medium and cells were pelleted.

Used supplements: LDN 193189 (T1935-5mg-TM, Biocat), SB 431542 (1614/10, R&D systems), rhBMP-4 (314-BP-010, R&D systems), CHIR 99021 (4423/10, R&D systems), SU-5402 (BV-1645-1, Biovision) and rhFGF2 (233-FB-010/CF, R&D systems).

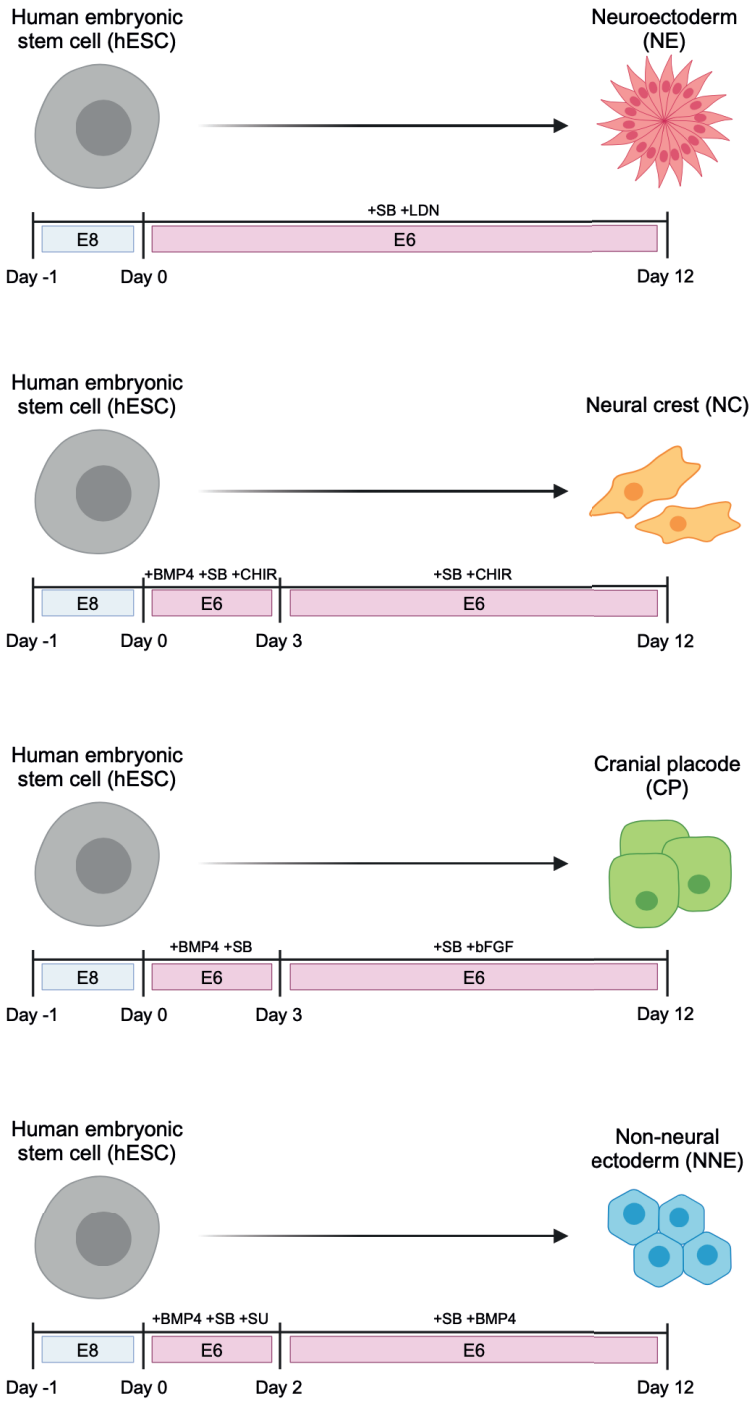

Figure 2.2: ***Ectodermal differentiation of hESCs.***
Protocol from Tchieu et al. 2017. Figure was made using Biorender.

2.1.5 Culture of iPSCs

Preparation of laminin coated plates

Induced pluripotent stem cells (iPSCs) were cultured on Laminin-521 coated plates. LN-521 (BioLamina) was diluted 20x in PBS +/+ (with calcium and magnesium, 14190-94, Life Technologies). One 6-well was coated with 1.5 ml and stored overnight at 4°C. Plates were warmed up at 37°C for 30 minutes before use.

Culture of iPSCs

The iPSC cell lines were cultured in Essential 8^{TM} medium with supplement (A1517001, Life Technologies) and passaged every 4 days. Medium change was performed daily. Cells were washed with PBS and 1 ml TrypLE Select (12563-011, Life Technologies) was added. Cells were incubated at 37°C for 5 minutes and afterwards transferred into a 2 ml E8 medium with ROCK inhibitor (Y-27632, SCM075, Millipore) containing falcon tube. Cells were pelleted for 3 minutes at 300xg and resuspended in 1 ml E8 plus ROCK inhibitor for counting. 180 thousand cells were seeded per 6-well in E8 medium with ROCK inhibitor.

2.1.6 Culture of NES cells

Preparation of laminin coated plates

Neuroepithelial stem cells (NES) were cultured on Laminin2020 coated plates. First, plates are coated with PolyOrnithine (PO). PO (P3655-100MG, Sigma Aldrich) was diluted 500x in PBS (without calcium/magnesium, 14190250, Life Technologies) to a final concentration of 100 µg/ml or a premade solution of Cultrex Poly-L-Ornithine was used (3436-100-01, R&D systems). Wells were coated with 1 ml and incubated at 37°C for 2 hours. Afterwards, wells were washed three times with PBS. Laminin2020 (L2020, Sigma Aldrich) was diluted 500x in PBS and wells were coated with 1.5 ml for either 4 hours at 37°C or overnight at 4°C. Before use, plates were warmed up at 37°C for 30 minutes.

Culture of NES cells

Both, NES cell lines from the Falk lab as well as the SAI1 cell line, were cultured in DMEM/F12 plus Glutamax medium (31331-028, Life Technologies) supplemented with N-2 (17502048, Life Technologies) and B-27 (17504044, Life Technologies), and with 10

ng/µl bFGF (CTP0261, Life Technologies or 233-FB-010/CF, R&D systems) and 10 ng/µl EGF (AF-100-15, PeproTech or PHG0314, Life Technologies). Medium change was performed daily. The cells were passaged every three days when they reached 100% confluency. First, cells were washed with PBS and 1 ml TrypLE Express (12604-013, Life Technologies) was added to detach the cells. After 5 minutes incubation at 37°C cells were resuspended and transferred in a flacon tube containing 2 ml medium. Cells were pelleted at 300xg for 3 minutes and resuspended in 1 ml medium for counting. 400 thousand cells were plated per 6-well.

2.2 siPOOL transfection

siPOOLs (siTOOLs Biotech) are pools of 30 siRNAs against the gene of interest, which greatly reduces off-target effects and allows for efficient and specific gene silencing. The used siPOOLs are listed in Table 2.3. A scrambled negative control siPOOL was used in all experiments.

Transfection of FaDu and Cal-33

Experiments in Cal-33 cells were performed by Marc Krontal. FaDu cells and Cal-33 cells were reverse transfected with 4 nM siPOOL. First, the transfection mixes (Table 2.2) were prepared, mixed and added to a 6-well. Next, 2.7 x 10^5 cells were added. The knockdown was carried out for 72 hours.

	Transfection mix	**Volume per well**
siPOOL (10 µM stock) + Opti-MEM™	0.8 µl + 249.2 µl	500 µl
RNAiMAX + Opti-MEM™	4 µl + 246 µl	
2.7 x 10^5 cells		1.5 ml

Table 2.2: *siPOOL transfection in FaDu and Cal33*

Gene	siPOOL
ADAT1	23536 ADAT1
ADAT2	134637 ADAT2
ADAT3	113179 ADAT3
ALKBH1	8846 ALKBH1
ALKBH8	91801 ALKBH8
BCDIN3D	144233 BCDIN3D
CDKAL1	54901 CDKAL1
CDK5RAP1	51654 CDK5RAP1
CTU1	90353 CTU1
CTU2	348180 CTU2
DNMT2	1787 TRDMT1
DUS2	54920 DUS2
DUS3L	56931 DUS3L
ELP1	8518 IKBKAP
ELP6	54859 ELP6
ELP3	55140 ELP3
FTSJ1	24140 FTSJ1
GTPBP3	84705 GTPBP3
KEOPS	84520 GON7
METTL1	4234 METTL1
METTL2A+B	339175 METTL2A+B
METTL6	131965 METTL6
METTL8	79828 METTL8
MOD5	54802 TRIT1

Gene	siPOOL
MTO1	25821 MTO1
NAT10	55226 NAT10
NSUN2	54888 NSUN2
NSUN3	63899 NSUN3
NSUN6	221078 NSUN6
OSGEPL1	64172 OSGEPL1
PUS7	54517 PUS7
PUS10	150962 PUS10
PUS1	80324 PUS1
PUS3	83480 PUS3
QTRT1	81890 QTRT1
TRMO	51531 TRMO
TRMT13	54482 TRMT13
TRMT44	152992 TRMT44
TRMT61A	115708 TRMT61A
TRMT10A	93587 TRMT10A
TRMT6	51605 TRMT6
TRMT9B	57604 KIAA1456
TRMT2A	27037 TRMT2A
TRMT11	60487 TRMT11
TRMT1	55621 TRMT1
TRMU	55687 TRMU
TYW1	55253 TYW1
WDR4	10785 WDR4

Table 2.3: *siPOOLs*

2.3 MitoTracker staining

MitoTracker staining for imaging

NES cells and iPSCs were growing on coated coverslips in a 24-well. They were stained with 100 nM MitoTracker™ Red CMXRos (M7512, Thermo Fisher) for 30 minutes at 37°C. Afterwards, the medium was removed and the cells were fixed with 4% Paraformaldehyde solution in PBS (sc-281692, Santa Cruz) for 15 minutes at room temperature in the dark. After washing two times with PBS, the cells were permeabilized with 0.5% TritonX-100 (T8787, Sigma Aldrich) in PBS for 5 minutes at room temperature in the dark. The cells were washed two times with PBS and then the nuclei were stained with DAPI (10236276001, Sigma Aldrich) for 5 minutes at room temperature. After another wash with PBS, coverslips were mounted on microscopy slides.

MitoTracker staining for flow cytometry

SAI1 cells and H1 cells were growing in 6-well format. Cells were treated with 100 nM MitoTracker™ Deep Red FM (M22426, Thermo Fisher) or 100 nM MitoTracker™ Red CMXRos for 45 minutes at 37°C. Cells were washed with PBS and detached with 1 ml TrypLE Express for 4 minutes at 37°C. After inactivation with 2 ml medium and centrifugation at 200xg (H1) or 300xg (SAI1) for 3 minutes, cells were fixed with 4% PFA solution for 15 minutes on ice, dark. Cells were washed two times with PBS and then directly used for flow cytometry analysis.

2.4 OP-puromycin incorporation

2.4.1 Global translation analysis

All cell lines (FaDu, Cal33, H1 and SAI1) were treated with 50 µM O-propargyl-puromycin (OP-puro) (Medchem Source) and one well was additionally treated with 50 µg/ml cycloheximide (CHX) (C4859-1ML, Sigma Aldrich) as a control. FaDu und Cal33 cells were treated for 1 hour at 37°C and H1 and SAI1 cells were treated for 45 minutes at 37°C. Afterwards, cells were washed with PBS and harvested according to their protocol. Cells were fixed with 4% PFA solution for 15 minutes on ice and washed two times with PBS (14190250, Life Technologies). For permeabilization, cells were incubated in PBS plus 3% FBS and 0.1% saponine (S7900-25G, Sigma Aldrich) for 5 minutes at room temperature. To fluorescently label the OP-puro, a Click-it reaction was performed for 30 minutes at room temperature in the dark, using the Click-iT™ cell reaction buffer kit (C10269, Thermo Fisher) with 2 µM Alexa Fluor™ azide (A10266 or A10277, Life Technologies). Afterwards, cells were washed twice with permeabilization buffer and finally resuspended in PBS for flow cytometry analysis.

2.4.2 Mitochondrial translation analysis

To analyze mitochondrial translation, H1 and SAI1 cells were treated with 50 µM OP-puro and 100 nM MitoTracker™ Deep Red FM (MitoTracker DR) for 30 min at 37°C. One 6-well plate was treated additionally with 2 µg/ml puromycin (P8833, Sigma Aldrich) as a control. Afterwards, cells were harvested as previously described and six 6-wells were pooled per sample. Next, mitochondria were isolated using the Mitochondria Isolation Kit

for Cultured Cells (89874, Thermo Fisher). Briefly, cells were resuspended in 800 µl Buffer A and disrupted using a dounce tissue grinder for 30 times (5 times douncer A and 25 times douncer B, D8938-1SET, Sigma Aldrich). One sample was processed at a time until centrifugation. After addition of 800 µl buffer C, cell debris was pelleted at 700xg, 4°C for 10 minutes. The mitochondria containing supernatant was transferred in a new tube and centrifuged at 12,000xg, 4°C for 15 minutes. The mitochondria pellet was washed with 500 µl buffer C and subsequently, the obtained mitochondria were fixed in 500 µl 1% PFA in PBS for 15 minutes on ice, dark. All further centrifugation steps were carried out at 12,000xg and 4°C. Fixed mitochondria were washed with PBS and permeabilized with PBS plus 3% FBS plus 0.1% saponine for 5 minutes at room temperature in the dark. Next, OP-puro was stained with the Click-it reaction as previously described (Chapter 2.4.1), mitochondria were washed two times with permeabilization buffer and resuspended in PBS for flow cytometry analysis.

2.5 Flow Cytometry

2.5.1 OP-puro analysis

Fluorescence of Alexa Fluor 488 was measured with BL-530/30 488 nm laser and of Alexa Fluor 647 was measured with RL-670/14 640 nm laser. The median intensity of the fluorescent signal of single cells was used as the value for OP-puro.

2.5.2 Mitotracker analysis

Fluorescence of CMXRos was measured with YG-610/20 531 nm laser and of DR was measured with RL-670/14 640 nm laser. The median intensity of fluorescent signal of single cells was used as the value of MitoTracker.

2.5.3 Cell cycle analysis

For cell cycle analysis, cells were stained with DAPI (10236276001, Sigma Aldrich) 1:3000 in PBS prior to flow cytometry analysis. DAPI fluorescence was measured with VL-450/50 405 nm laser. Cell cycle phases were determined by the signal peaks of single cells.

2.5.4 Apoptosis assay

To measure apoptosis, all cells of interest (e.g. knockdown FaDu cells after OP-puro treatment) were harvested, including floating cells in the supernatant. Cells were washed two times with PBS and resuspended in 1 ml PBS for counting. 5 x 105 cells were resuspended in 500 µl 1x binding buffer (556454, BD Pharmingen™) of which 100 µl were transferred in a new tube. Next, 5 µl FITC Annexin V (556419, BD Pharmingen™) were added, as well as 10 µl Propidium iodide staining solution (PI) (556463, BD Pharmingen™). Cells were gently vortexed and incubated for 15 minutes at room temperature in the dark. Finally, 400 µl 1x binding buffer were added and cells were analyzed by flow cytometry. Unstained cells, only FITC Annexin V and only PI cells were used as controls to set up the cytometer. Fluorescence was measured with BL-530/30 488 nm laser and BL-670/LP 488 nm laser.

2.5.5 Marker staining

Cells were harvested as previously described (Chapter 2.1.4) and fixed with 4% PFA in PBS. After washing, cells were permeabilized with PBS plus 10% FBS plus 0.1% saponine. Incubation with primary antibodies (Table 2.4) was 30 minutes at room temperature. After three rounds of washes with permeabilization buffer, cells were stained with secondary antibodies (Table 2.4) for 30 minutes at room temperature. After another three rounds of washes with permeabilization buffer, cells were resuspended in PBS and analyzed by flow cytometry.

	1st Antibody	**2nd Antibody**
NE	anti-FOXG1, rabbit, 5 µg (702554, Life Technologies)	anti-rabbit 647, 1:1,000 (A31573, Thermo Scientific)
NC	anti-SOX10, mouse, 25 µg/ml (MAB2864-SP, Bio-techne)	anti-mouse 647, 1:1,000 (A21235, Thermo Scientific)
CP	anti-SIX1, rabbit, 2 µg/ml (ATA-HPA001893-100, Biozol)	anti-rabbit 647, 1:1,000 (A31573, Thermo Scientific)
NNE	anti-TFAP2A, mouse, 5 µg/ml (3B5, DHSB)	anti-mouse 647, 1:1,000 (A21235, Thermo Scientific)

Table 2.4: *Antibodies used for marker staining in differentiated cells*

2.6 Microscopy

2.6.1 Brightfield imaging

Brightfield images were acquired using the ZEISS Axio Vert.A1 microscope.

2.6.2 Mitotracker imaing and analysis

Images for MitoTracker analysis were acquired using a ZEISS Axio Imager.M2 microscope. Images were processed and analyzed using Fiji. Mitochondrial length was measured in µm. Per cell line, three to five images were analyzed and per image, 50 to 250 mitochondria were measured using the freehand line tool in Fiji.

2.7 mRNA expression analysis

2.7.1 RNA extraction

RNA, which was only used for RT-qPCR, was isolated using the RNeasy Mini kit (74104, Qiagen) according to the manufacturer's instructions. Briefly, cell pellets were lysed in 350 µl RLT buffer, RNA was bound to a column and finally eluted in 30 µl nuclease-free water (10977035, Thermo Fisher). RNA concentration was quantified using NanoDrop™ One Spectrophotometer (Thermo Scientific).

Total RNA was isolated using TRIzol (15596018, Life Technologies). Cell pellets were resuspended in 1 ml TRIzol and incubated for 5 minutes at room temperature. 200 µl chloroform (22720.360, VWR) was added, samples were vortexed and incubated for 3 minutes. After centrifugation at 12,000xg, 4°C for 15 minutes, the upper aqueous phase was transferred into a new tube and 500 µl 2-propanol (Fisher Scientific) were added. The samples were mixed by inverting and incubated for 10 minutes. After another centrifugation at 12,000xg, 4°C for 10 minutes, the RNA pellet was washed with 75% Ethanol (1.00983.2511, Supelco). The dried pellet was resuspended in 30 µl nuclease-free water. RNA concentration was measured with NanoDrop or with the Qubit RNA BR assay (Q10210, Life Technologies).

2.7.2 Reverse transcription

Reverse transcription of RNA into cDNA was performed with 1 µg of RNA. RNA was mixed with 0.5 µl random primers (10 mM stock, C1181, Promega) and 1 µl dNTPs (10 mM stock, N0447S, NEB). After incubation at 65°C for 5 minutes, 4 µl 5x first strand buffer (18080093, Thermo Fisher), 1 µl DTT (0.1 M stock, 18080093, Thermo Fisher), 1 µl RNasin® Plus (N2615, Promega) and 1 µl SuperScript™ III Reverse Transcriptase were added. The reaction was incubated at 25°C for 5 minutes, at 50°C for 60 minutes and at 70°C for 15 minutes.

2.7.3 Real-time quantitative PCR

For RT-qPCR, 1 µl of cDNA was mixed with 5 µl TaqMan™ Fast Advanced Master Mix (4444557, Thermo Fisher), 3.5 µl nuclease-free water and 0.5 µl TaqMan™ gene expression assay (Thermo Fisher) (Table 2.5). PCR was carried out using a Quantstudio 3 applied biosystems real-time PCR system (Thermo Fisher). Probes against house-keeping genes are used for normalization. Fold changes in gene expression were calculated using the delta delta Ct method.

Gene	Taqman probe
ADAT1	Hs00201527_m1
ADAT2	Hs00699339_m1
ADAT3	Hs00707957_s1
ALKBH1	Hs00195696_m1
ALKBH8	Hs00299122_m1
BCDIN3D	Hs00416915_m1
CDK5RAP1	Hs01001899_m1
CDKAL1	Hs00214949_m1
CTU1	Hs00293325_m1
CTU2	Hs00419111_m1
DUS2	Hs00250393_m1
DUS3L	Hs01116425_m1
ELP3	Hs00986846_m1
ELP6	Hs01015876_m1
FBLL1	Hs01584505_s1
FTSJ1	Hs01125798_g1
GON7	Hs01897983_s1
GTPBP3	Hs00378443_m1
IKBKAP	Hs00175353_m1
KIAA1456	Hs00332747_m1
METTL1	Hs01096147_g1
METTL2A+B	Hs00276553_m1
METTL6	Hs00379179_m1
METTL8	Hs00227054_m1
MTO1	Hs00969127_g1
NAT10	Hs00226545_m1
NSUN2	Hs00214829_m1
NSUN3	Hs00222961_m1
NSUN6	Hs01013871_m1
OSGEPL1	Hs01088658_g1
PUS1	Hs01124619_m1
PUS10	Hs00328708_m1
PUS3	Hs00229938_m1
PUS7	Hs01031425_m1
QTRT1	Hs00229674_m1
TRIT1	Hs01091215_m1
TRMO	Hs00939134_m1
TRMT1	Hs01551973_g1
TRMT10A	Hs01083083_m1
TRMT11	Hs00935252_m1
TRMT13	Hs01052225_m1
TRMT2A	Hs00224133_m1
TRMT44	Hs01013769_m1
TRMT5	Hs00418256_m1
TRMT6	Hs01017508_m1
TRMT61A	Hs00293457_m1
TRMU	Hs00972705_m1
TYW1	Hs04989072_m1
WDR4	Hs00218742_m1
ELAVL4	Hs00956610_mH
HES5	Hs01387463_g1
HMX1	Hs00232746_m1
KRT16	Hs00373910_g1
PAX6	Hs01088114_m1
POU5F1	Hs00999632_g1
SIX1	Hs00195590_m1
SMYD1	Hs00400855_m1
SOX1	Hs01057642_s1
SOX10	Hs00366918_m1
FOXG1	Hs01850784_s1
TFAP2A	Hs01029413_m1
WISP1	Hs05047584_s1
ZNF229	Hs00970996_g1
LHX2	Hs00180351_m1
OTX2	Hs00222238_m1
SIX3	Hs00193667_m1
GBX2	Hs00230965_m1
PAX5	Hs05040337_s1
HOXB2	Hs01911167_s1
TBP	Hs00427620_m1
18S	Hs99999901_s1

Table 2.5: *Taqman probes*

2.8 Measuring modifications with Mass Spectrometry

Mass Spectrometry was performed to measure tRNA modifications. Per sample, 5 µg total RNA was sent to Dr. Cathrine Broberg Vågbø, Proteomics and Modomics Experimental Core (PROMEC), NTNU, Trondheim, Norway.

The following text was written by Cathrine Broberg Vågbø: "tRNA was enriched using an Agilent 1260 Infinity II Analytical-Scale LC-UV Purification System with a Bio SEC-3 300 Å, 2.1 x 300 mm column (Agilent Technologies) chromatographed isocratically with 100 mM ammonium acetate pH 7 at 0.280 ml/min and 40°C for 20 minutes. Chromatograms were recorded at 260 nm and tRNA collected, lyophilized and dissolved in water. The collected tRNA was enzymatically digested using benzonase (Santa Cruz Biotech) and nuclease P1 (Sigma) in 10 mM ammonium acetate pH 6.0, 1 mM MgCl2 and 100 µM erythro-9-Amino-β-hexyl-α-methyl-9H-purine-9-ethanol at 40 °C for 1 h, added ammonium bicarbonate to 50 mM, phoshodiesterase I and alkaline phosphatase (Sigma) and incubated further at 37 °C for 1 h. Digested samples were precipitated with 3 volumes of acetonitrile and supernatants were lyophilized and dissolved in internal standard (I.S.) solution for LC-MS/MS analysis. An Agilent 1290 Infinity II UHPLC system with an ZORBAX RRHD Eclipse Plus C18 150 x 2.1 mm (1.8 µm) column protected with an ZORBAX RRHD Eclipse Plus C18 5x2.1 mm (1.8 µm) guard (Agilent) was used for chromatographic separation. The mobile phase consisted of A: water and B: methanol (both added 0.1% formic acid) at 0.22 ml/min, starting with 5% B for 0.5 min followed by 2.5 min of 5-20% B, 3.5 min of 20-95% B, and 4 min re-equilibration with 5% B. Mass spectrometric detection was performed using an Agilent 6495 Triple Quadrupole system monitoring the mass transitions 268.1-136.1 (A), 284.1-152.1 (G), 244.1-112.1 (C), 245.1-113.1 (U), 282.1-150.1 (m^6A and m^1A), 296.1-164.1 ($m^{6,6}A$), , 283.1-151.1 (m^1I), 298.1-166.1 (m^1G, m^2G and m^7G), 312.1-180.1 ($m^{2,2}G$ and $m^{2,7}G$), 258.1-126.1 (m^3C and m^5C), 274.1-142.1 (hm^5C), 272.1-140.1 (f^5C), 286.1-154.1 (ac^4C), 258.1-112-1 (Cm), 302.1-170.1 (ncm^5U), 317.1-185.1 (mcm^5U), 333.1-183.1 (R/S-$mchm^5U$), 333.1-201.1 (mcm^5s^2U), 259.1-113.1 (Um), 285.1/153.1 (d3-m^6A, I.S.), 286.1-154.1 (d3-m^1I, I.S.), 261.1-112.1 (d3-Cm, I.S.), 301.1-152.1 (d3-m^7G, I.S.), 301.1-152.1 (d3-Gm, I.S.), 264.1-127.1 (13C5-m^5U, I.S.), 273.1/136.1 (13C5-A, I.S.), 246.1/114.1 (d2-C, I.S.) in positive ionization mode, and 267.1-135.1 (I) and 272.1-135.1 (13C5-I, I.S.) in negative ionization mode."

2.9 Sequencing

2.9.1 RNA sequencing

iPSC and NES cells

Samples were first treated with DNase. 4 µg of RNA in 50 µl nuclease-free water was mixed with 5 µl 10x TURBO™ buffer and 1 µl TURBO™ DNase (AM2239, Thermo Fisher) and was incubated at 37°C for 30 minutes. Afterwards, samples were cleaned up using the RNeasy Mini kit (Qiagen) and eluted in 25 µl nuclease-free water. Concentrations were measured with the Qubit RNA BR kit.

To determine the RNA integrity number (RIN), samples were analyzed with the Bioanalyzer RNA 6000 Nano kit (5067-1511, Agilent).

Finally, RNA samples were submitted to the DKFZ sequencing facility. For library prep, the TruSeq Stranded protocol was used and samples were sequenced on a NovaSeq 6K PE 100 S4 split.

H1 and differentiated lines

4 µg RNA was DNase treated as described above. Libraries for sequencing were prepared from 100 ng RNA using the Illumina Stranded Total RNA Prep with Ribo-Zero Plus kit (20040525, Illumina) according to the manufacturer's protocol. The IDT for Illumina RNA UD Indexes Set A kit (20040553, Illumina) was used for indexes. Concentrations of libraries were measured with the Qubit 1x dsDNA HS assay (Q33230, Life Technologies) and library sizes were determined using the TapeStation Agilent High Sensitivity D1000 ScreenTape assay (5067-5585, Agilent). One multiplex was created from the libraries with a concentration of 10 nM. Present adapters were cleaned up using AMPure XP beads (A63881, Beckman Coulter). The multiplex was sequenced on 2 lanes of a NovaSeq 6K PE 100 SP.

2.9.2 tRNA pool sequencing

The tRNA pool sequencing protocol was developed by Kristen et al. in Prof. Dr. Mark Helms lab (Figure 3.11). The libraries were prepared in collaboration with Marc Lander. 2 µg of total RNA was used and filled up to 7 µl with nuclease-free water. A mix of

2 µl cytosolic oligos (6-FAM labelled), 2 µl mitochondrial oligos (Cy-5 labelled), 3 µl 10x hybridization buffer (150 mM HEPES pH 7.5, 500 nM potassium acetate) and 1 µl nuclease-free water was added per sample. The sample was denatured for 2 minutes at 94°C and gradually cooled down to 25°C. tRNA/oligo hybrids were subsequently separated from unhybridized RNAs on a Native 10% PAGE run at 12 W for 40 minutes. The gel was stained and the hybrid band was excised. The gel pieces were crushed, transferred in a tube and 300 µl 0.5 M ammonium acetate was added. The tube was incubated for 15 minutes at -80°C and shook overnight at 15°C. The next day, everything was transferred on a Nanosep spin column and centrifuged for 5 minutes in a table top centrifuge. Flow through was transferred into a new tube, 1 µl glycogen was added as well as 700 µl 100% ethanol (-80°C cold) and then the tube was incubated for 1 hour at -80°C followed by centrifugation at 4°C for 1 hour. The pellet was washed with 300 µl cold 75% ethanol and centrifuged at 4°C for 30 minutes. The pellet was dried and resuspended in 5 µl nuclease-free water.

Next, 2.5 µl sample was amplified in a PCR using 1 µl i5 primer (10 µM), 1 µl i7 primer (10 µM), 2 µl 10x Standard Taq reaction buffer, 1.2 µl MgCl2, 1 µl dNTPs, 10.3 µl water and 1 µl Taq polymerase. The PCR was run for 6 cycles and cleaned-up on a denaturing 10% PAGE gel for 2 hours at 14 W. PCR product band was excised and the libraries were extracted as described above. Pellets were eluted in 5 µl water.

Concentrations of libraries were measured with the Qubit 1x dsDNA HS assay and sizes were determined with the Bioanalyzer DNA 1000 kit. Libraries were pooled to a multiplex and sequenced on 2 lanes of a MiSeq V3 PE 75.

2.10 Protein expression analysis

2.10.1 Protein extraction

Protein for Western Blot analysis was extracted from cells by adding 75 µl (to cells from 6-well) RIPA buffer (50 mM Tris-HCl pH 7.4, 1% NP-40, 150 mM NaCl, 0.1% SDS, 0.5% sodium deoxycholate) supplemented with cOmplete™ EDTA-free protein inhibitor cocktail (11873580001, Sigma Aldrich) and PhosSTOP™ phosphatase inhibitor cocktail (4906837001, Sigma Aldrich) to each well. Cells were scraped off and transferred to an Eppendorf tube on ice. Tubes were incubated on ice for 15 minutes and then

centrifuged at maximum speed, 4°C for 15 minutes. The protein containing supernatant was transferred into a new tube and stored at -80°C until use.

Protein used in proteomics analysis was extracted as follows: cells were washed two times with ice cold PBS before storing as cell pellets at -80°C. For lysis, cells were resuspended in 40 µl lysis buffer (Table 2.6) and incubated on ice for 1 hour. After centrifugation at 20,000xg, 4°C for 60 minutes, the protein containing supernatant was transferred in a new tube and stored at -80°C.

10 ml	RIPA buffer	SLCC5042, Sigma Aldrich
100 µl	1 M NaF	215309-10G, Sigma Aldrich
10 µl	1 M Na_3VO_4	450243-10G, Sigma Aldrich
1 pill	Complete EDTA free protease inhibitor	4693159001, Merck
1 pill	Phsopho Stop	4906845001, Merck
10 µl	Benzonase (2500 U)	
37 µl	DNase 1 (100 U)	

Table 2.6: *Lysis buffer for Proteomics*

Protein concentrations were determined using Pierce™ BCA protein assay kit (23225, Thermo Fisher) according to the manufacturer's protocol. Absorbance was measured with the GloMax Explorer spectrophotometer (Promega). Samples were measured in three technical replicates.

2.10.2 Western Blot

50 µg of protein was used for Western Blot. First, samples were mixed with 4x Laemmli buffer (1610747, Bio-Rad) plus 2-Mercaptoethanol (21985023, Life Technologies) and denatured at 98°C for 5 minutes. To separate samples according to their size, they were run on an SDS-PAGE (4-15% Mini-PROTEAN® TGX™ Precast Protein Gel, 4561084DC, Bio-Rad) in electrophoresis buffer (1 g SDS, 14 g Glycine, 3.03 g Trizma-base in 1 l water) for 20 minutes at 40 V and for 1 hour at 140 V. Next, proteins were plotted onto a PVDF membrane (Amersham™ HybondTM 0.45 PVDF, 10600023, GE Healthcare) in a wet

transferring system in transfer buffer (3.03 g Trizma-base, 14.4 g glycine, 200 ml methanol in 1 l water) for 1 hour at 400 mA.
The membrane was blocked in 5% skim milk (42590.01, Serva) in PBS-Tween (524653-1EA, Sigma Aldrich) for 1 hour at room temperature. Primary antibodies (Table 2.7) were incubated in 5% skim milk in PBS-T at 4°C overnight.

Protein of interest	**Protein size**	**Antibody**	**Dilution**
ADAT2	21 kDa	ab135429, abcam, rabbit	1:1,000
ADAT3	38 kDa	ab125540, abcam, rabbit	1:1,000
METTL1	31 kDa	PA580810, Life Technologies, rabbit	1:1,000
ALKBH1	44 kDa	MA535781, Life Technologies, rabbit	1:1,000
PUS3	56 kDa	A304-958A-M, Biomol, rabbit	1:1,000
TRIT1	53 kDa	PA531715, Life Technologies, rabbit	1:1,000
Hsp90	90 kDa	Sc-13119, Santa Cruz, mouse	2 µl in 5 ml block

Table 2.7: *Primary Antibodies for Western Blot*

The next day, the membrane was washed three times with PBS-Tween and then incubated with the secondary antibody (Table 2.8) for 1 hour at room temperature. After another three rounds of washes with PBS-Tween, detection was done with the ECL™ Prime Western Blotting Detection Reagents (GERPN2232, Sigma Aldrich) and with the ChemiDoc System (Bio-Rad).

Species	**Antibody**	**Dilution**
anti-rabbit IgG, HRP linked	6401-05, BioVision	1:10,000
anti-mouse IgG, HRP linked	6402-05, BioVision	1:10,000

Table 2.8: *Secondary Antibodies for Western Blot*

2.10.3 Proteomics analysis

Proteomics analysis was performed with 20 µg protein in 10 µl lysis buffer. LC-MS analysis with label-free quantification was performed in the Proteomics Core Facility of the DKFZ.

2.11 Bioinformatic Analysis

2.11.1 RNA sequencing analysis

Bioinformatic RNA sequencing data analysis was performed by Dr. Anke Heit-Mondrzyk: "RNA sequencing data was processed by the DKFZ One Touch Pipeline (OTP) using the RNA-seq workflow version 1.3.0 in combination with the workflow management system Roddy version 3.5.9 or 3.5.10. In brief, RNA sequencing data was aligned against the reference genome 1KGRef_PhiX (generated from the 1000 Genomes assembly, based on hs37d5 and including decoy sequences merged with PhiX contigs to be able to align spike in reads) using the STAR aligner version 2.5.3a. Duplicate marking was performed using Sambamba version 0.6.5 and quality control was performed using Samtools version 1.6 flagstat as well as rnaseqc version 1.1.8. FeatureCounts of the Subread package version 1.5.1 was used for gene specific quantification of reads on the GENCODE version 19 gene annotation in the strand-specific counting mode. Additionally, FPKM and TPM values were calculated.

Raw gene count values were then used as input for a differential gene expression analysis using DESeq2 version 1.28.1 within R version 4.0.0 which was made using default conditions besides fitType="local". For iPSC and NES samples, the sex of the cell lines was included as a variable in the design formula while building the DESeqDataSet. Results tables were then generated for each differentiated cell line compared to stem cells (NE/NC/CP/NNE vs H1; NES vs iPSC). PCA plots were generated using the plotPCA function from transformed data by Variance stabilizing transformation."

2.11.2 tRNA pool sequencing analysis

Bioinformatic tRNApool sequencing data analysis was performed by Dr. Sabrina Weser. The analysis was performed according to Kristen et al. (Kristen et al., 0, unpublished). Downsampling of read counts was performed when necessary. For the analysis, she used

command line tools. First, reads were trimmed with Trimmomatic version 0.38 to a length of 40 nucleotides corresponding to the cDOQ sequence. Trimmed reads were assigned to the cDOQ sequences and quantified using alignment-free Sailfish version 0.10.1., based on k-mer indexing and counting.

In principal component analysis, samples first clustered by library size so they were batch corrected for this. Differential expression analysis was performed in R version 4.3.0 using limma version 3.58.1.

2.11.3 Proteomics analysis

Bioinformatic analysis of proteomics data was performed by Dr. Sabrina Weser. Transformed intensity values were provided by proteomics facility. Differential protein expression analysis on log2 transformed intensity values was performed in R version 4.3.0 using limma version 3.58.1.

2.12 Data analyis and Statistical tests

Data was analyzed and plotted using RStudio packages, GraphPad Prism 8 and ClustVis (Metsalu and Vilo, 2015). Gene ontology analysis was performed with Gorilla (Eden et al., 2007, Eden et al., 2009). Statistical testing was performed with GraphPad Prism 8 and RStudio. Significance depicted by either directly shown p-value or via asteriks (* for $P < 0.05$, ** for $P < 0.01$, *** for $P < 0.001$, **** for $P < 0.0001$).

3 Results

3.1 Modelling early ectodermal cell states by differentiation of human pluripotent stem cells

Development is a highly complex process and is heavily dependent on accurate regulation of gene expression. However, development is also the process that displays the power of gene expression regulation best by forming a whole organism from one initial cell type. Modifications on tRNA are one part of this regulatory program that have been shown to be crucial during development (Frye et al., 2018). Especially the development of the brain is sensitive to mutations in tRNA modifying enzymes (see Chapter 1.4). Studying human nervous system development *in vivo* is limited due to ethical reasons. Therefore, most research in this field is made in animal models. However, brain development in humans differs in various ways which already appears in the first stages of development (Rossant and Tam, 2017). The alternative is to use human embryonic stem cells and differentiate them *in vitro*.

Previous work in the Frye group demonstrated that embryonic stem cells optimize codon usage depending on the inosine modification at the wobble position of tRNAs and showed that tRNA modifications affect already early cell fate decisions (Bornelöv et al., 2019). The early ectoderm (consisting of neuroectoderm, neural crest, cranial placodes and non-neural ectoderm) constitutes the very beginning of brain development.

To model this early step, I used the human embryonic stem cell line H1 which originates from human blastocyst (James A. Thomson et al., 1998) and differentiated it into the four major ectodermal cell types (Figure 3.1A):

- Neuroectoderm (NE), which will give rise to central nervous system.
- Neural crest (NC), which will give rise to pigment cells, cartilage and bone, gland cells and connective tissue.
- Cranial placode (CP), which will form sensory organs and ganglia.
- Non-neural ectoderm (NNE), which will form the epidermis, hair and nails.

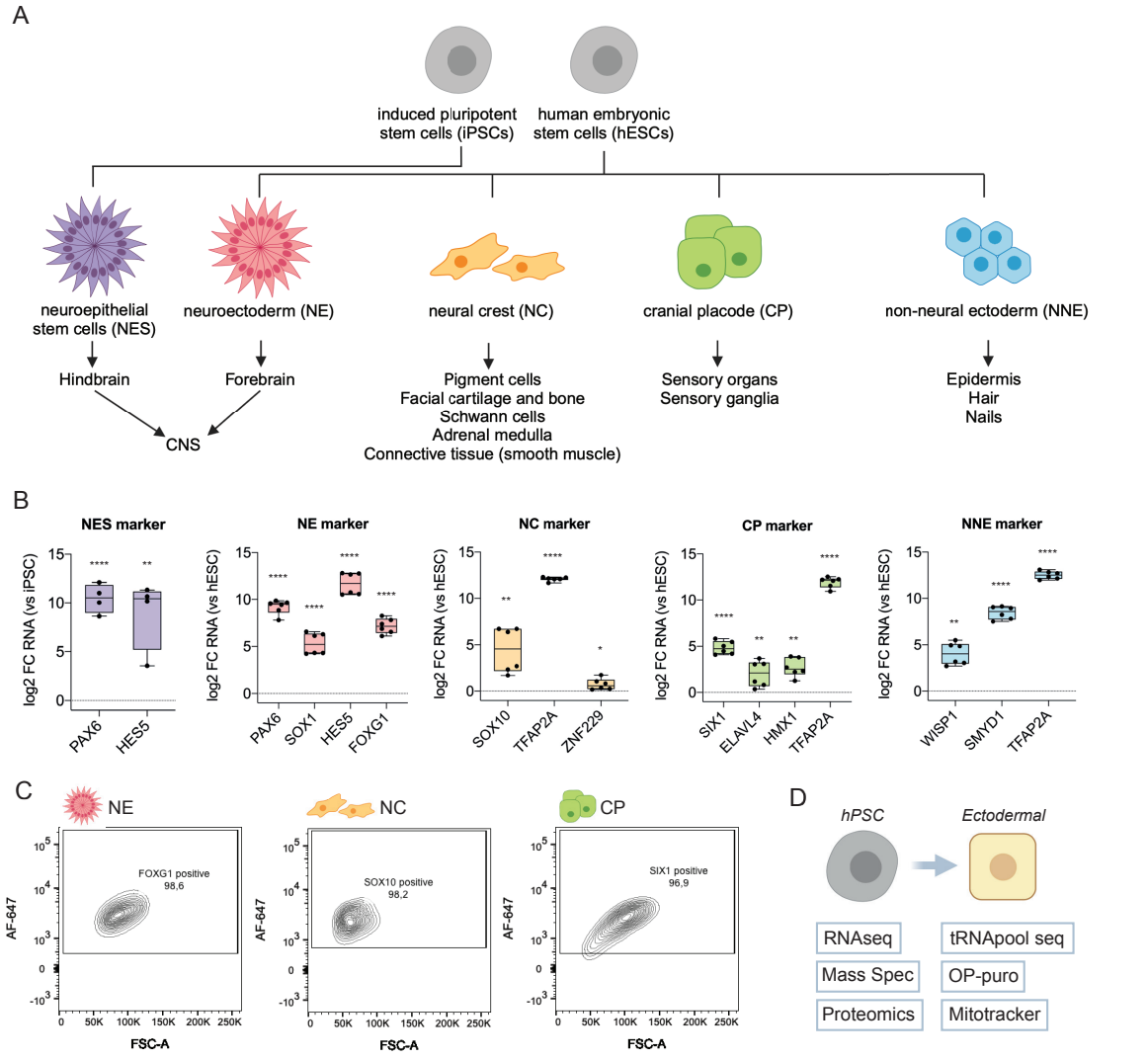

Figure 3.1: ***Differentiation of human pluripotent stem cells into early ectodermal cell types.***
(A) *Neuroepithelial stem cells (NES) were derived from induced pluripotent stem cells (iPSCs) (both cell types provided by Prof. Dr. Anna Falk). Human embryonic stem cells (hESCs) were differentiated into neuroectoderm (NE), neural crest (NC), cranial placode (CP) and non-neural ectoderm (NNE) using a protocol from Tchieu et al., 2017. Figure was generated with Biorender.* ***(B)*** *Analysis of lineage markers by RT-qPCR. RNA expression levels are depicted as log2-transformed fold changes relative to RNA expression in human pluripotent stem cells (hPSCs). Each data point represents a biological replicate and the mean of two technical replicates. Significance determined by unpaired t-test compared to hPSC. Box plot shows minimum, first quartile, median, third quartile and maximum.* ***(C)*** *Flow cytometry analysis of lineage markers. For each cell line, one representative plot of three biological replicates is shown.* ***(D)*** *Overview of used methods to analyze mechanisms steering this early ectodermal differentiation step.*

The protocol used for differentiation was published by Tchieu et al. in 2017 and allows for efficient differentiation in twelve days. Since the cells have to be confluent from the

beginning of differentiation and cannot be passaged, they are slightly overgrown at the end of the differentiation protocol and might have exited the cell cycle. Therefore, I included another neuroectodermal cell type: the neuroepithelial stem cells (NES) derived from induced pluripotent stem cells (Figure 3.1A) to exclude proliferation-dependent differences. These two cell lines were made and provided by Prof. Dr. Anna Falk from Lund University (Falk et al., 2012). An overview of how they differentiated the iPSC into NES cells is provided in Chapter 2.1.1. They transformed the NES cells into a stable cell line which allowed for far more application options and continuous culturing and could therefore be used as a culture-independent control. While iPS cells grew in typical colonies (Figure 3.2A), the NES cells showed the typical rosette structures (Figure 3.2B).

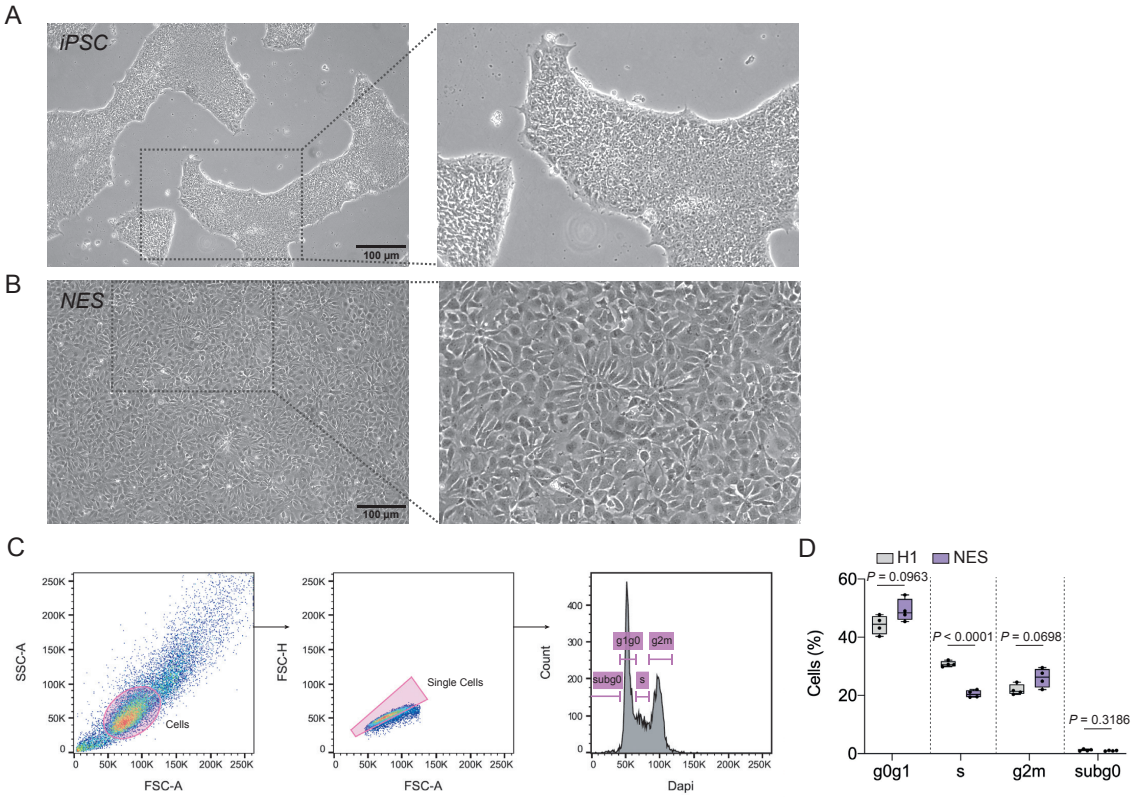

Figure 3.2: ***hPSC and NES cells in culture.***
Representative bright field images of iPSCs ***(A)*** *and NES cells* ***(B)****. NES cells show typical rosette structures. Scale bars, 100 µm.* ***(C)*** *Gating strategy for cell cycle analysis using Dapi staining flow cytometry analysis.* ***(D)*** *Cell cycle analysis of hESCs (H1) and SAI1 cells (NES). Each data point represents one biological replicate. Box plot shows minimum, first quartile, median, third quartile and maximum. P = unpaired t-test.*

Measuring their cell cycle through DAPI staining, NES cells exhibited an increase of cells in G1 and G2M phase and reduction of cells in S phase compared to hESCs

(Figures 3.2C and 3.2D). Embryonic stem cells have a shortended G1 phase due to rapid proliferation (Bigarella et al., 2014).

To test for correct differentiation, I analyzed lineage marker expression by RT-qPCR (Figure 3.1B). Both, NES and NE, expressed the neuroectoderm markers PAX6 (Osumi et al., 2008) and HES5. Neural crest is defined by SOX10 expression, cranial placode by SIX1 expression and non-neural ectoderm by expression of transcription factor AP2α (TFAP2A) (Tchieu et al., 2017). All markers were significantly enriched compared to expression in human pluripotent stem cells (hPSC), proving successful differentiation. To control for cell population purity, I stained NE, NC and CP cells with a lineage marker antibody and performed flow cytometry analysis (Figure 3.1C). For all three cell types, I observed over 95% positively stained cells, suggesting a relatively homogeneous population.

These two model systems, iPSC – NES and H1 – NE – NC – CP – NNE, could then be used to analyze changes in gene expression during ectodermal differentiation by RNA sequencing, mass spectrometry, proteomics, tRNA pool sequencing, OP-puromycin treatment and mitotracker staining (Figure 3.1D).

I started with performing RNA sequencing on these cells. Bioinformatic analysis was assisted by Dr. Anke Heit-Mondrzyk. Principle component analysis based on the top 500 genes with highest row variance clearly separated human pluripotent stem cells and differentiated cells (Figures 3.3A and 3.3B). Differentiated cell types NE, NC, CP and NNE could be separated as well with PC2, with NE and NNE being furthest apart highlighting their clear future distinction into nervous system and epidermis. Lineage marker expression, depicted as z-scores of normalized read counts, was also confirmed using this RNA sequencing data (Figure 3.3C). As expected, pluripotency markers were only expressed by H1. Some counter expressions of neural, neural crest, placode and non-neural ectoderm marker could be explained by either some impurities in cell population or the close proximity of cell types, e.g. cranial placodes are specialized regions of the non-neural ectoderm. Nevertheless, this could be tolerated due to clear separation in the PCA plot and good lineage marker expression, showing that the majority of cells was the desired cell type.

NE and NES are both neuroectodermal cell types but they differ in the aspect, that NE resembles forebrain cells and NES resembles hindbrain cells (Figure 3G). I confirmed

this by looking at marker expression in the RNA sequencing data (Figure 3.3D) and RT-qPCR (Figures 3.3E and 3.3F).

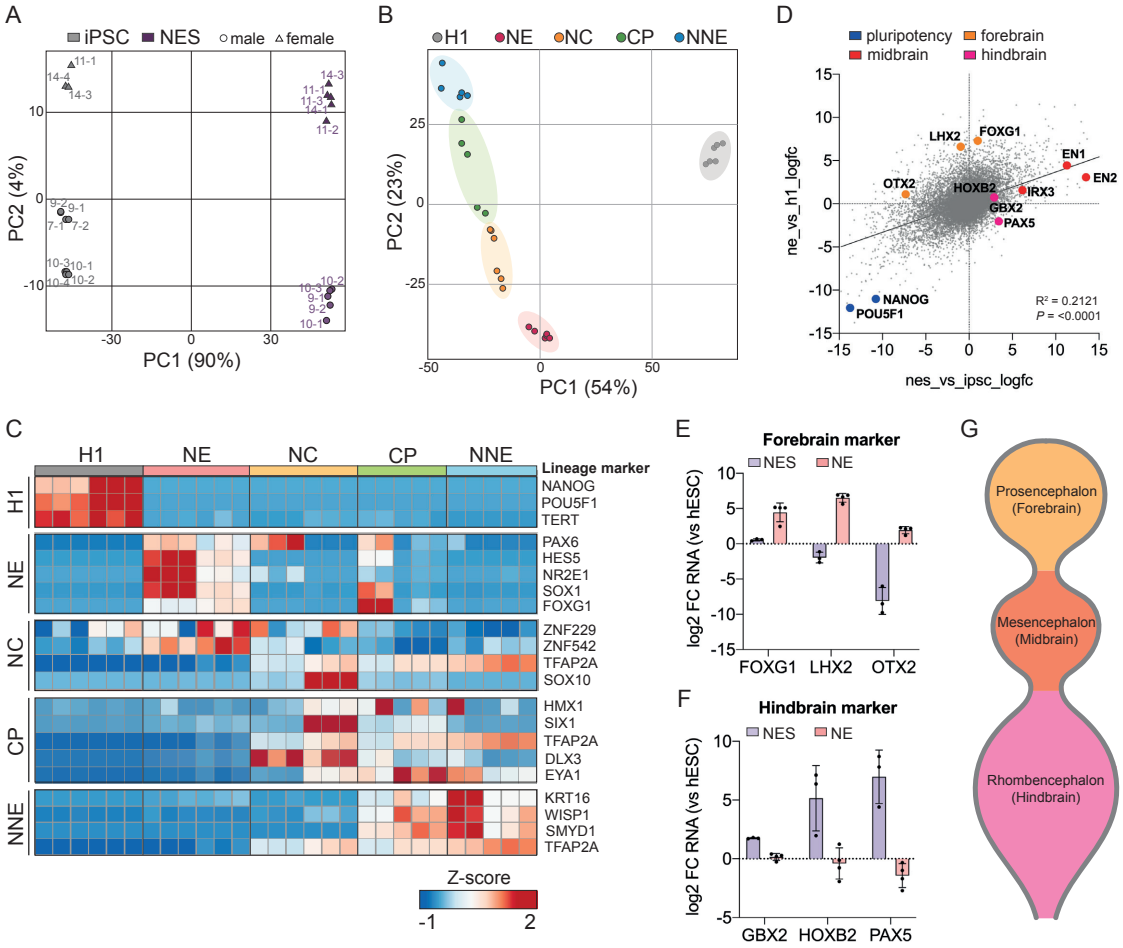

Figure 3.3: ***NE and NES depict forebrain and hindbrain.***
(A) *Principal component analysis of top 500 genes with highest row variance of iPSC and NES cells. Each data point represents one biological replicate.* ***(B)*** *Principal component analysis of top 500 genes with highest row variance of H1, NE, NC, CP and NNE cells. Each data point represents one biological replicate.* ***(C)*** *Heatmap depicting z-scores of lineage marker expression. Each column represents one biological replicate.* ***(D)*** *Log2 fold change of gene expression of all genes in NE was plotted against NES. Marker for pluripotency (blue), forebrain (orange), midbrain (red) and hindbrain (pink) are highlighted. Simple linear regression line.* ***(E + F)*** *Log2 fold change of RNA expression in NES and NE vs hESCs measured by RT-qPCR. Each data point represents a biological replicate and the mean of two technical replicates.* ***(G)*** *Overview of brain vesicles forebrain, midbrain and hindbrain.*

Next, I performed gene ontology analysis on significantly up and down regulated genes in differentiated cells compared to stem cells. In NES cells, I found a lot of microtubule and neuron related terms upregulated and signaling, translation and metabolism related terms downregulated (Figure 3.4A). In NE, genes related to cell migration and neuron fate were upregulated, and DNA and metabolic related genes downregulated (Figure 3.4B). In NC, CP and NNE mostly cell type specific GO terms were upregulated and translation, signaling, metabolic and DNA related GO terms were downregulated (Figures 3.4C, 3.4D and 3.4E).

Since a lot of the observed GO categories seem to be similar across the different cell types, I performed gene ontology analysis on up and down regulated genes shared between all of them. I found 1825 genes commonly upregulated compared to gene expression in stem cells, which were mostly related to developmental processes and differentiation (Figure 3.5A). The 2168 commonly downregulated genes mostly fell into translation and RNA related GO categories (Figure 3.5B and Suppl. Figure 5.1). This suggested, that translation and its regulation through modifications are changed during differentiation and are part of the characteristics of early ectodermal cell types.

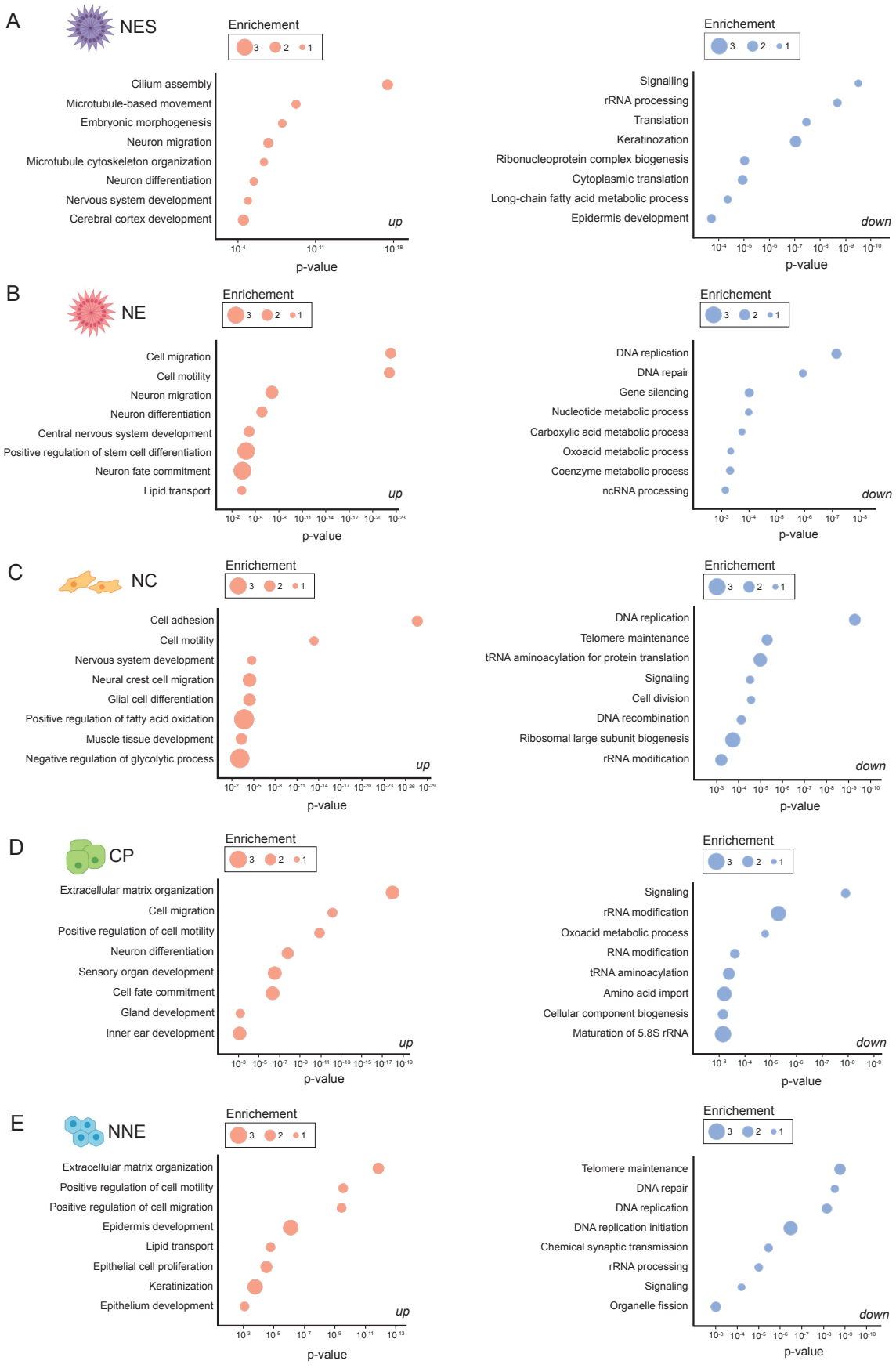

Figure 3.4: ***Gene ontology analysis of differentially expressed genes compared to hPSCs.*** *Caption on next page.*

Figure 3.4: *(Previous page.) GO analysis of significant > 0.5 log2FC up (red) and < -0.5 log2FC down (blue) regulated genes in* ***(A)*** *NES vs iPSC,* ***(B)*** *NE vs hESC,* ***(C)*** *NC vs hESC,* ***(D)*** *CP vs hESC and* ***(E)*** *NNE vs hESC. Chosen categories are representative for all results. GO analysis was performed with GOrilla (Eden et al., 2007, Eden et al., 2009).*

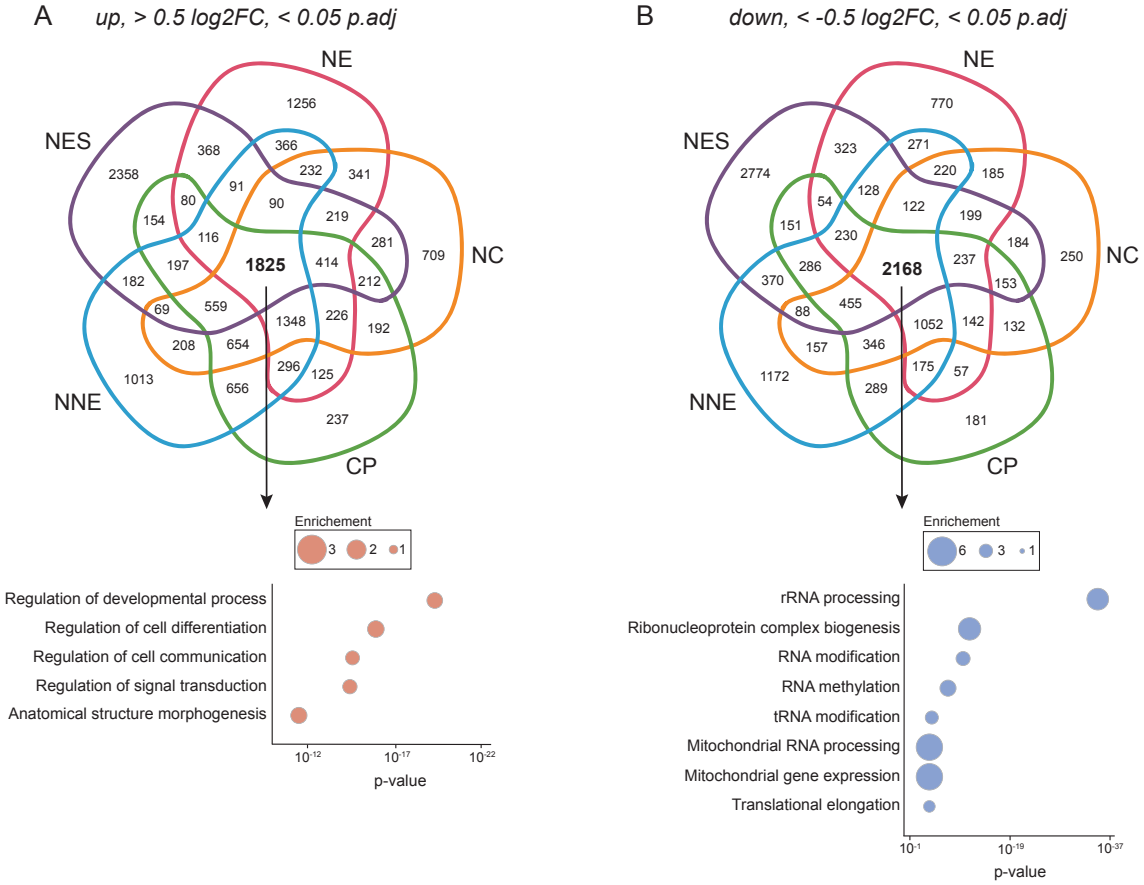

Figure 3.5: ***Early ectodermal cells commonly downregulate translation and RNA related genes.***
Gene ontology analysis of shared significant ***(A)*** *> 0.5 log2FC up (red) and* ***(B)*** *< -0.5 log2FC down (blue) regulated genes in all differentiated cell types compared to stem cells. Chosen categories are representative for all results. GO analysis was performed with Gorilla (Eden et al., 2007, Eden et al., 2009).*

Taken together, I established a model suited for studying changes in gene expression between pluripotent stem cells and early ectodermal cell types.

3.2 tRNA modifying enzymes are downregulated in early ectodermal cell types

Genes related to translation and its regulation were differentially expressed in all early ectodermal cell types compared to stem cells (Figure 3.5B). A key role in regulating protein synthesis is played by RNA modifications (Agris et al., 2007, Novoa and Ribas de Pouplana, 2012, Roundtree et al., 2017). Due to the involvement of especially tRNA modifications in many neurodevelopmental diseases, I was particularly interested in studying whether abundance and expression levels changed during differentiation.

First, I wanted to investigate expression levels of the enzymes that modify tRNAs (Suppl. Table 5.1). Principal component analysis based on the expression of these enzymes allowed clear separation of differentiated and stem cells by PC1 (Figures 3.6A and 3.6B). Additionally, neuroectoderm NE and non-neural ectoderm NNE could be separated by PC2. Implying that they have a different composition of tRNA modifying enzymes expressed. Looking at the log2 fold change of enzyme expression in differentiated cells versus stem cells, I observed that most tRNA modifying enzymes were downregulated (Figure 3.6C).

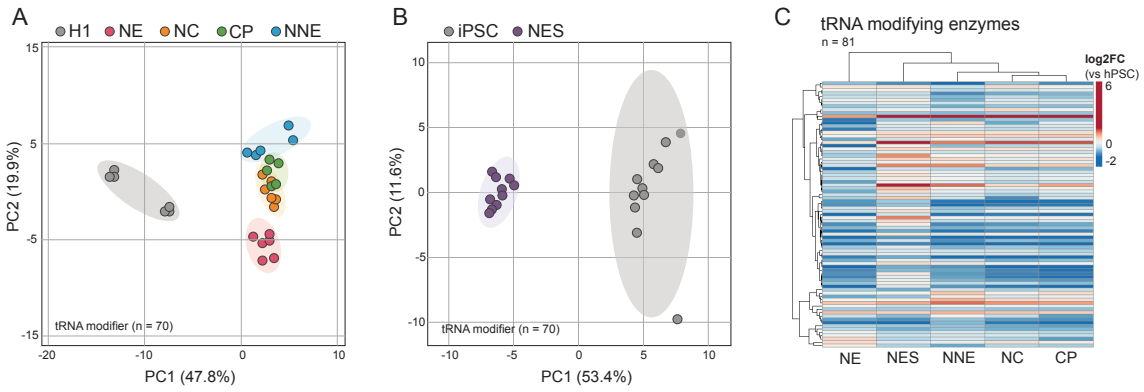

Figure 3.6: ***Expression of tRNA modifying enzymes changes during differentiation.***
Principal component analysis based on z-scores of n = 70 tRNA modifying enyzmes of ***(A)*** *H1, NE, NC, CP and NNE and* ***(B)*** *iPSC and NES. Z-scores calculated from normalized read counts.* ***(C)*** *Heatmap showing log2 fold changes of tRNA modifier expression vs. hPSC. Unbiased clustering based on correlation distance and average linkage. PCA plots and heatmap made with ClustVis (Metsalu and Vilo, 2015).*

When I applied unbiased clustering on the cell types, I observed that NC and CP clustered closest together while the neuroectodermal cell types NE and NES clustered further apart from each other. The hindbrain NES cells even clustered closer to the not neuroectodermal cell types NC, CP and NNE than to the forebrain NE cells. Whether this depends on culture conditions or is a hindbrain characteristics cannot be concluded here.

To look at the tRNA modifying enzymes and their expression throughout early ectodermal differentiation in more detail, I calculated z-scores based on normalized read counts in H1, NE, NC, CP and NNE (Figure 3.7A). Confirming what was seen in the fold change analysis (Figure 3.6C), most tRNA modifiers were highest expressed in embryonic stem cells. NE had the lowest expression of the different cell types. Unbiased clustering resulted in three major tRNA modifier cluster. Looking at their expression levels across differentiation they could be separated into cluster 1 (containing 4 modifiers) with no significant change in expression, cluster 2 (containing 24 modifiers) with significant downregulation in NE while significant upregulation in NES, CP and NNE, and cluster 3 (containing 53 modifiers) with significant downregulation in all early ectodermal cell lines (Figure 3.7B). This second cluster distinguished neuroectoderm NE from NES and the other cell types. Interestingly, 22 of the 24 tRNA modifiers in this cluster only modify cytoplasmic tRNAs.

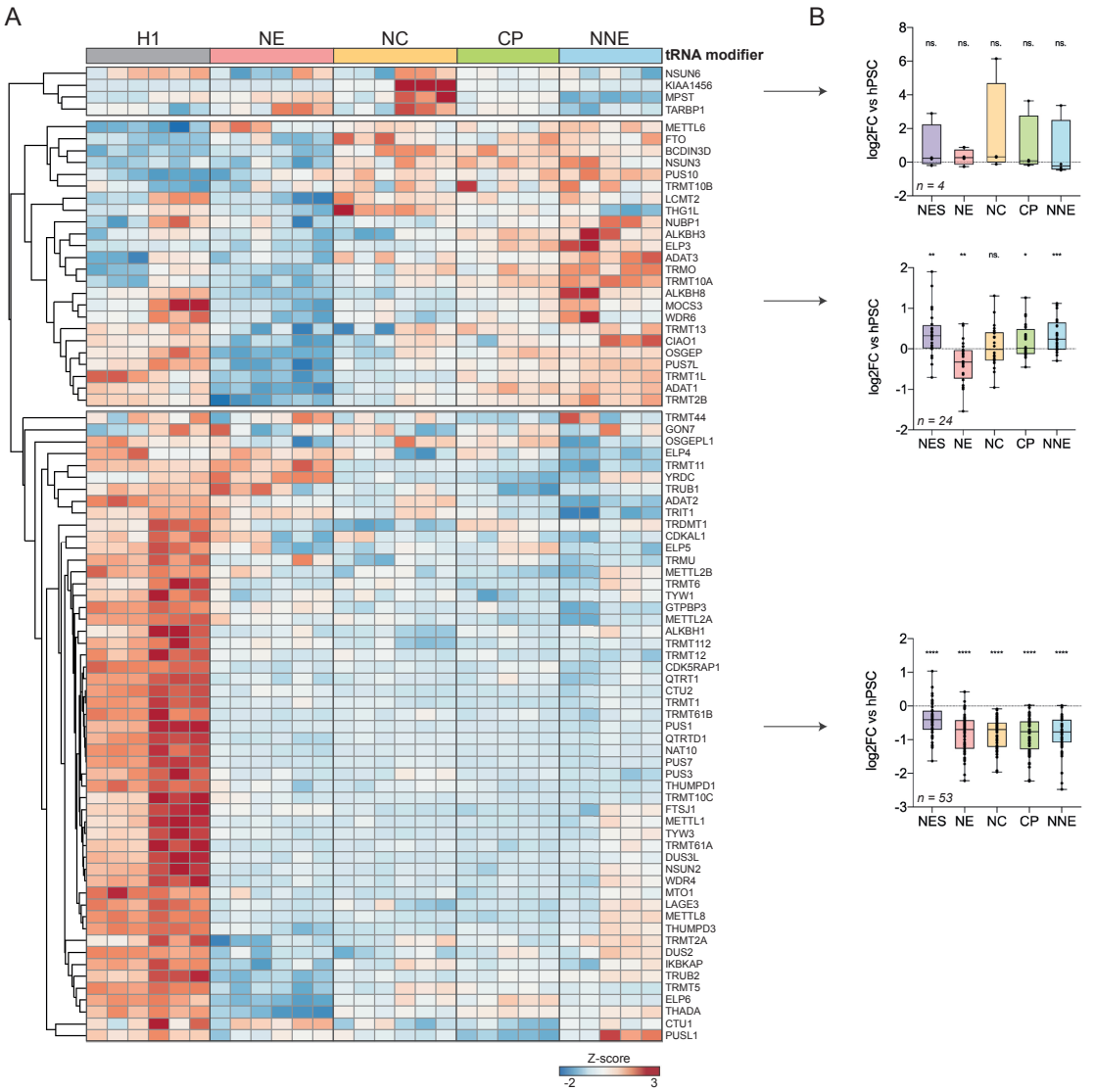

Figure 3.7: ***Landscape of tRNA modifying enzymes during early ectodermal differentiation.***
(A) *Heatmap showing z-scores of normalized read counts of tRNA modifier expression across the different lineages. A high z-score indicates a higher expression of a gene compared to mean expression across all lines. Heatmap and unbiased clustering made with ClustVis.* ***(B)*** *Log2 fold change of tRNA modifier expression of differentiated cell types vs expression in stem cells. Significance determined by paired t-test compared to hPSC. Box plot shows minimum, first quartile, median, third quartile and maximum.*

In NES cells 23 tRNA modifying enzymes were significantly downregulated (with log2FC $<$ -0.5) (Figure 3.8A). The most downregulated enzymes were METTL8, which produces m^3C in mitochondrial tRNAs, PUS1, which produces pseudouridine in both cytoplasmic and mitochondrial tRNAs, and ADAT2, which modifies the wobble position in cytoplasmic tRNAs into inosine (Figures 3.8H and 3.8I). Significantly upregulated (with log2FC $>$ 0.5) were 10 modifiers, with TRMT10A, producing m^1G in both types of

tRNA, with BCDIN3D, producing mmpG in cytoplasmic tRNAs, and with KIAA1456 upregulated the most. KIAA1456 is also known as TRMT9B, a homolog of yeast Trm9, and is thought to produce mchm^{5}U at the wobble position in cytoplasmic tRNAs. However, no experimental prove for its methylation ability on tRNAs is available yet (Hogan et al., 2023). TRMT9B was fount to be enriched in the nervous system and is important for synapse function (Hogan et al., 2023).

To determine changes in protein levels of tRNA modifying enzymes, I performed a proteomics analysis on NES cells and iPS cells. Bioinformatic analysis was assisted by Dr. Sabrina Weser. On protein level, 24 modifiers were significantly downregulated (with log2FC $<$ -0.5), with PUS1, PUS7 and TARBP1 having the biggest fold change. 7 modifiers were significantly upregulated, with LCMT2, TRMT10A and PUS10 being mostly up (Figure 3.8B). Downregulated PUS7 produces pseudouridine and TARBP1 produces 2'-O-methylguanosine (Gm), both in cytoplasmic tRNAs. Upregulated LCMT2 produces wybutosine and PUS10 produces pseudouridine, both in cytoplasmic tRNAs as well. RNA levels and protein levels of tRNA modifying enzymes correlated really well (Figure 3.8C).

In the forebrain neuroectodermal cell type NE, 44 tRNA modifying enzymes were significantly downregulated (with log2FC $<$ -0.5) and only 2 significantly upregulated (with log2FC $>$ 0.5) (Figure 3.8D). In neural crest, 38 modifiers were significantly downregulated and 5 significantly upregulated (Figure 3.8E). In cranial placode, 36 modifying enzymes were significantly down- and 6 significantly upregulated (Figure 3.8F). And in non-neural ectoderm, 37 tRNA modifiers were significantly down- and 8 significantly upregulated (Figure 3.8G). The enzymes whose expression changed the most during differentiation modify both types of tRNA in various positions (Figures 3.8H and 3.8I).

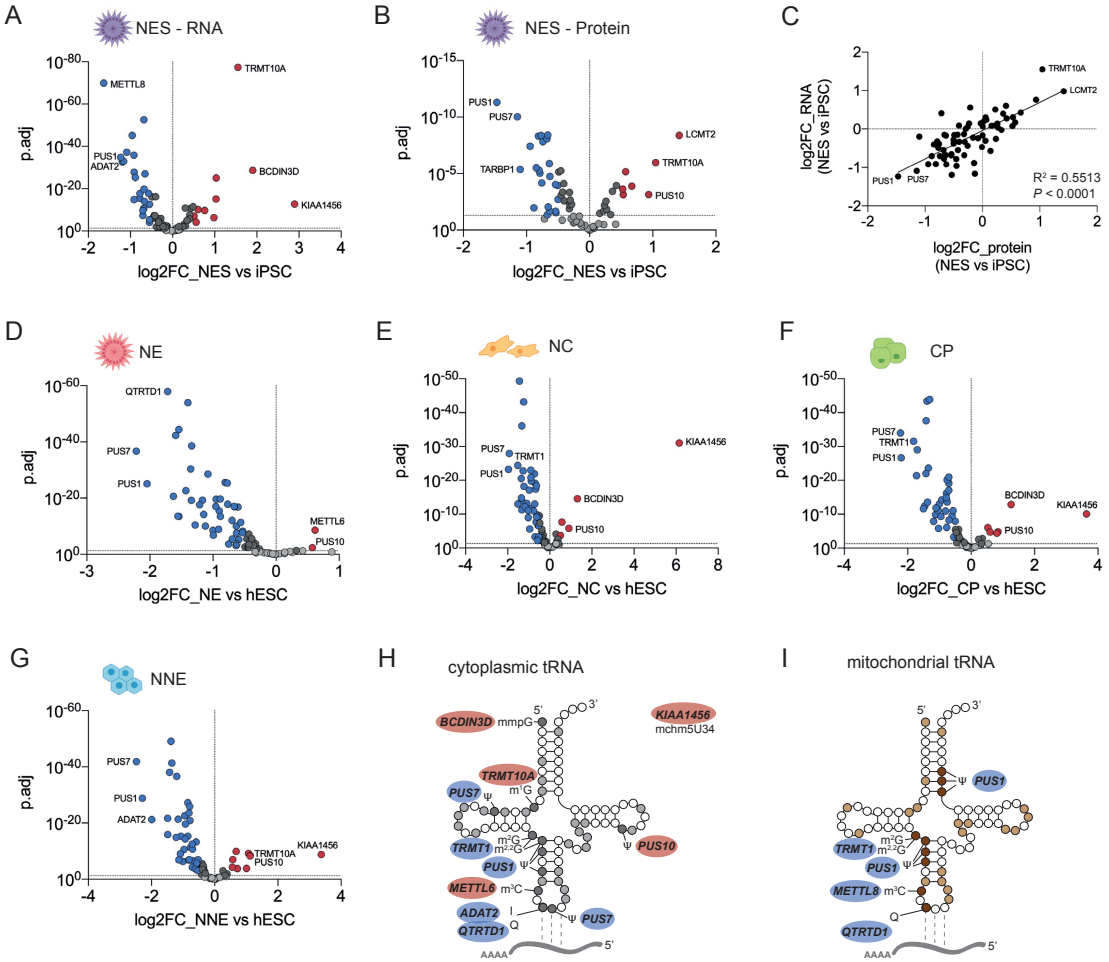

Figure 3.8: ***Early ectodermal cells downregulate tRNA modifiers.*** ***(A)*** *Log2 fold change of RNA expression of tRNA modifiers in neuroepithelial stem cells (NES) vs. induced pluripotent stem cells (iPSC).* ***(B)*** *Log2 fold change of protein expression of tRNA modifiers in NES cells vs. iPSCs.* ***(C)*** *Correlation of RNA expression vs. protein expression of tRNA modifiers in NES cells vs. iPSCs. Simple linear regression line.* ***(D)*** *Log2 fold change of RNA expression of tRNA modifiers in neuroectoderm cells (NE) vs. human embryonic stem cells (hESC).* ***(E)*** *Log2 fold change of RNA expression of tRNA modifiers in neural crest cells (NC) vs. hESCs.* ***(F)*** *Log2 fold change of RNA expression of tRNA modifiers in cranial placode cells (CP) vs. hESCs.* ***(G)*** *Log2 fold change of RNA expression of tRNA modifiers in non-neural ectoderm cells (NNE) vs. hESCs.* ***(A, B, D - G)*** *Dotted lines at p.adj 0.05 marks significance. Each data point represents the mean of 5-6 biological replicates. All not significant data points colored in light grey, all significant data points with -0.5 < log2FC > 0.5 colored in dark grey, all significant data points with log2FC < -0.5 colored in blue and all significant data points with log2FC > 0.5 colored in red.* ***(H + I)*** *Schematic representation of a human cytoplasmic tRNA and a mitochondrial tRNA with highlighted modifications and modifying enzymes. Enzymes highlighted in red were most upregulated in differentiated cells and enzymes highlighted in blue most downregulated. mmpG – 5'-monomethylmonophosphate guanosine; m1G – 1-methylguanosine; - pseudouridine; m2G – 2-methylguanosine; m2,2G – 2,2-dimethylguanosine; m3C – 3-methylcytosine; I – Inosine; Q – Queosine; mchm5U – 5-(carboxyhydroxymethyl)uridine methyl ester.*

Overall, in all cell types the modifying enzymes were mostly downregulated, especially in the hESC derived ectodermal cell types. This could be related to culture conditions and limited growth capacity of H1 derived cells. NES cells were always harvested before becoming confluent and their undisturbed possibility to cycle could allow a higher translation and therefore higher dependency and usage of tRNA modifications.

To out rule hits influenced by culture conditions, I checked which up- and downregulated tRNA modifiers were shared between all cell types. Only 2 enzymes were collectively upregulated: METTL6 and PUS10 (Figure 3.9A). Collectively downregulated were 33 enzymes (Figure 3.9B). While NES cells had a lot more individual upregulated modifiers, most of the modifiers that were downregulated during differentiation were shared between the different cell types. Human embryonic stem cells derived cells shared additional 8 downregulated modifiers. Interestingly, there were no neural cell type specific differentially expressed tRNA modifying enzymes. Nevertheless, expression in NE correlated with expression in NES (Figure 3.9C). Looking at the distribution of enzymes modifying only cytoplasmic tRNAs versus enzymes modifying both or only mitochondrial tRNAs it stands out that mt-tRNA modifiers were more consistently down regulated. This stronger downregulation compared to cytoplasmic tRNA only modifiers was significant (Figure 3.9D).

Taken together, I found that tRNA modifying enzymes were downregulated in early ectodermal cell types compared to pluripotent stem cells. This downregulation was most prominent in mitochondrial tRNA modifiers. The next chapters describe, how this might influence modifications, tRNAs and protein synthesis.

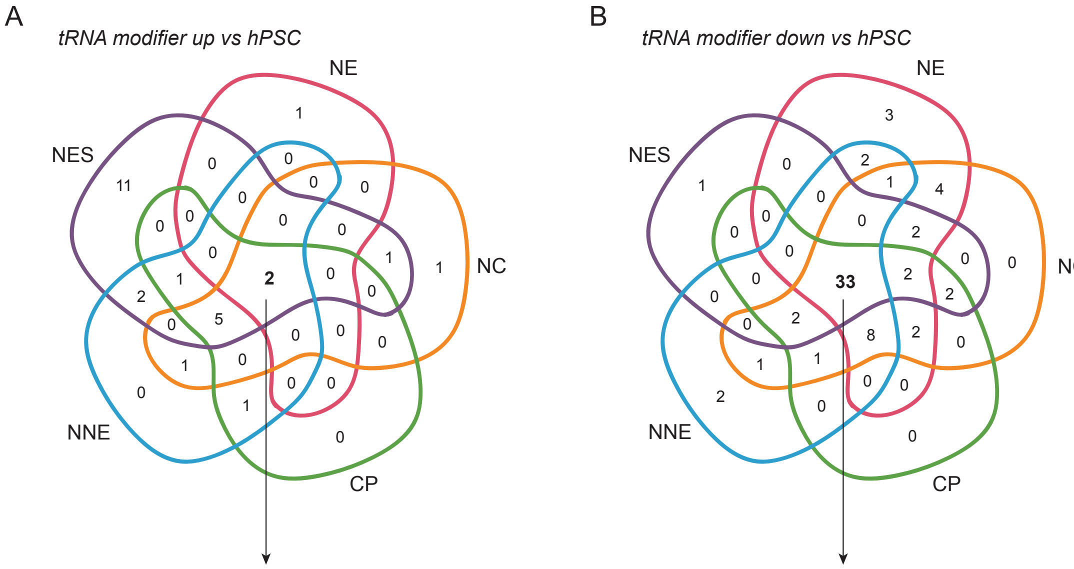

Cell types	total	tRNA modifying enzymes	
NES NE NC CP NNE	2	METTL6	PUS10

Cell types	total	tRNA modifying enzymes		
NES NE NC CP NNE	33	ADAT2	ALKBH1	CDK5RAP1
		CDKAL1	CTU2	DUS2
		FTSJ1	GTPBP3	IKBKAP
		LAGE3	METTL2A	METTL2B
		METTL8	MTO1	NAT10
		NSUN2	PUS1	PUS3
		PUS7	QTRTD1	THADA
		THUMPD1	THUMPD3	TRMT1
		TRMT10C	TRMT112	TRMT12
		TRMT5	TRMT61A	TRMT61B
		TRUB2	TYW1	WDR4

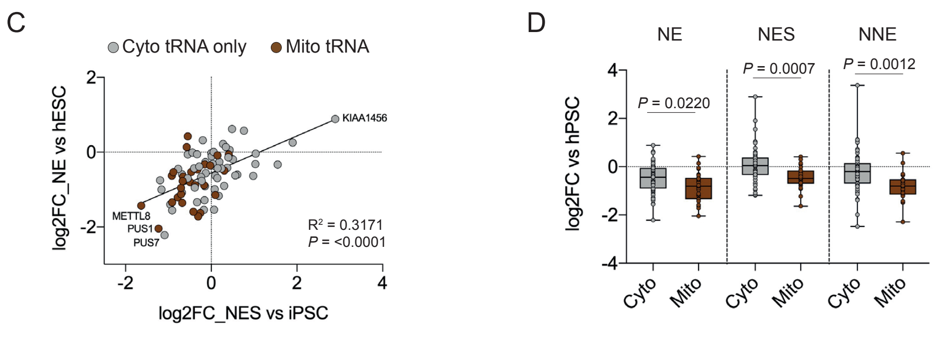

Figure 3.9: ***Early ectodermal lines commonly downregulate mitochondrial tRNA modifier.***
(A) *Shared significantly upregulated tRNA modifying enzymes.* ***(B)*** *Shared significantly downregulated tRNA modifying enzymes.* ***(C)*** *Correlation of log2 fold change RNA expression of tRNA modifier in NE vs. NES. Simple linear regression line. Enzymes modifying only cytoplasmic tRNAs colored in grey, enzymes modifying both or only mitochondrial tRNAs colored in brown.* ***(D)*** *Log2 fold change RNA expression of modifiers of only cytoplasmic tRNAs (grey) or modifiers of both/only mitochondrial tRNAs (brown) in NE, NES and NNE. P-value determined by unpaired t-test. Box plot shows minimum, first quartile, median, third quartile and maximum.*

3.3 tRNA modifications and tRNA anticodon pools are largely stable during early ectodermal differentiation

As previously mentioned, tRNA modifications regulate gene expression and are thought to be an instrument for cell state transitions (reviewed in Frye et al., 2018). However, there are almost no studies so far analyzing the landscapes and dynamics of tRNA modifications and tRNA pools during development, except a study in the amoeba *Dictyostelium discoideum* (Hoffmann et al., 2021), a study in Drosophila (White et al., 1973) and a recently published study in zebrafish (*Danio rerio*) (Rappol et al., 2024). The reason for this, besides earlier mentioned ethical limitations regarding human development, is probably related to the technical difficulties to detect tRNA modifications and to sequence tRNAs. Transfer RNAs are highly modified which interferes with reverse transcription into cDNA, a step that almost all sequencing methods rely on. Additionally, the huge variety of chemical modifications represents another challenge.

I used mass spectrometry to analyze modification levels on tRNAs. Mass spectrometry enables the quantification of many modifications in one sample and is a direct detection method. Other available methods depend on misincorporations or stops of the reverse transcriptase (Behrens et al., 2021, Rappol et al., 2024) and therefore detect modifications indirect. I used three biological replicates of each cell type and sent total RNA to Dr. Cathrine Broberg Vågbø in Norway, who isolated small RNAs via high-performance liquid chromatography and who performed the mass spectrometry analysis on 20 types of modifications. The same RNA was also used in RT-qPCR, RNA sequencing and tRNA sequencing.

Surprisingly, most measured modification levels seemed to not change upon differentiation (Figures 3.10A – 3.10E), although the majority of modifying enzymes was downregulated. Modification levels did not correlate with modifier enzyme expression (Figures 3.10F – 3.10J). Rappol et al. made the same observation in zebrafish development (Rappol et al., 2024). They also observed, that expression levels of tRNA modifying enzyme expression did not correlate with their observed modification levels throughout

development.

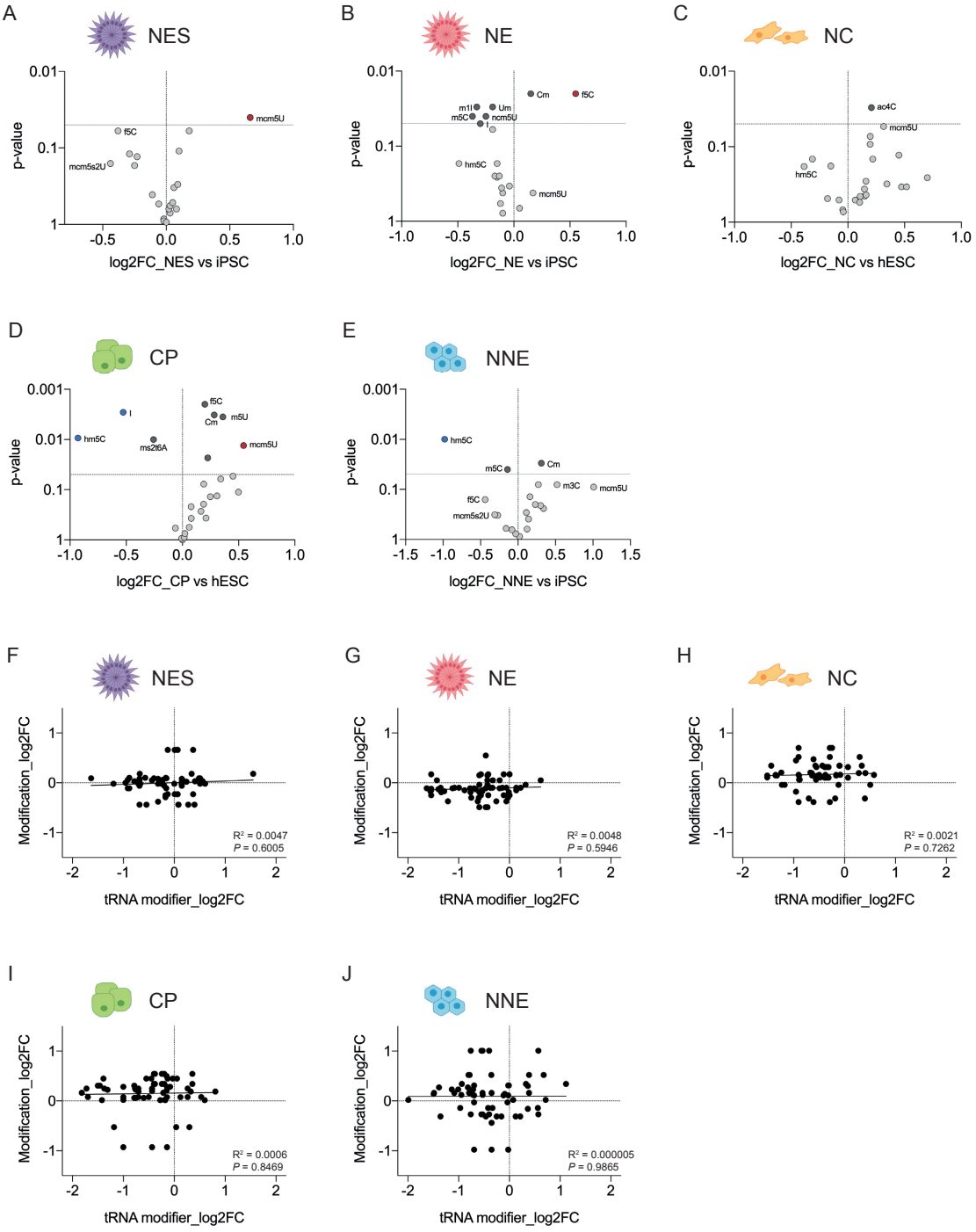

Figure 3.10: ***tRNA modifications stay mostly stable during early ectodermal differentiation.***
(A – E) *Log2 fold change of modification levels measured by mass spectrometry in differentiated cells vs. stem cells. P-value determined by unpaired t-test compared to stem cells. Each data point represents the mean of 3 biological replicates. All not significant data points colored in light grey, all significant data points with -0.5 < log2FC > 0.5 colored in dark grey, all significant data points with log2FC < -0.5 colored in blue and all significant data points with log2FC > 0.5 colored in red. (Caption continued on next page.)*

Figure 3.10: *(Previous page. Caption continued here.)* mcm^5U – *5-methoxycarbonylmethyluridine;* f^5C – *5-formylcytosine;* mcm^5s^2U – *5-methoxycarbonylmethyl-2-thiouridine;* m^1I – *1-methylinosine; Um – 2'-O-methyluridine;* ncm^5U – *5-carbamoylmethyluridine;* m^5C – *5-methylcytosine; I – inosine; Cm – 2'-O-methylcytosine;* ac^4C – *N4-acetylcytidine;* ms^2t^6A - *2-methylthio-N6-threonylcarbamoyladenosine;* m^5U – *5-methyluridine;* hm^5C – *5-hydroxymethylcytosine;* m^3C – *3-methylcytosine.* ***(F – J)*** *Correlation of modification levels with RNA expression of the matching modifying enzyme. Log2 fold changes compared to stem cells. Simple linear regression line.*

The disadvantage of using mass spectrometry to detect modifications is, that sequence information is lost. Since several modifications can be present at different positions in the tRNA and being produced by different enzymes, it could be that changes in modification levels are balanced out and result in visually no change here. Regarding the hESC derived samples (NE, NC, CP and NNE), it could be also due to 'older' modified tRNAs that still being around in the cell. The differentiation protocol is twelve days long and the effect of downregulation of modifying enzymes could be not visible yet, since tRNAs have a relatively long half-life of more than four days (Choe and Taylor, 1972). Additionally, modification levels also depend on the presence of the tRNA itself.

Therefore, I sequenced the tRNA anticodons pools in pluripotent stem cells and early ectodermal cells. Prof. Dr. Mark Helms group developed a protocol which overcomes artefacts from cDNA synthesis (Kristen et al., unpublished). The quantitative information of the tRNA pool is directly transferred onto DNA oligonucleotides which are then used for library preparation (Figure 3.11). Library preparation was assisted by Marc Lander and bioinformatic analysis was assisted by Dr. Sabrina Weser. First, total RNA of 4-6 biological replicates of all cell types were incubated with 44 complementary DNA molecules for cytoplasmic tRNAs and 22 complementary DNA molecules for mitochondrial tRNAs. The formed hybrids where then visualized on a gel, isolated and then used for library preparation.

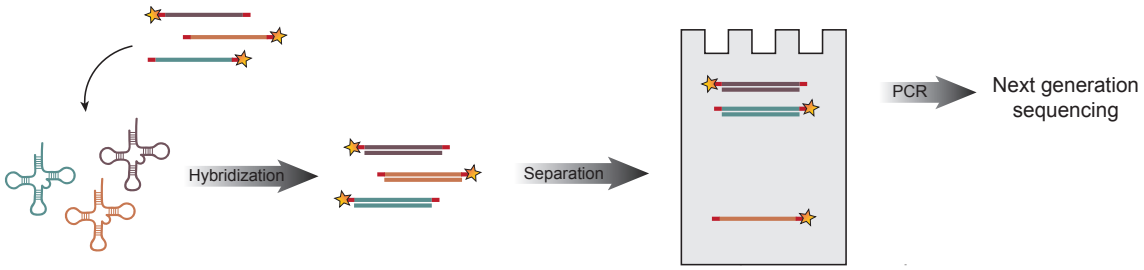

Figure 3.11: ***Overview of tRNA anticodon pool sequencing.***
Protocol was developed by Kristen et al. First, RNA is incubated with fluorescently labelled complementary DNA oligonucleotides that contain adapter sequences for final library preparation. The formed hybrids of tRNA and DNA oligonucleotides are then separated from unhybridized RNAs and oligonucleotides on a gel. The hybrid band can then be excised and used in an index PCR to generate a library for next-generation sequencing. Figure adapted from Kristen et al.

Looking at a principal component analysis based on all measured tRNAs, stem cells and differentiated cells clustered separately (Figures 3.12A and 3.12B), suggesting that tRNA anticodon pool changed. The overall composition of cytoplasmic tRNAs was mostly stable across cell types (Figure 3.12C). High abundant tRNAs as e.g. tRNA(Asn)GTT, tRNA(Ile)AAT_GAT and tRNA(Val)AAC_CAC_TAC stayed high abundant throughout differentiation. Same applied for low abundant tRNAs. The mitochondrial pool was dominated by the tRNA(Val)TAC (Figure 3.12D). It was by far the highest abundant mt-tRNA in all cell types. This tRNA substitutes the 5S rRNA in mitochondrial ribosomes. Interestingly, it was significantly downregulated in all differentiated cells (Figure 3.12E) which might influence mitochondrial protein synthesis. While most mitochondrial tRNAs seemed to be stably expressed from iPSCs to NES cells, more differences in abundance was observable in H1 differentiation. Overall, the proportion of cytoplasmic tRNA reads to mitochondrial tRNA reads changed significantly (Figure 3.12F).

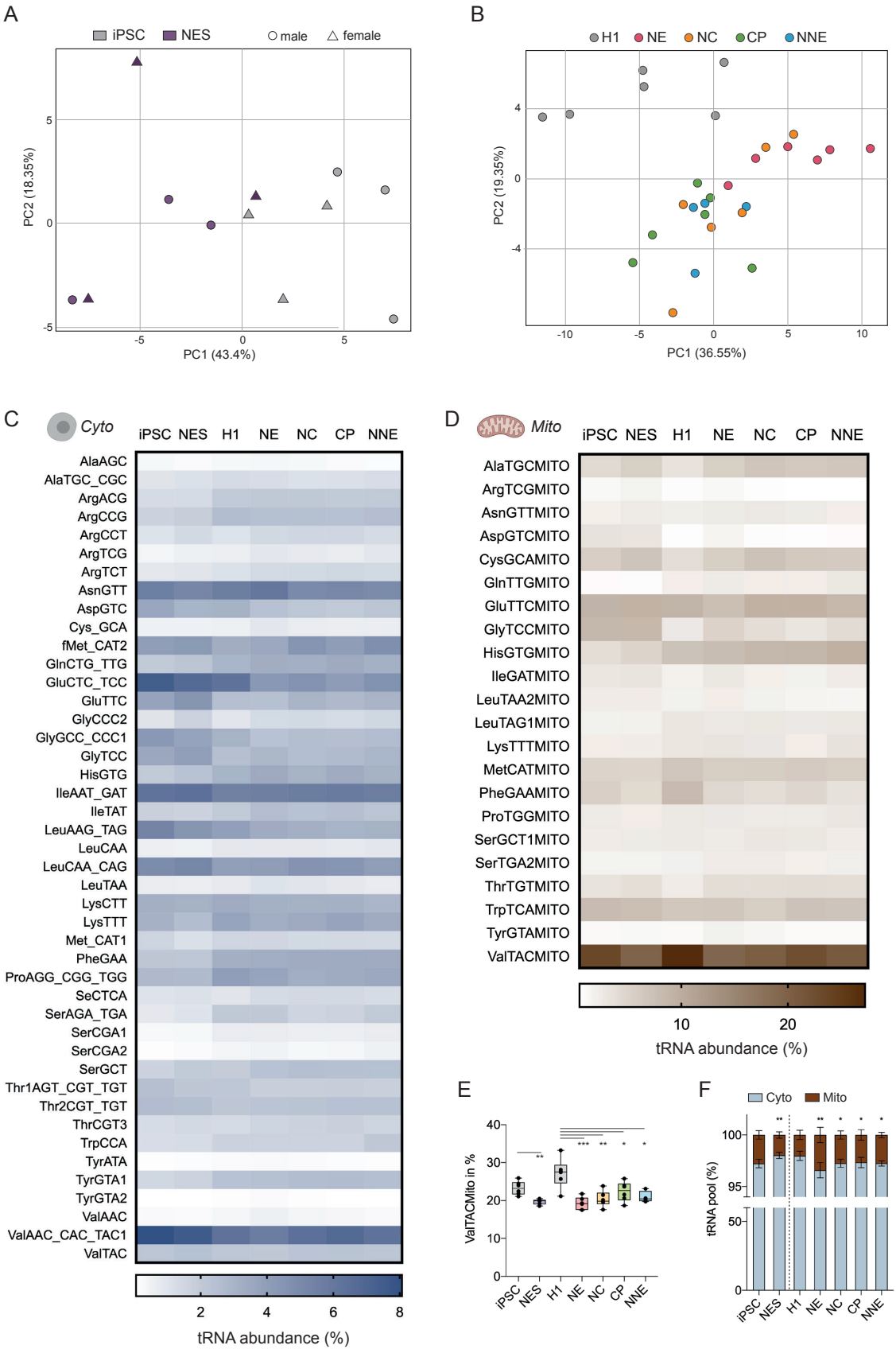

Figure 3.12: ***Landscape of tRNA anticodons in early ectodermal differentiation.*** ***(A)*** *Principal component analysis on counts per million of all 66 genes in iPSC and NES cells. Each data point represents one biological replicate. (Caption continued on next page.)*

Figure 3.12: *(Previous page. Caption continued here.)* ***(B)*** *Principal component analysis on counts per million of all 66 genes in hESC and differentiated cells. Each data point represents one biological replicate.* ***(C)*** *Composition of cytoplasmic tRNA anticodon pool in stem cells and differentiated cells. Heatmap displays abundance of tRNAs in % of cytoplasmic tRNA reads.* ***(D)*** *Composition of mitochondrial tRNA anticodon pool in stem cells and differentiated cells. Heatmap displays abundance of tRNAs in % of mitochondrial tRNA reads.* ***(C + D)*** *tRNAs labeled in three-letter amino acid code. Multiple anticodons listed when DNA oligos target multiple isoacceptors. Anticodons are numbered when different isodectoders are targeted.* ***(E)*** *Amount of mitochondrial tRNA(Val)TAC in % of mitochondrial tRNA reads. Significance determined by unpaired t-test compared to stem cells.* ***(F)*** *tRNA pool composition of cytoplasmic and mitochondrial tRNAs. Significance determined by unpaired t-test compared to stem cells.*

In the hindbrain neuroepithelial stem cells mitochondrial tRNAs were clearly downregulated (Figure 3.13A), reflecting the reduction in mitochondrial tRNA fraction.

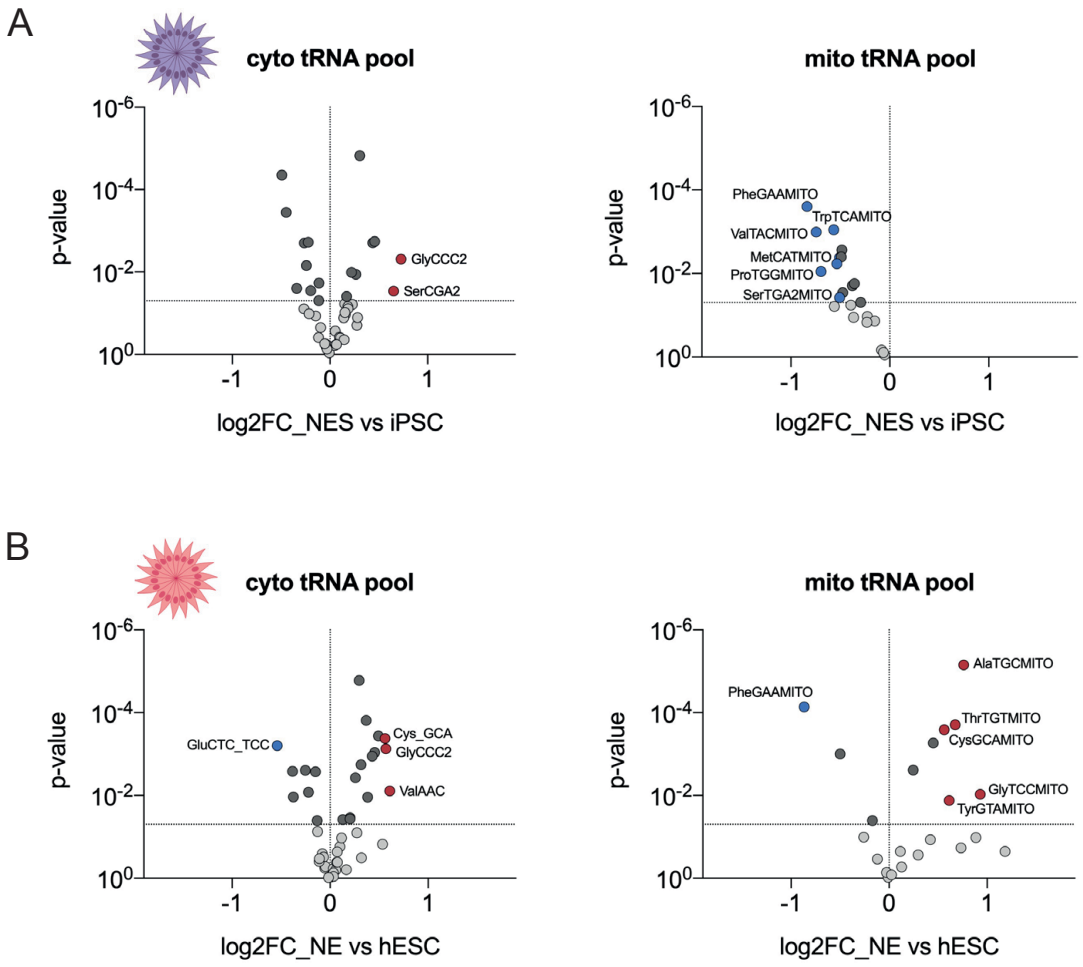

Figure 3.13: ***Differential expression of tRNAs during early ectodermal differentiation.***
(Figure and caption continued on next page.)

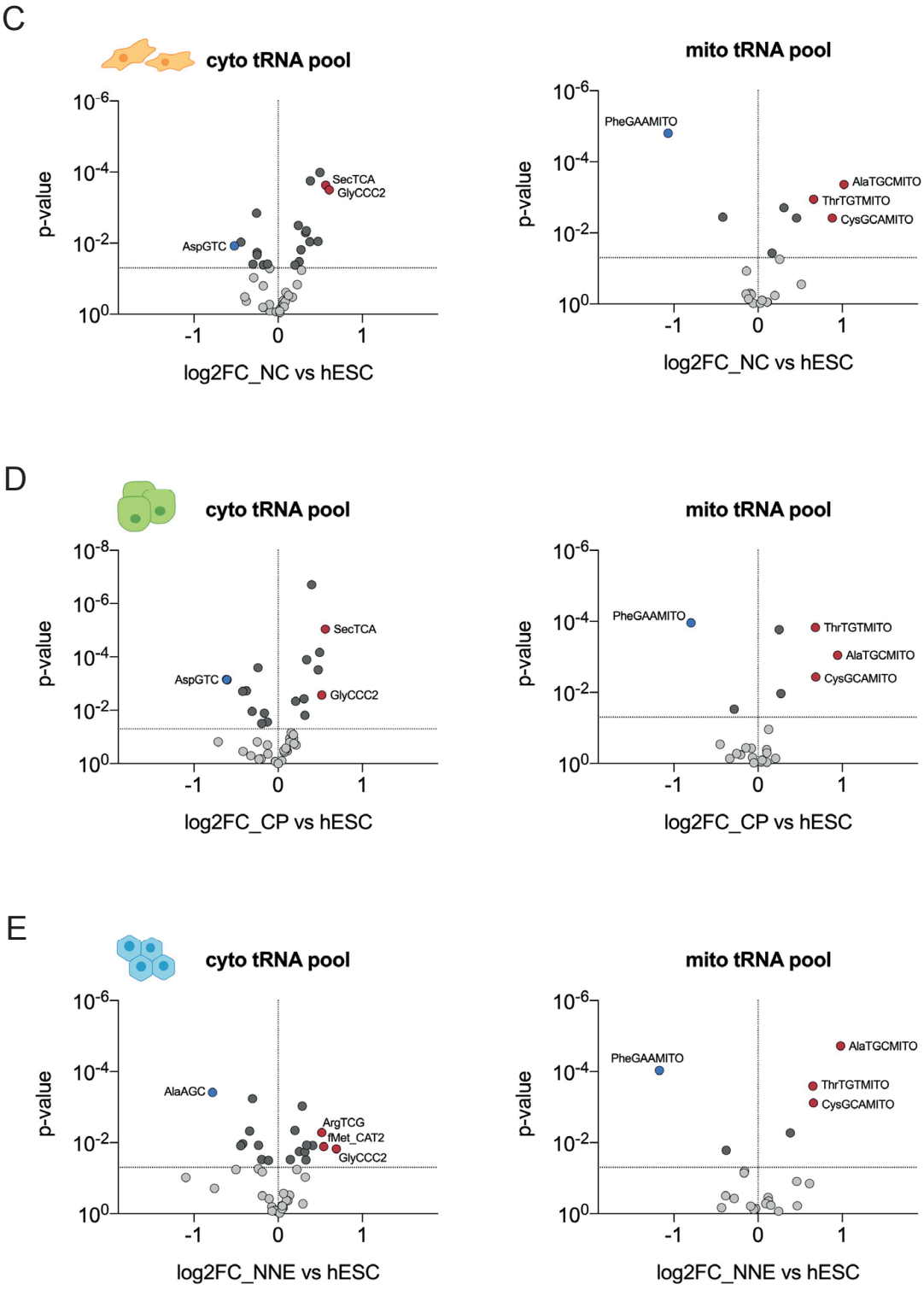

Figure 3.13: *(Figure and caption continued here from previous page.)* ***(A – E)*** *Log2 fold change of abundance (%) of cytoplasmic and mitochondrial tRNAs in differentiated cells vs. stem cells. Each data point represents mean of 4-6 biological replicates. Significance determined by unpaired t-test. Dotted line at 0.05 marks significance. All not significant data points colored in light grey, all significant data points with -0.5 < log2FC > 0.5 colored in dark grey, all significant data points with log2FC < -0.5 colored in blue and all significant data points with log2FC > 0.5 colored in red.*

In the other cell types, an upregulation of mitochondrial tRNAs was observed (Figures 3.13B – 3.13E). However, mito-tRNA(Phe)GAA was commonly downregulated. Only a few cytoplasmic tRNAs were differentially expressed, with tRNA(Gly)CCC significantly upregulated in all.

I wondered where the difference in mitochondrial tRNA expression between NES and the other differentiated cells came from, when they commonly downregulate genes associated to mitochondrial gene expression and RNA processing (Figure 3.5B). Looking at the RNA expression of mitochondrial protein coding genes, they were downregulated in all ectodermal lines (Figure 3.14A). The mitochondrial tRNA genes were on the other hand slightly up or downregulated in the RNA sequencing data. As previously mentioned, RNA sequencing is not ideal to measure tRNA expression. However, since in mitochondria the whole DNA is transcribed into one transcript, carrying both protein coding and non-coding RNAs, gene expression of proteins and tRNAs should be roughly the same. And the whole mitochondrial gene expression machinery was downregulated in all ectodermal cell types (Figures 3.14B – 3.14E). The same was observed on protein level of genes in the MitoCarta3.0 category 'Central dogma', including genes associated with mtDNA maintenance, mtRNA metabolism and mitochondrial translation (Figure 3.14F).

Taken together, NES cells and the H1 derived ectodermal cell types looked the same regarding mitochondrial gene expression when compared to pluripotent stem cells. Therefore, also mitochondrial tRNA expression levels should be roughly similar when compared to pluripotent stem cells. However, genes for biogenesis of cytoplasmic tRNAs were downregulated only in H1 derived cells (Figure 3.14G). A reduction in cytoplasmic tRNAs could have indirectly led to the observed increase of the mitochondrial tRNA fraction.

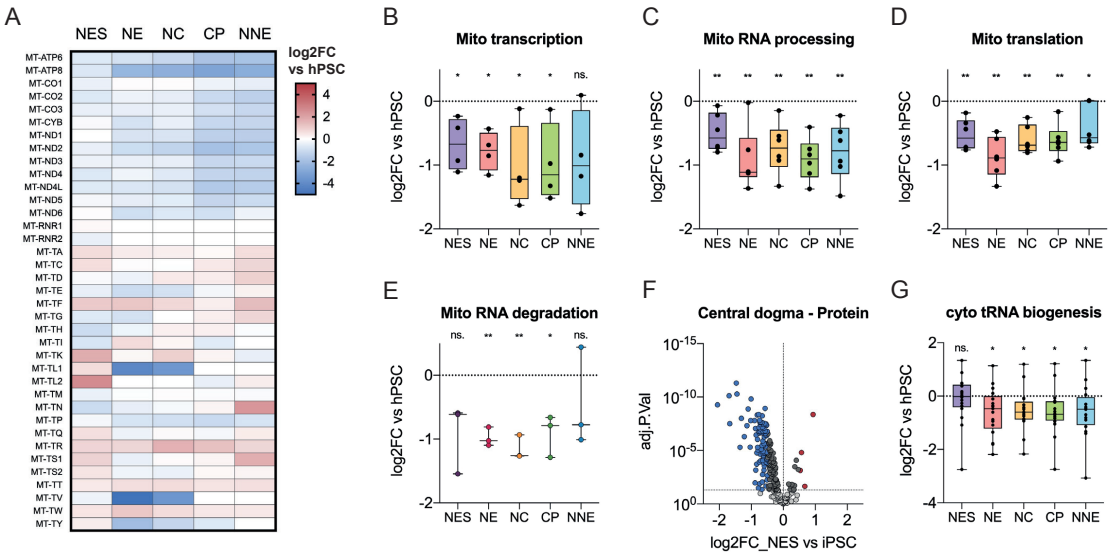

Figure 3.14: ***Genes related to mitochondrial gene expression are downregulated in early ectodermal cells.***
(A) *Heatmap displaying log2 fold change of mitochondrial encoded genes in differentiated cells vs. stem cells.* ***(B)*** *Log2 fold change of mito transcription genes. Analyzed genes: TFAM, POLRMT, TFB2M, TEFM.* ***(C)*** *Log2 fold change of mito RNA processing genes. Analyzed genes: TRMT10C, HSD17B10, KIAA0391, ELAC2, GRSF1, RPUSD4.* ***(D)*** *Log2 fold change of mito translation genes. Analyzed genes: TACO1, TUFM, GFM2, GFM1, MTIF3, MTIF2.* ***(E)*** *Log2 fold change of mito RNA degradation genes. Analyzed genes: PNPT1, SUPV3L1, REXO2.* ***(F)*** *Differential expression of mito central dogma proteins in log2 fold change of NES vs. iPS cells. Each data point represents the mean of six biological replicates. All not significant data points colored in light grey, all significant data points with -0.5 < log2FC > 0.5 colored in dark grey, all significant data points with log2FC < -0.5 colored in blue and all significant data points with log2FC > 0.5 colored in red.* ***(G)*** *Log2 fold change of cyto tRNA biogenesis genes. Analyzed genes: POLR3A, BRF1, GTF3C1, RPP14, RPP21, RPP25, POP4, RPP30, RPP38, RPP40, POP1, POP5, TSEN54, TSEN2, TSEN34, TSEN15, RTCB.*

In summary, the modification landscape stayed mostly stable upon differentiation. Cytoplasmic transfer RNA anticodon pools stayed mostly stable as well with a few minor changes in abundance. However, mitochondrial tRNAs were downregulated in NES cells.

3.4 Mitochondrial tRNA modifications shape both mitochondrial and cytoplasmic translation

In the previous chapters, I analyzed the expression of tRNA modifying enzymes, tRNA modifications and tRNA anticodon pool in stem cells and early ectodermal cells. I found that especially tRNA modifying enzymes were downregulated during differentiation. In this chapter I am analysing the consequences of this downregulation for protein synthesis.

I started by performing a knockdown screen of 47 different modifiers and analyzed how this affected protein synthesis. Although several tRNA modifying enzymes and their involvement in gene expression have been studied in certain contexts, for most modifiers their importance for global translation has not been studied yet. To knockdown the tRNA modifying enzymes I used so called siPOOLs, which consist of 30 siRNAs against the gene of interest and allow for an efficient knockdown. For the screen I used a highly proliferative and easy to transfect cancer cell line (FaDu). After 72 hours of knockdown, I measured protein synthesis via incorporation of OP-puromycin and flow cytometry and compared it to a scrambled negative control siPOOL (Figure 3.15A).

I observed a significant reduction in global protein synthesis for 26 out of the 47 analyzed tRNA modifying enzymes (Figure 3.15B). The strongest downregulation was measured in ALKBH1, NSUN2 and TRIT1 knockdown. Interestingly, an upregulation of protein synthesis was observed for METTL1. The knockdown efficiency was measured via RT-qPCR (Suppl. Figure 5.2) and did not affect results of OP-puromycin (Figure 3.15C). Additionally, efficient reduction of protein levels in 72 hours was controlled by Western Blot for four modifiers (Suppl. Figure 5.3). Reduction in protein synthesis was also not due to dying cells. Cell state was controlled by Annexin/PI staining in knockdown cells with highest reduction in translation (Figures 3.15D and 3.15E).

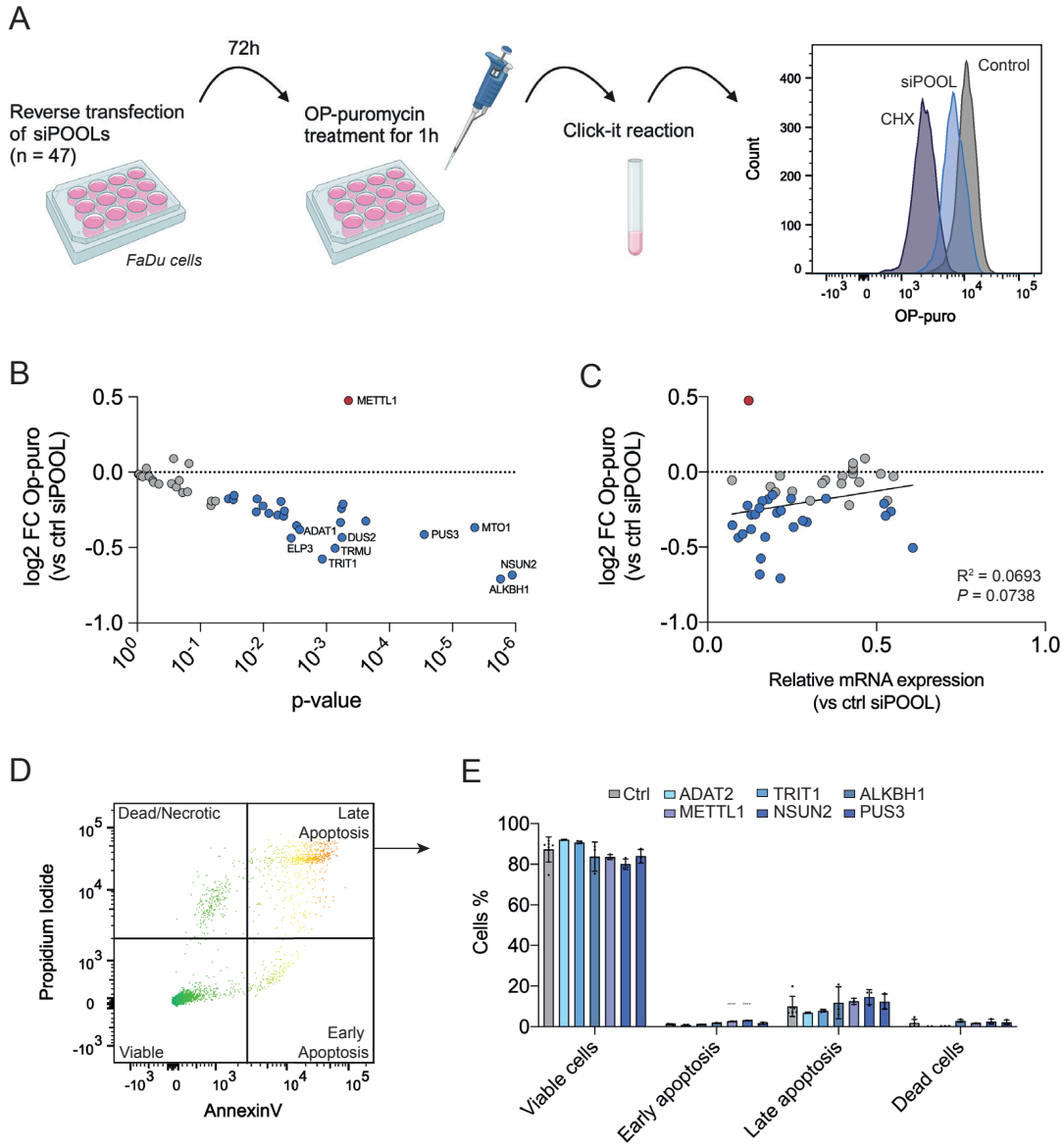

Figure 3.15: ***Knockdown screen of 47 tRNA modifier to assess their importance for translation.***
(A) *Experimental outline of knockdown screen. Figure was generated with Biorender.* ***(B)*** *Log2 fold change of OP-puromycin signal compared to scrambled negative control siPOOL. Each data point represents mean of 5 replicates. Non-significant points colored in light grey, significantly downregulated points in blue, significantly upregulated data points in red. P-value determined by unpaired t-test.* ***(C)*** *Log2 fold change of OP-puromycin signal vs relative mRNA expression, both compared to scrambled negative control siPOOL. Each data point represents mean of 5 replicates. Simple linear regression line. Non-significant points colored in light grey, significantly downregulated points in blue, significantly upregulated data points in red (based on OP-puro).* ***(D)*** *Gating strategy of apoptosis assay.* ***(E)*** *Percentage of cells in each category: viable, early apoptosis, late apoptosis and dead. Significance determined by unpaired t-test compared to scrambled negative control.*

These knockdown experiments were repeated with 29 siPOOLs in a different cancer cell line (Cal33) by Marc Krontal under my supervision (Figure 3.16A). Results in Cal33

cells correlated with the results obtained in FaDu cells. In both cell lines, knockdown of ALKBH1 and NSUN2 resulted in the strongest reduction of protein synthesis, while knockdown of METTL1 led to an increase (Figure 3.16B).

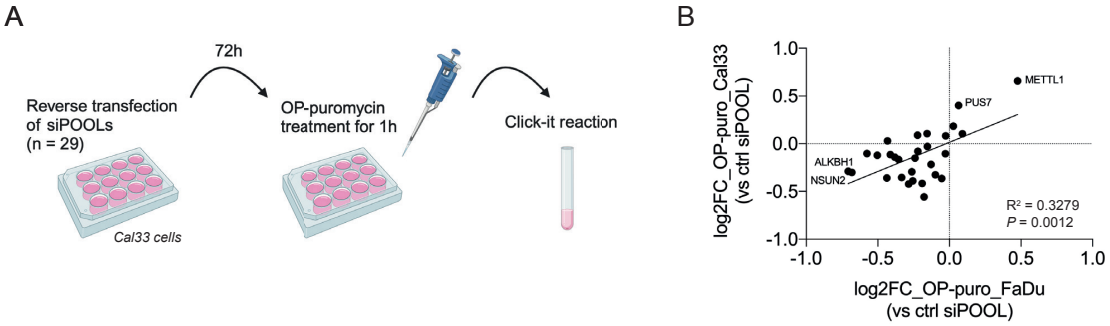

Figure 3.16: ***Knockdown screen of tRNA modifiers in Cal33 cells correlates with results in FaDu cells.***
(A) *Experimental outline of knockdown screen of 29 tRNA modifier in Cal33 cells. Experiments were performed by Mark Krontal under my supervision.* ***(B)*** *Correlation of log2 fold change of OP-puromycin signal vs. scrambled negative control siPOOL in FaDu and in Cal33 cells. Linear regression line.*

The general consent is, that modifications in the anticodon loop play an important role in translation, while modifications in the body of the tRNA stabilize its structure. I analyzed if this holds true by looking at relative translation rate compared to position of the modification in the tRNA (Figure 3.17). Enzymes modifying only cytoplasmic tRNAs and enzymes modifying either only mitochondrial tRNAs or both types, were separated. Indeed, depletion of almost all modifications in the wobble position led to a significant decrease of global protein synthesis (Figure 3.17A).

FTSJ1, for which no reduction in translation was observed, is a 2'-O-methyltransferase and modifies 11 tRNAs (Nagayoshi et al., 2021). Previously it has been shown, that depletion of FTSJ1 affects decoding of phenylalanine codons and leads to reduction of gene specific translation (Nagayoshi et al., 2021). Therefore, it is likely that the effect cannot be seen in the here measured global translation rate or that FaDu cells do not express FTSJ1 dependent transcripts.

Depletion of ALKBH1 had, together with NSUN2, the strongest effect on translation. ALKBH1 produces f^5C in the wobble position of mitochondrial tRNAs, but also demethylates m^1A in the T loop (F. Liu et al., 2016). The f^5C modification depends on a previous m^5C modification by NSUN3. Knockdown of NSUN3 did not significantly reduce

translation rate (Figure 3.17A). Since this modification is only found in mitochondrial tRNAs, global translation was not affected in this experimental setup. Regarding the other function of ALKBH1, the m^1A demethylation activity, a depletion was previously linked to an increase in translation initiation and elongation (F. Liu et al., 2016). Whether the here observed effect is then due to its f^5C modification, if ALKBH1 has another yet uncovered function or if it depends on a certain cell stage remains unknown.

NSUN2 is a methyltransferase and produces m^5C at the wobble position on one cytoplasmic tRNA and in the variable loop of both cytoplasmic and mitochondrial tRNAs (Figures 3.17A and 3.17B) (Brzezicha et al., 2006, Blanco et al., 2011). The modification in the variable loop protects the tRNA from enzymatic cleavage and a depletion of the modification leads to the biogenesis of tRNA derived fragments which inhibit protein synthesis (Tuorto et al., 2012, Blanco et al., 2014). Therefore, the strong reduction in translation rates coincides with previously published literature.

Another enzyme modifying in the variable loop is METTL1, producing m^7G together with WDR4 in a complex. Interestingly, knockdown of METTL1 led to an increase of translation (Figure 3.17B). Knockdown of WDR4 on the other hand did not change translation rate. A previous study in mouse embryonic stem cells showed, that lack of this m^7G modification led to a translation defect (Lin et al., 2018). If METTL1 has another function related to translation needs to be further investigated.

Interestingly, I found modifying enzymes significantly affecting translation in all positions of the tRNA, not only in the anticodon loop (Figures 3.17C – 3.17G), but also modifying enzymes in all positions that did not affect translation.

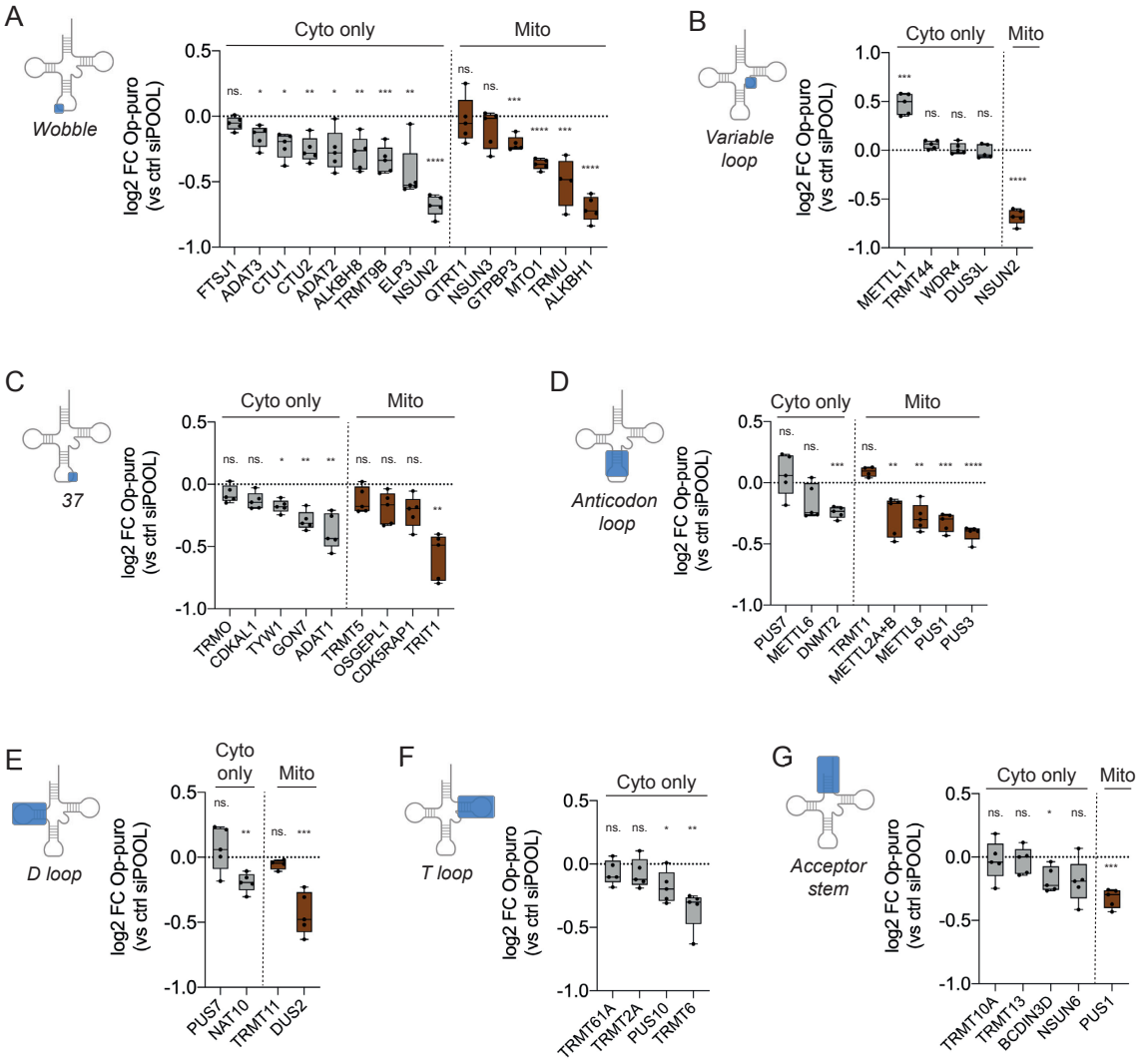

Figure 3.17: ***Effect on translation assessed based on the modification position in the tRNA.***
Log2 fold change of OP-puromycin signal compared to a scrambled negative control siPOOL of modifications in ***(A)*** *wobble position,* ***(B)*** *variable loop,* ***(C)*** *position 37,* ***(D)*** *anticodon loop,* ***(E)*** *D loop,* ***(F)*** *T loop and* ***(G)*** *acceptor stem. Enzymes modifying only cytoplasmic tRNAs at this position colored in grey, enzymes modifying mitochondrial or both tRNAs at this position colored in brown. Significance determined by unpaired t-test compared to scrambled control siPOOL.*

Looking at overall translation rates of enzymes modifying only cytoplasmic tRNAs and enzymes modifying mitochondrial tRNAs, it stands out, that knockdown of mitochondrial tRNA modifiers had a stronger effect on translation (Figure 3.18A). The difference between only cytoplasmic tRNA modifier and mitochondrial tRNA modifier was significant (Figure 3.18B). Therefore, mitochondrial tRNA modifiers and modifications shape both cytoplasmic and mitochondrial translation.

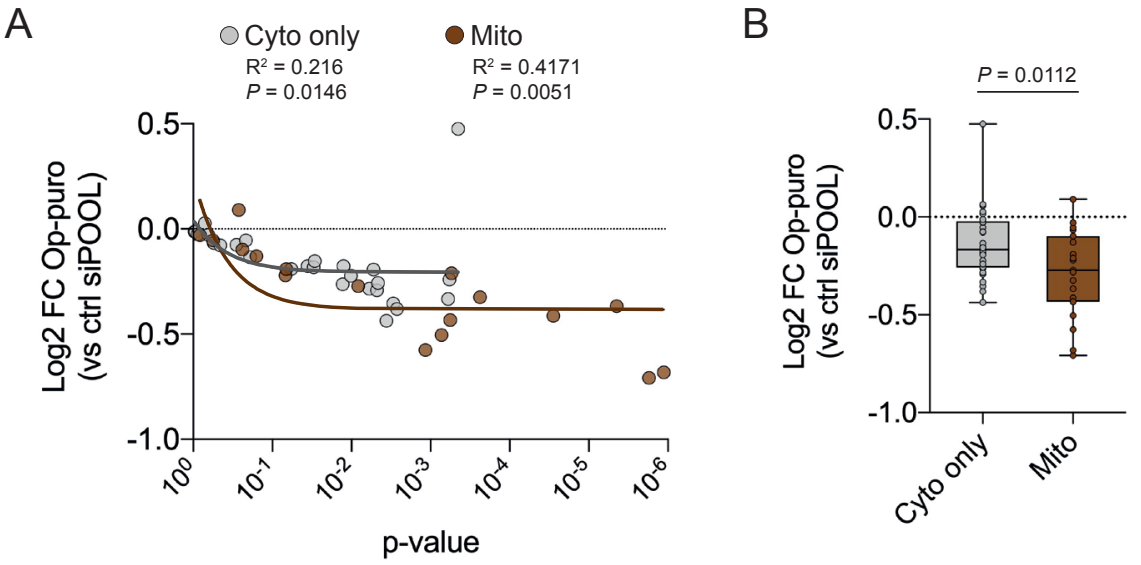

Figure 3.18: ***Knockdown of mitochondrial tRNA modifier affects translation more than cytoplasmic tRNA modifier.***
(A) *Log2 fold change of OP-puromycin signal vs. p-value compared to scrambled negative control siPOOL. Each data point represents mean of 5 replicates. Enzymes modifying only cytoplasmic tRNAs are colored in grey, enzymes modifying mitochondrial or both tRNAs are colored in brown. P-value determined by unpaired t-test. Simple regression lines for both.* ***(B)*** *Log2 fold change of OP-puromycin signal compared to scrambled negative control siPOOL for enzymes modifying only cytoplasmic tRNAs (grey) or mitochondrial or both tRNAs (brown). Significance determined by unpaired t-test compared to cyto only.*

With the data obtained from the screen, I know that downregulation of many tRNA modifying enzymes leads to a reduction in translation. Therefore, I measured global translation as well as mitochondrial translation in NES cells and embryonic stem cells. I used OP-puromycin incorporation and measured global translation rate in whole cells (Figures 3.19A and 3.19B) and mitochondrial translation rate in isolated mitochondria (Figures 3.19C – 3.19E).

Global translation rate was strongly reduced in NES cells compared to stem cells (Figure 3.19B). Looking at mitochondrial translation, I found that the number of mitochondria with a high translation rate was reduced compared to H1 (Figure 3.19D). Translation rate was also slightly reduced, but not significantly (Figure 3.19E).

Additionally, I looked at expression of translation initiation and elongation factors in cytoplasmic and mitochondrial translation (Figures 3.19F and 3.19G). They were also downregulated in ectodermal cells and confirmed the observed reduced protein synthesis, together with the previously found reduction in mito-tRNA(Val) (Figure 3.12E).

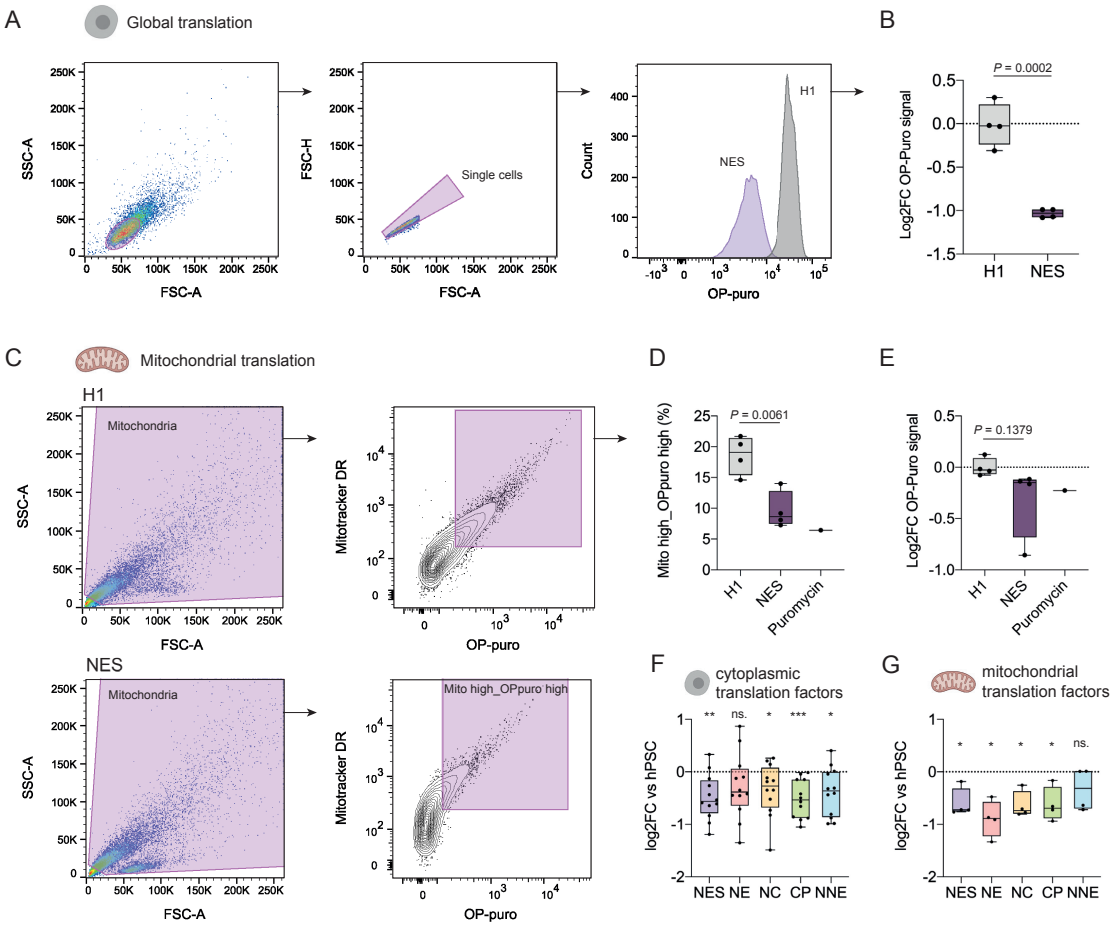

Figure 3.19: ***Protein synthesis is reduced in early ectodermal cells.*** *(**A**) Gating strategy for measuring global translation rate via OP-puromycin incorporation by flow cytometry. (**B**) Log2 fold change of OP-puromycin signal compared to H1. Significance determined by unpaired t-test compared to H1. (**C**) Gating strategy for measuring mitochondrial translation rate in isolated mitochondria via OP-puromycin incorporation by flow cytometry. Mitochondria stained with Mitotracker DR. (**D**) Percentage of Mitotrack DR high and OP-puromycin high mitochondria. Puromycin as control. Significance determined by unpaired t-test. (**E**) Log2 fold change of OP-puromycin signal compared to H1. Significance determined by unpaired t-test compared to H1. (**F**) Log2 fold change of RNA expression of cytoplasmic translation initiation and elongation factors in ectodermal cells compared to stem cells. Significance determined by paired t-test compared to stem cells. (**G**) Log2 fold change of RNA expression of mitochondrial translation initiation and elongation factors in ectodermal cells compared to stem cells. Significance determined by paired t-test compared to stem cells.*

Overall, I showed which tRNA modifiers are important for global translation and I showed, that the downregulation of tRNA modifiers in early ectodermal cells compared to stem cells resulted in lower translation rate.

3.5 Mitochondrial dynamics and activity during early ectodermal differentiation

In the previous chapters, I found several indications that regulation of mitochondrial gene expression is a strong characteristics of early ectodermal cell types. I found that during early ectodermal differentiation especially mitochondrial tRNA modifying enzymes were downregulated, the mitochondrial tRNA(Val) which is part of the mitochondrial ribosome was downregulated, mitochondrial tRNA anticodon pool fractions were changing and both, cytoplasmic and mitochondrial, protein synthesis pathways were downregulated. How did the differential regulation of mitochondrial gene expression affected mitochondrial function?

Previously it was shown, that the main energy resource in stem cells is glycolysis (Gu et al., 2016) and in differentiated cells OXPHOS. Here, I am looking at very early differentiated cells which are still multipotent stem cells. So far, Khacho et al. analyzed neural stem cells in mouse, which are equivalent to NE and NES, and found that they have elongated mitochondria but are not using OXPHOS for energy production (Khacho et al., 2016). I aim to identify mitochondrial dynamics and activity in all major human early ectodermal cell types.

I started by looking at mitochondrial morphology by staining mitochondria with Mitotracker in induced pluripotent stem cells and neuroepithelial stem cells. I observed fragmented mitochondria in iPSCs (Figure 3.20A), which was also seen in previous studies (J. Zhang et al., 2011). They had a median mitochondrial length of 1 µm (Figure 3.20B). In NES cells, the mitochondria appeared elongated (Figure 3.20A), which is usually associated with more metabolically active mitochondria (Yao et al., 2019). Their median length was with 2.25 µm more than double the length of mitochondria in iPSCs (Figure 3.20B). Overall, the pluripotent stem cells had a significantly larger percentage of small mitochondria ($< 0.5 - 1$ µm) while NES cells had a significantly larger percentage of long mitochondria (> 2 µm) (Figure 3.20C). Besides longer mitochondria, I observed less mitochondria in NES cells compared to stem cells by measuring Mitotracker DR staining via flow cytometry (Figure 3.20D).

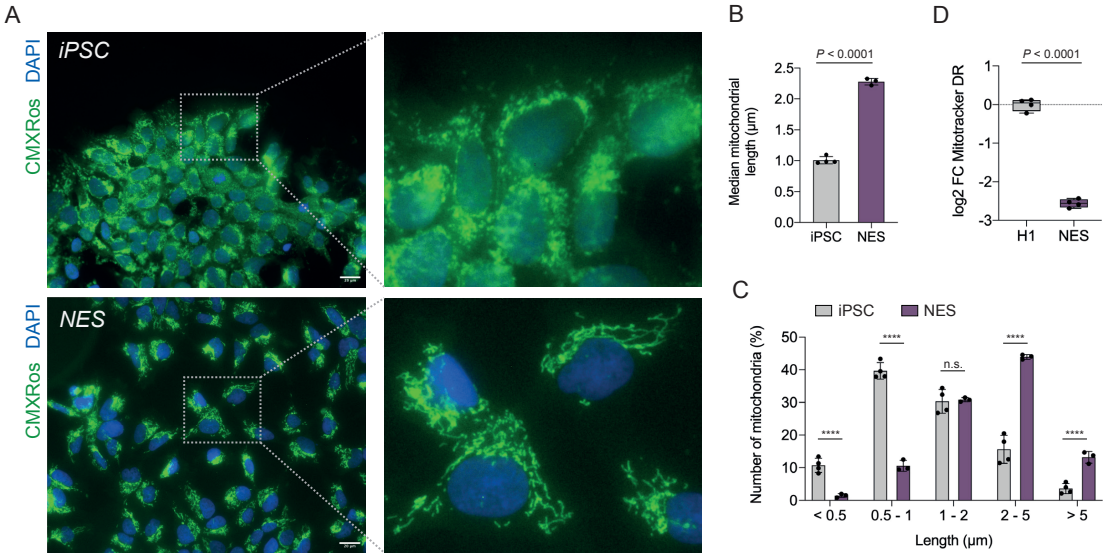

Figure 3.20: ***Mitochondrial network grows during early neural differentiation.*** ***(A)*** *Representative images of induced pluripotent stem cells (iPSCs) and neuro-epithelial stem cells (NES) stained with Mitotracker CMXRos and DAPI. Scale bar: 20 µm.* ***(B)*** *Median mitochondria length (µm) in iPSCs and NES cells. Significance determined by unpaired t-test compared to iPSCs.* ***(C)*** *Comparison of mitochondrial length distribution in iPSCs and NES cells. Each dot represents one cell line; per cell line 3 to 5 images with each 50 to 250 mitochondria were measured. Significance determined by unpaired t-test compared to iPSC.* ***(D)*** *Log2 fold change of Mitotracker DR signal. Mitotracker DR stains mitochondria independent of activity. Significance determined by unpaired t-test compared to H1.*

To analyze how mitochondrial function is affected during differentiation, I looked at the expression of genes encoding the mitochondrial proteome, cataloged in the MitoCarta3.0 dataset (Rath et al., 2021). The genes are categorized into the following 'MitoPathways': 'Small molecule transport', 'Signaling', 'Central dogma', 'Protein import, sorting and homeostasis', 'Metabolism', 'OXPHOS' and 'Dynamics and surveillance' (Figures 3.21A and 3.21B).

Genes in 'Central dogma', which contains genes related to mtDNA maintenance, mtRNA metabolism and translation, were, as shown in Chapter 3.3, significantly downregulated in all ectodermal cell types (Suppl. Figure 5.4A). 'Protein import, sorting and homeostasis' was also significantly downregulated in all cell types compared to stem cells (Suppl. Figure 5.4B). Genes in 'Metabolism', which comprises all metabolic pathways taking place in mitochondria, were also slightly downregulated in all differentiated cells (Suppl. Figure 5.4C). Expression of genes in categories 'Small molecule transport', 'Signaling' and 'Dynamics and surveillance' was mostly unchanged (Suppl. Figures 5.4D – 5.4F).

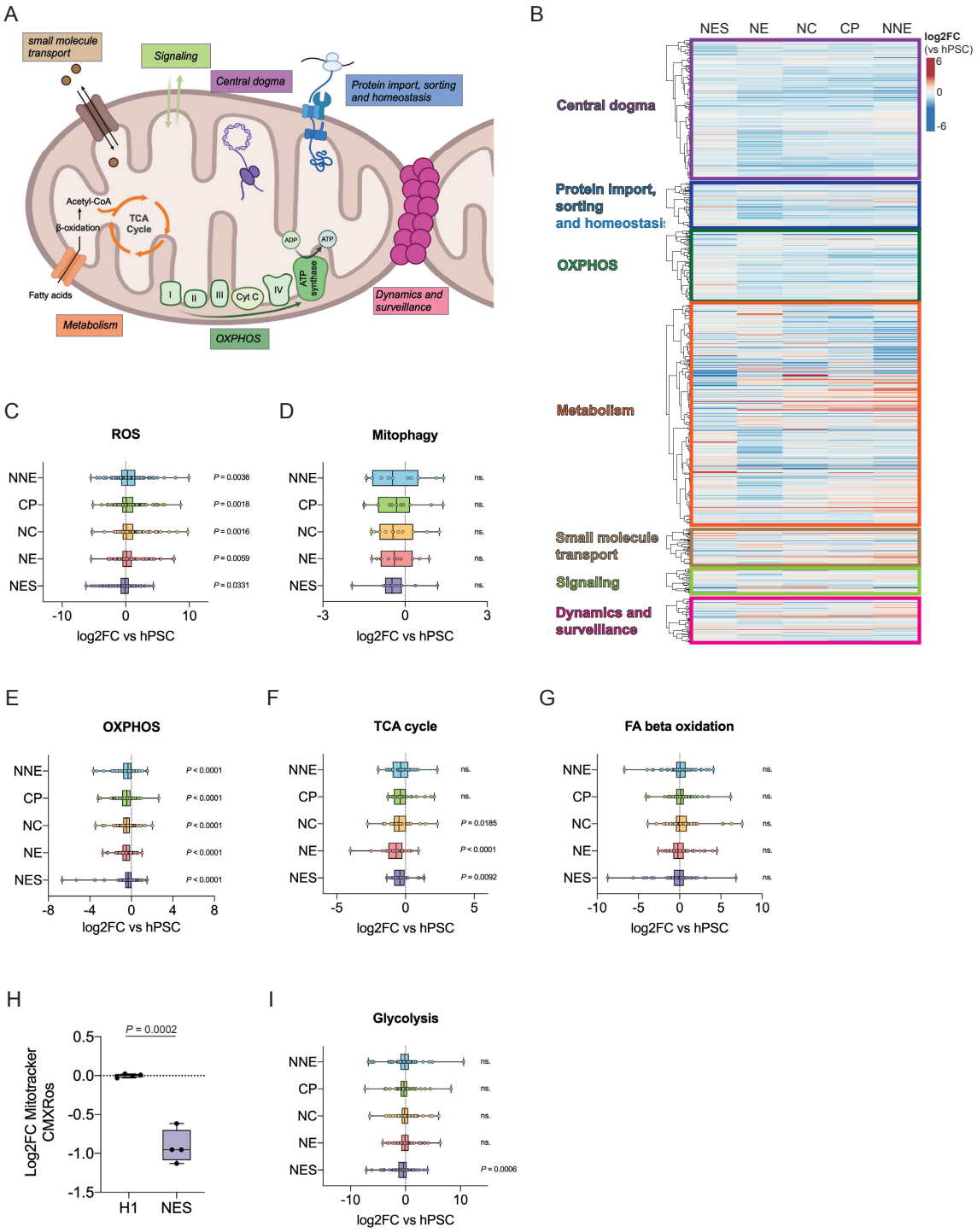

Figure 3.21: ***Mitochondrial activity is downregulated during early ectodermal differentiation.***
(A) *Overview of 'MitoPathways' defined in the MitoCarta3.0 dataset. Figure generated with Biorender.* ***(B)*** *Heatmap depicting log2 fold change of gene expression in differentiated cells vs. stem cells of 'MitoPathways'.* ***(C)*** *Log2 fold change of genes involved in ROS pathways in differentiated cells vs. stem cells. Gene set from GSEA. Significance determined by paired t-test compared to hPSC.* ***(D)*** *Log2 fold change of genes involved in mitophagy in differentiated cells vs. stem cells. Gene set from MitoCarta3.0 dataset. Significance determined by paired t-test compared to hPSC. (Caption continued next page.)*

Figure 3.21: *(Previous page. Caption continued here.)* ***(E)*** *Log2 fold change of genes involved in OXPHOS in differentiated cells vs. stem cells. Gene set from MitoCarta3.0 dataset. Significance determined by paired t-test compared to hPSC.* ***(F)*** *Log2 fold change of genes involved in TCA cycle in differentiated cells vs. stem cells. Gene set from GSEA. Significance determined by paired t-test compared to hPSC.* ***(G)*** *Log2 fold change of genes involved in fatty acid beta oxidation in differentiated cells vs. stem cells. Gene set from GSEA. Significance determined by paired t-test compared to hPSC.* ***(H)*** *Log2 fold change of Mitotracker CMXRos staining in NES cells vs. H1 cells measured by flow cytometry. Each data point represents one biological replicate. Significance determined by unpaired t-test.* ***(I)*** *Log2 fold change of genes involved in glycolysis in differentiated cells vs. stem cells. Gene set from GSEA. Significance determined by paired t-test compared to hPSC. All box plot show minimum, first quartile, median, third quartile and maximum.*

Mitochondria are the major source for intracellular reactive oxygen species (ROS) (de Almeida et al., 2022). ROS, which act as signaling molecules, have been shown to regulate stem cell function (Bigarella et al., 2014) and are involved in differentiation and lineage commitment (Khacho et al., 2016). Genes related to ROS were slightly upregulated in hESC derived cells, while being slightly downregulated in NES cells (Figure 3.21C). Higher ROS in neural stem cells was shown to stabilize the master redox regulator NRF2, which leads to upregulation of genes for differentiation (Khacho et al., 2016). NRF2 was upregulated in NE and NNE but unchanged in NES, NC and CP compared to expression in stem cells (Suppl. Figure 5.4G). This could mean that neuroectoderm (NE) and non-neural ectoderm (NNE) were already more committed than the other lines.

To control if mitochondrial quality suffered under downregulation of several mitochondrial pathways, I analyzed mitophagy related genes (Figure 3.21D). These genes were downregulated although not significantly in differentiated cells, which shows that mitochondria were functional and were not discarded.

Finally, I wanted to check energy production pathways in differentiated cells (Figures 3.21E, 3.21H – 3.21J). OXPHOS related genes were significantly downregulated during differentiation (Figure 3.21E). Genes involved in the Krebs cycle were also downregulated, although not significantly in cranial placode and non-neural ectoderm (Figure 3.21F). Fatty acid beta oxidation was unchanged compared to stem cells (Figure 3.21G). Therefore, early ectodermal cells were not switching their metabolism to OXPHOS and mitochondria dependent energy production yet as more final differentiated cell types would do. Downregulation of OXPHOS was also confirmed by a strongly reduced Mitotracker

CMXRos signal in NES cells compared to stem cells, which stains mitochondria depending on their membrane potential (Figure 3.21H). The membrane potential results from the proton gradient which forms in the electron transport chain during OXPHOS (Zorova et al., 2018).

Glycolysis seemed to be still the main resource for ATP in early ectodermal cells since genes were mostly unchanged (Figure 3.21I). Only in NES cells, glycolysis was also slightly downregulated.

In summary, mitochondria underwent morphological changes during ectodermal differentiation into neuroepithelial stem cells. The discovered downregulation of mitochondrial tRNA modifying enzymes and translation came along with a downregulation of mitochondrial dependent energy production pathways in early ectodermal cells and resulted in overall less abundant and less active mitochondria.

4 Summary, Discussion and Future perspectives

4.1 Summary and Key findings

In my PhD project I aimed to better understand the influence of tRNA modifications in human early ectodermal differentiation, which defines the origin of central nervous development. I investigated the landscape of tRNA modifications and modifying enzymes and whether tRNA anticodon pools change during differentiation of human pluripotent stem cells into the major early ectodermal cell types: fore- and hindbrain neuroectoderm, neural crest, cranial placode and non-neural ectoderm. Furthermore, I analyzed the importance of tRNA modifications and tRNA modifying enzymes in global protein synthesis and mitochondrial function.

The main findings from this thesis are:

- tRNA modifying enzymes are mostly downregulated in early ectodermal cell types compared to pluripotent stem cells.
- Modification levels are largely stable and therefore, do not correlate with downregulation of modifying enzymes.
- Cytoplasmic tRNA anticodon pool stays largely stable during differentiation.
- In neuroepithelial stem cells (NES), mitochondrial tRNAs are downregulated.
- Downregulation of many tRNA modifying enzymes reduces global translation rate.
- This downregulation does not depend on the location of the modification in the tRNA molecule.
- Mitochondrial tRNA modifying enzymes shape not only mitochondrial but also cytoplasmic translation.
- The observed downregulation of tRNA modifying enzymes during differentiation is accompanied by reduced global and mitochondrial translation in NES cells.

- Mitochondria change their morphology during differentiation from fragmented in pluripotent stem cells to elongated in neuroepithelial stem cells.
- Early ectodermal cells are in a low metabolic state and clearly reduce mitochondrial related energy production.

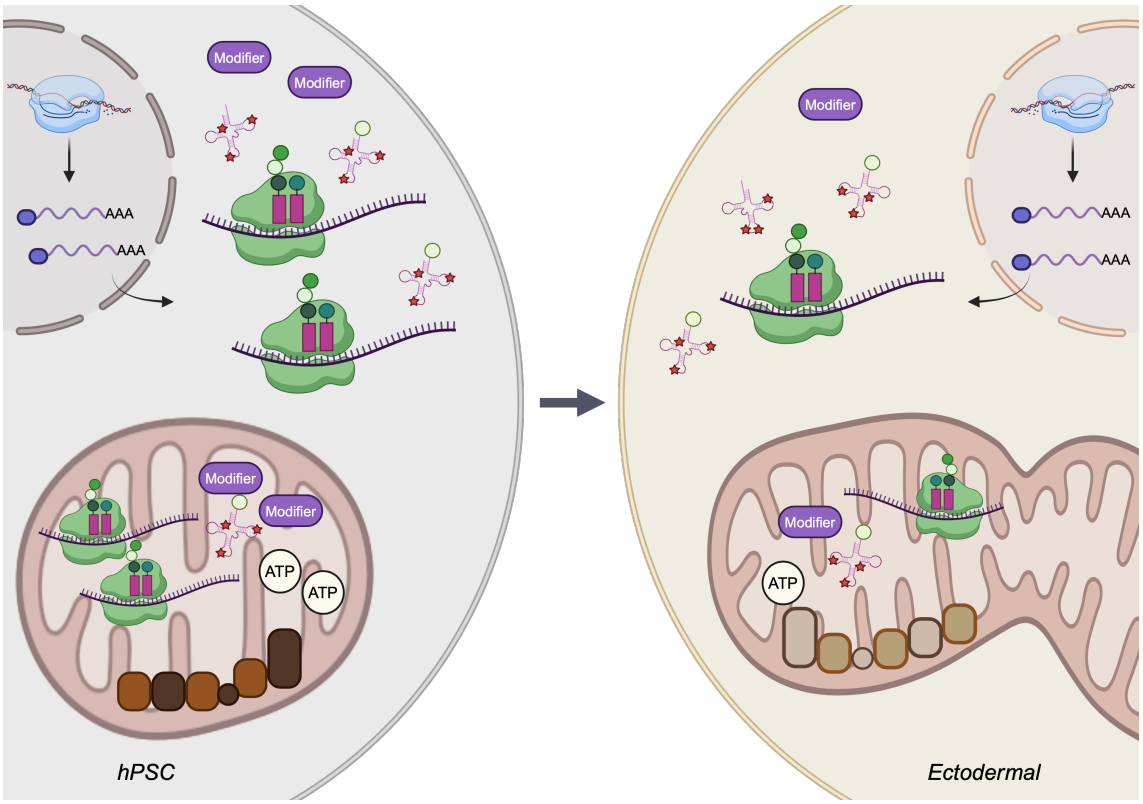

Figure 4.1: ***Key findings.***
This figure summarizes my key findings. hPSC = human pluripotent stem cells. Figure was generated with Biorender.

4.2 Discussion

4.2.1 Modelling early ectodermal cell states by differentiation of human pluripotent stem cells

The Epitranscriptome, comprising RNA modifications on all types of RNA including transfer RNAs, gained more and more attention in the last years. While for a long time, the study of tRNAs was hindered by lack of good methods, the development of new technologies in the last years allowed to analyze and discover their function in more depth. The involvement of tRNAs and tRNA modifications in proper cell function has been shown in several studies (rewied in Torres et al., 2014, Kirchner and Ignatova, 2015, L. Wang and Lin, 2023). Nevertheless, there are still a lot of open questions to be answered. Several tRNA modifying enzymes have been linked to neurodevelopmental disorders (Table 1.1). Here in this thesis, I aimed to understand better why tRNA modifications are so important for proper neural development.

Most research on neural and brain development was made in animal models. However, there are critical differences between human development and e.g. mouse development (Lui et al., 2011, Rossant and Tam, 2017, Haldipur et al., 2019). Therefore, I wanted to study tRNA modification function solely in a human model. I used human pluripotent stem cells, induced (iPSC) and embryonic (ESC), and differentiated them into the major early ectodermal cell types neuroectoderm (NE), neural crest (NC), cranial placode (CP) and non-neural ectoderm (NNE) using a protocol from Tchieu et al. (Tchieu et al., 2017). In human development, these cell types are formed early on after gastrulation at around the fifth week of gestation.

In general, there are several protocols published to generate neural stem cells, neuroepithelial stem cells or neural progenitor cells (Dhara and Stice, 2008, Falk et al., 2012, Reinhardt et al., 2013). However, they either differ in the aspect of which brain vesicle they represent, depict different points in time of differentiation or are more unspecific by using retinoic acid or embryoid bodies. To generate the other ectodermal cell types (NC, CP and NNE), there are also several protocols available, but they would differ in length and medium composition. Therefore, the protocol by Tchieu et al. offered the option

to generate all of the four mentioned cell types in twelve days by simple adjustment of supplements in the medium.

My results showed that differentiation into the desired cell types was successful and they expressed distinct gene sets consisten with their cell fate. However, I did observe some counter marker expression across some cell types. It would be possible that the cell types still share some resemblance due to fact that their formation during development is really close to each other. Additionally, all of these cell types are still multipotent stem cells and not finally differentiated.

One downside of the used protocol was, that cells were completely confluent at the end of differentiation and further passaging was not possible. Therefore, I included the neuroepithelial NES cell lines (Falk et al., 2012, Tailor et al., 2013) which enabled continuous culturing and allowed to exclude proliferation-dependent differences.

4.2.2 Landscape of tRNA modifying enzymes, tRNA modifications and tRNA anticodon pools in early ectodermal differentiation

When looking at the expression of tRNA modifying enzymes in early ectodermal cell types compared to expression in pluripotent stem cells, I observed that most of them were downregulated. Interestingly, expression levels changed quite similarly in the different cell types. I could not observe a neural or non-neural expression profile. So far, there are no studies looking at the landscape of tRNA modifier expression of human embryonic stem cell differentiation neuroectoderm, neural crest, cranial placode and non-neural ectoderm. Most studies on tRNA modifier function in neurodevelopment look at later steps in differentiation (Flores et al., 2017, Brazane et al., 2023) or use a different model organism (Lin et al., 2018, Wu et al., 2023). The other ectodermal cell types NC, CP and NNE have not been investigated in the context of tRNA modifications at all.

Downregulation of most tRNA modifying enzymes in early ectodermal cells did not correlate with levels of modifications, which remained quite stable during differentiation. Recently, Rappol et al. published an analysis on tRNA modification landscape in zebrafish development (Rappol et al., 2024). They developed a new method for tRNA

sequencing, called tRAM-seq, and identified tRNA modifications via reverse transcription stops. In their analysis, modification levels were highest in activated eggs and the very early embryonic stages. Mitochondrial tRNA modifications were stable throughout differentiation. They also observed like me, that expression levels of modifying enzymes did not correlate with modification levels.

I used mass spectrometry to measure the levels of tRNA modifications. This method offered the measurement of 20 different modifications in the same sample. However, sequence information is lost. Other methods to measure modifications are based on reverse transcription stops or mismatches (Behrens et al., 2021, Rappol et al., 2024) or only allow the detection of a specific modification (Schaefer et al., 2009, Lin et al., 2019). In the last years, more and more of these methods were developed and together with the ability to directly sequence tRNA molecules with Nanopore sequencing (Garalde et al., 2018, Lucas et al., 2024), detection and evaluation of tRNA modifications will be come much easier and more precise in the future.

The research of tRNAs has been difficult in the past, since normal RNA sequencing fails to properly detect tRNAs. Transfer RNAs are small, highly structured and highly modified. Only in the last years, new methods were developed that overcame these issues by either removing modifications prior library generation, usage of improved reverse transcriptase molecules (Behrens et al., 2021, Rappol et al., 2024) or by usage of complementary DNA oligos that allow transfer of tRNA quantity onto these oligos without the need of reverse transcription (Kristen et al., unpublished). To measure whether the tRNA anticodon pools change during early ectodermal differentiation, I used the method from Kristen and colleagues.

In the past, Gingold et al. found that the tRNA composition changes from proliferating cells to differentiated cells and that the anticodons correspond to changes in codon usage (Gingold et al., 2014). Back then, no specific tRNA sequencing protocols were available yet, so they used microarrays and histone modification maps to determine tRNA pools. However, two recent publications by Gao et al. (Gao et al., 2024) and Rappol et al. (Rappol et al., 2024) also investigated tRNA pools in development. Gao et al. found, that anticodons were robustly expressed during differentiation of induced pluripotent stem cells to neural progenitor cells (NPCs) and even to neurons. They reasoned that

stable expression ensures constant decoding rates throughout development and would minimize translation errors and protein misfoldings (Nedialkova and Leidel, 2015). Both publications showed, that anticodon expression did not correlate with cell type-specific codon usage but rather with mRNAs that are stably expressed throughout differentiation (Gao et al., 2024, Rappol et al., 2024).

Like Gao et al., I observed a mitochondrial tRNA fraction of less than 4%. When they looked into tRNA anticodon expression in iPSCs and NPCs, they also observed an upregulation of cytoplasmic tRNA(Gly)CCC and tRNA(Sec)TCA, like me. Both of us found tRNA(Asp)GTC downregulated. This shows, that both used methods, mim-tRNAseq and the method from Kristen et al., are reliable and confirm each other.

Interestingly, I found that overall non-neural ectodermal lines neural crest (NC), cranial placode (CP) and non-neural ectoderm (NNE) are really similar to the neural lines neuroectoderm (NE) and neuroepithelial stem cells (NES) in prospect of tRNA modification landscape. It seems that this point of time during development, around neural tube closure, requires lower expression of tRNA modifying enzymes but stable modifications and tRNA anticodon pools.

4.2.3 Mitochondrial tRNA modifications shape both mitochondrial and cytoplasmic translation and affect mitochondrial activity in early ectodermal cell types

Previously, it has been shown, that protein synthesis is rather low in embryonic stem cells (Buszczak et al., 2014). Upon differentiation of mouse ESCs into embryonic bodies, global translation increases (Sampath et al., 2008, Ingolia et al., 2011). However, looking into a model that resembles more closely my study, Chau et al. showed in mouse forebrain development *in vivo*, that upon neural tube closure, ribosome biogenesis and translation rate are strongly downregulated (Chau et al., 2018). This matches what I observed in human early ectodermal cells.

I could show, that downregulation of tRNA modifying enzymes reduces protein synthesis rate. Since many tRNA modifiers were downregulated in early ectodermal cell types compared to stem cells, this could explain the observed downregulation of protein

synthesis rate.

Additionally, I observed, that downregulation of mitochondrial tRNA modifiers even affected global translation more than downregulation of only cytoplasmic tRNA modifiers. Mitochondrial tRNAs need to be highly modified to be functional in mitochondrial translation (Kopajtich et al., 2014). Impaired mitochondrial protein synthesis reduces mitochondrial function and energy generation (Delaunay et al., 2022), and since protein synthesis is the most highly energy consuming process in cells (Buttgereit and Brand, 1995), reduced mitochondrial function affects also global protein synthesis.

I also observed lower mitochondrial function and metabolism in ectodermal cells compared to stem cells, accompanied by a structural change from fragmented to elongated mitochondria. These dynamics in morphology were also observed in mouse forebrain development (Fame et al., 2019) and in mouse ESC differentiation to neural stem cells (Khacho et al., 2016). Khacho et al. further reported, that mitochondria return to a fragmented state in neural progenitor cells before reaching their final elongated state in neurons.

There are several publications showing reduced mitochondrial activity in neural stem cells. Baser et al. observed low protein synthesis rate and low cellular metabolism in adult neural stem cells (Baser et al., 2017). Khacho et al. could show, that mouse neural stem cells have low OXPHOS activity and predominantly use glycolysis (Khacho et al., 2016). And Lees et al. found that human neural progenitor cells have less mitochondrial mass and lower mitochondrial membrane potential than iPSCs (Lees et al., 2018).

This low metabolic state was also previously shown to exist in pre-migratory neural crest cells (Bhattacharya et al., 2021).

Overall, it was known that early neural stem cells adopt a more quiescent metabolic state compared to pluripotent stem cells. My findings showed, that this reduced mitochondrial activity is linked to reduced mitochondrial protein synthesis due to low expression of tRNA modifying enzymes. Interestingly, this observation was made in all human major ectodermal cell types and not only neural stem cells.

4.3 Future perspectives

Work in this thesis shows that all major human early ectodermal cell types downregulate the expression of tRNA modifying enzymes which is accompanied by reduced mitochondrial protein synthesis, reduced mitochondrial metabolic activity and reduced global protein synthesis. To understand the impact of tRNA modifications in brain development further, this work could be continued in the following ways:

- Modification mapping could be improved by usage of further detection methods, e.g. bisulfite sequencing, mim-tRNAseq and Nano-tRNAseq.

- There are indications that already the exit of pluripotency marks a big turn of events. Lees et al. observed a metabolic exit event 24 hours after introduction of differentiation (Lees et al., 2018). Therefore, it could be interesting to investigate the tRNA modification landscape already from the beginning of differentiation.

- Furthermore, it has been shown, that cells switch to mitochondrial dependent energy production during further neural differentiation (Khacho et al., 2016). Additionally, Harnett et al. showed in mouse that a burst of gene expression regulation occurs at day E15.5 (roughly 5 days after neural tube closure) (Harnett et al., 2022). Analysis of tRNA modification landscape during later timepoints in development would be also interesting.

- The function of tRNA modifications in ectodermal differentiation could be analyzed more in detail by manipulating their expression levels in either pluripotent stem cells or ectodermal cells and analyze how this affects self-renewal and differentiation capabilities, but also how protein synthesis and metabolism are affected.

5 Appendix

5.1 Supplementary materials

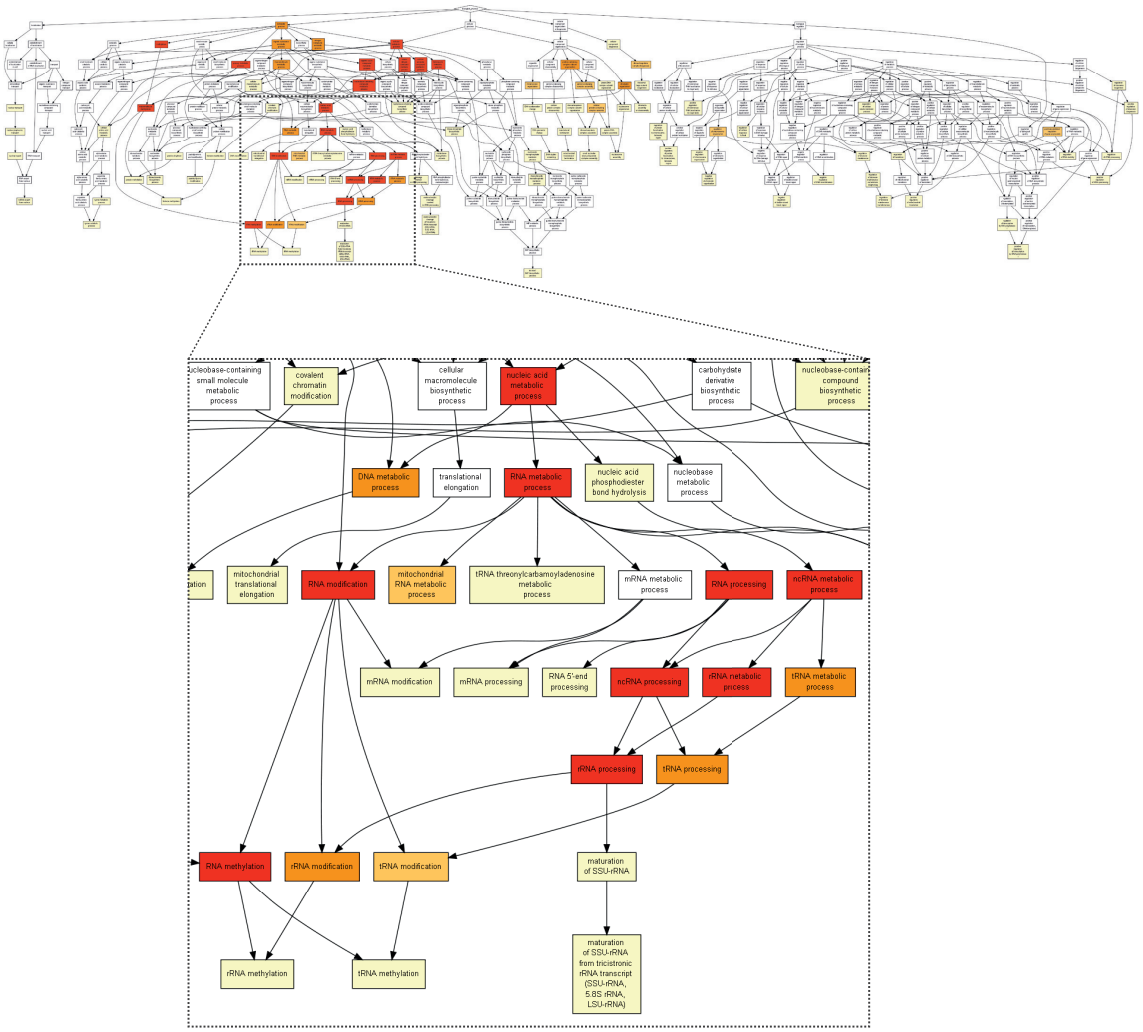

Figure 5.1: ***RNA related GO categories downregulated in early ectoderm.*** *GO analysis was performed with Gorilla (Eden et al., 2007, Eden et al., 2009).*

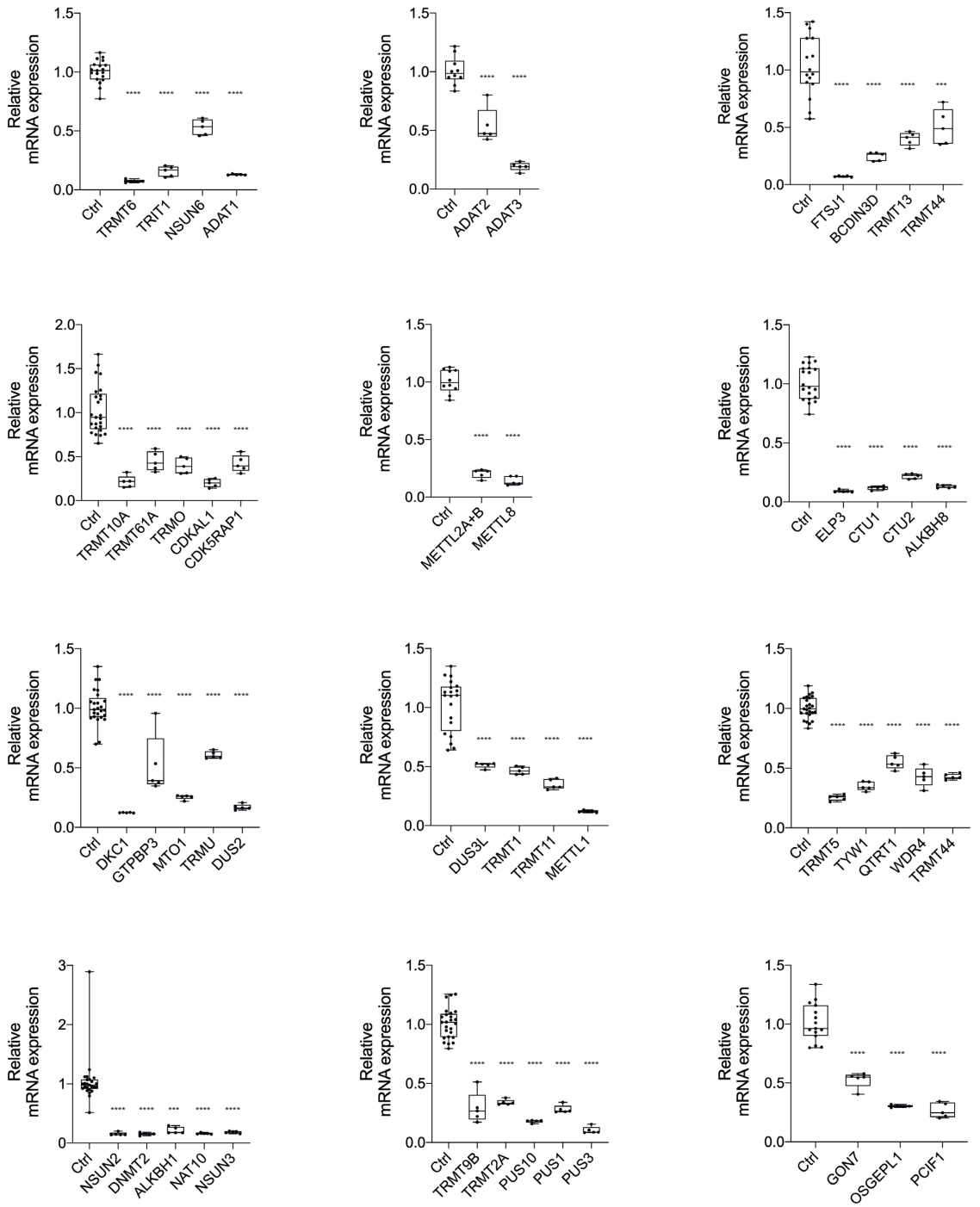

Figure 5.2: ***Relative RNA expression after knockdown using siPOOLs.***
Relative RNA expression measured with RT-qPCR compared to negative control siPOOL.

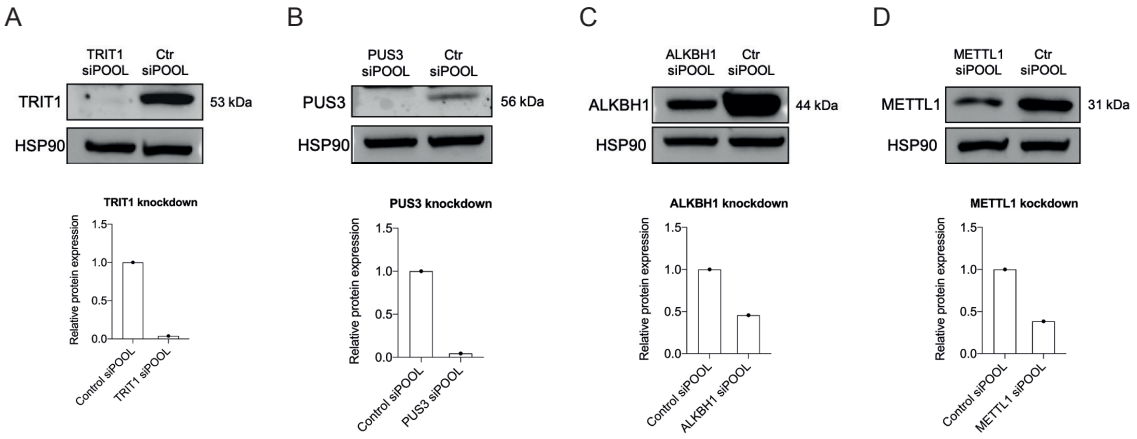

Figure 5.3: ***Western Blot showing protein expression after knockdown using siPOOLs.***
(A) TRIT1 protein expression after siPOOL knockdown. (B) PUS3 protein expression after siPOOL knockdown. (C) ALKBH1 protein expression after siPOOL knockdown. (D) METTL1 protein expression after siPOOL knockdown.

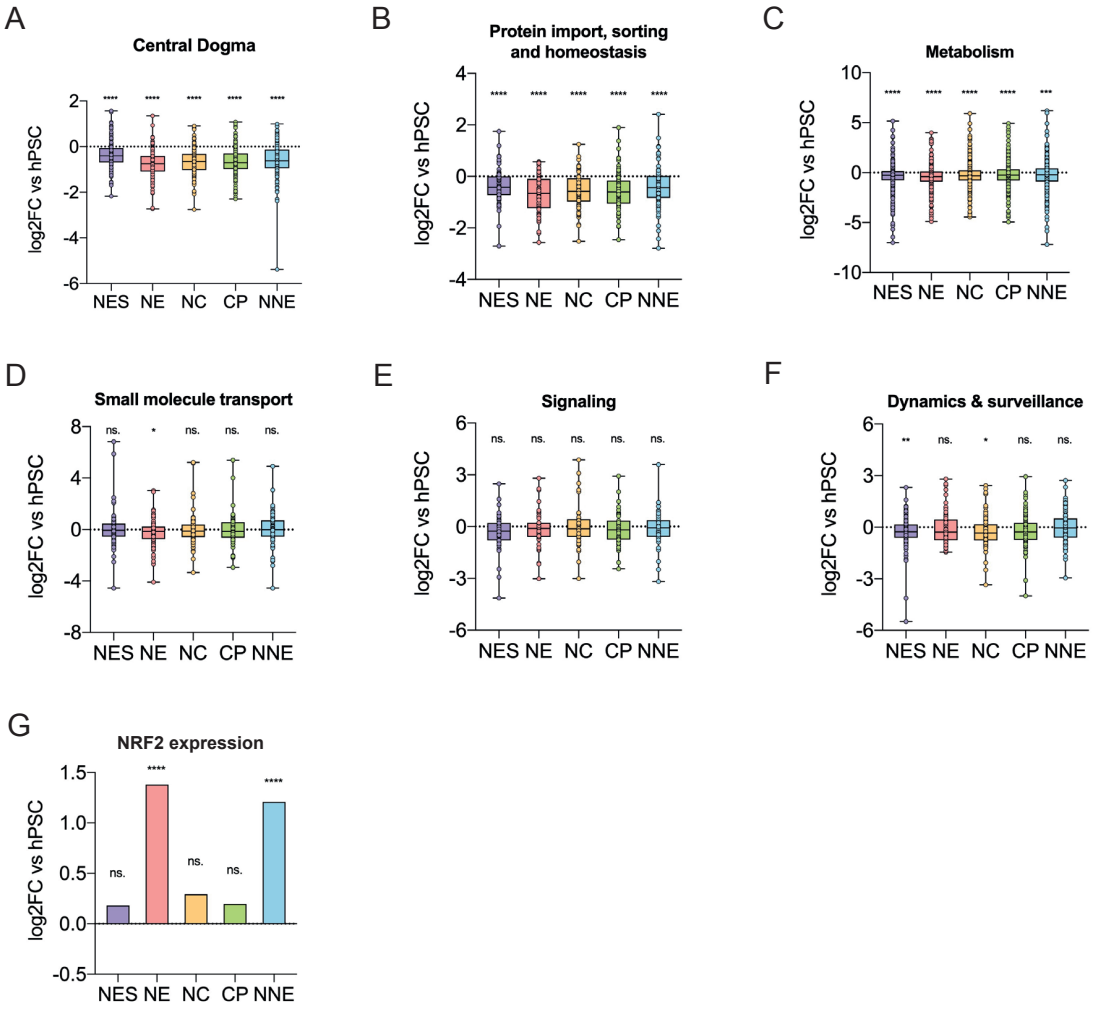

Figure 5.4: ***Differential expression of MitoCarta3.0 genes.***
Log2 fold changes of genes of MitoCarta3.0 categories in early ectodermal cell types compared to human pluripotent stem cells. Significance determined by paired t-tests compared to hPSCs. Box plot shows minimum, first quartile, median, third quartile and maximum. ***(A)*** *Category 'Central Dogma' which comprises genes related to mtDNA maintenance, mtRNA metabolism and translation.* ***(B)*** *Category 'Protein import, sorting and homeostasis'.* ***(C)*** *Category 'Metabolism' which comprises genes related to carbohydrate metabolism, amino acid metabolism, lipid metabolism, nucleotide metabolism, metals and cofactor metabolism, vitamin metabolism, detoxification and electron carriers.* ***(D)*** *Category 'small molecule transport'.* ***(E)*** *Category 'Signaling'.* ***(F)*** *Category 'Dynamics and surveillance' which comprises genes involved in fusion, fission and mitophagy.* ***(G)*** *Log2 fold change of NRF2 RNA expression compared to hPSC. Bars represent mean fold change of six biological replicates. Significance displayed as adjusted p-value.*

Table 5.1: *tRNA modifying enzymes*

Enzyme	Mod symbol	Mod name	Position	tRNA species	Reference
ADAT1	I	Inosine	A37	cytoplasmic	De Crécy-Lagard et al., 2019
ADAT2	I	Inosine	A34	cytoplasmic	De Crécy-Lagard et al., 2019
ADAT3	I	Inosine	A34	cytoplasmic	De Crécy-Lagard et al., 2019
ALKBH1	m^1A	1-methyladenosine	A58 (removal)	cytoplasmic	F. Liu et al., 2016
ALKBH1	f^5C	5-formylcytidine	C34	mitochondrial	F. Liu et al., 2016
ALBKH3	m^1A	1-methyladenosine	A58 (removal)	cytoplasmic	Z. Chen et al., 2019
ALKBH3	m^3C	3-methylcytidine	C20, C32, C47 (removal)	cytoplasmic	Z. Chen et al., 2019
ALKBH8	mcm^5U, (S)-mchm5U	5-methoxycarbonylmethyluridine, (S)-5-methoxycarbonylhydroxymethyluridine	U34	cytoplasmic	De Crécy-Lagard et al., 2019
BCDIN3D	mm(pN)	5'-monomethylmonophosphate	5'	cytoplasmic	Tomita and Liu, 2018
CKD5RAP1	ms^2i^6A	2-methylthio-N6-isopentenyladenosine	A37	mitochondrial	De Crécy-Lagard et al., 2019
CDKAL1	ms^2i^6A	2-methylthio-N6-isopentenyladenosine	A37	cytoplasmic	De Crécy-Lagard et al., 2019
CIAO1	s^2U, mcm^5s^2U	2-thiouridine, 5-methoxycarbonylmethyl-2-thiouridine	U34	cytoplasmic	De Crécy-Lagard et al., 2019
CTU1	s^2U, mcm^5s^2U	2-thiouridine, 5-methoxycarbonylmethyl-2-thiouridine	U34	cytoplasmic	De Crécy-Lagard et al., 2019
CTU2	s^2U, mcm^5s^2U	2-thiouridine, 5-methoxycarbonylmethyl-2-thiouridine	U34	cytoplasmic	De Crécy-Lagard et al., 2019
DUS1L	D	Dihydrouridine	U16, U17	cytoplasmic	De Crécy-Lagard et al., 2019
DUS2	D	Dihydrouridine	U20	both	De Crécy-Lagard et al., 2019
DUS3L	D	Dihydrouridine	U47	cytoplasmic	De Crécy-Lagard et al., 2019
ELP3	cm^5U	5-carboxymethyluridine	U34	cytoplasmic	De Crécy-Lagard et al., 2019
ELP4	cm^5U	5-carboxymethyluridine	U34	cytoplasmic	De Crécy-Lagard et al., 2019
ELP5	cm^5U	5-carboxymethyluridine	U34	cytoplasmic	De Crécy-Lagard et al., 2019
ELP6	cm^5U	5-carboxymethyluridine	U34	cytoplasmic	De Crécy-Lagard et al., 2019
FTO	m^1A	1-methyladenosine	removal	cytoplasmic	
FTSJ1	Nm	2'-O-methylation	32, 34	cytoplasmic	De Crécy-Lagard et al., 2019
GTPBP3	tm^5U	5-taurinomethyluridine	U34	mitochondrial	De Crécy-Lagard et al., 2019
GON7	t^6A	N6-threonylcarbamoyladenosine	A37	cytoplasmic	Srinivasan et al., 2011
IKBKAP	cm^5U	5-carboxymethyluridine	U34	cytoplasmic	De Crécy-Lagard et al., 2019
LAGE3	t^6A	N6-threonylcarbamoyladenosine	A37	cytoplasmic	De Crécy-Lagard et al., 2019
LCMT2	yW	Wybutosine	G37	cytoplasmic	De Crécy-Lagard et al., 2019
METTL1	m^7G	7-methylguanosine	G46	cytoplasmic	De Crécy-Lagard et al., 2019
METTL2A	m^3C	3-methylcytidine	C32	cytoplasmic	De Crécy-Lagard et al., 2019
METTL2B	m^3C	3-methylcytidine	C32	both	De Crécy-Lagard et al., 2019
METTL6	m^3C	3-methylcytidine	C32	cytoplasmic	De Crécy-Lagard et al., 2019
METTL8	m^3C	3-methylcytidine	C32	mitochondrial	Kleiber et al., 2022
MOCS3	s^2U, mcm^5s^2U	2-thiouridine, 5-methoxycarbonylmethyl-2-thiouridine	U34	cytoplasmic	De Crécy-Lagard et al., 2019
MPST	s^2U, mcm^5s^2U	2-thiouridine, 5-methoxycarbonylmethyl-2-thiouridine	U34	cytoplasmic	De Crécy-Lagard et al., 2019
MTO1	tm^5U	5-taurinomethyluridine	U34	mitochondrial	De Crécy-Lagard et al., 2019
NAT10	ac^4C	N4-acetylcytidine	C12	cytoplasmic	De Crécy-Lagard et al., 2019
NSUN2	m^5C	5-methylcytidine	C34, C48-50	both	De Crécy-Lagard et al., 2019
NSUN3	m^5C	5-methylcytidine	C34	mitochondrial	De Crécy-Lagard et al., 2019
NSUN6	m^5C	5-methylcytidine	C72	cytoplasmic	De Crécy-Lagard et al., 2019
NUBP1	s^2U, mcm^5s^2U	2-thiouridine, 5-methoxycarbonylmethyl-2-thiouridine	U34	cytoplasmic	De Crécy-Lagard et al., 2019
OSGEP	t^6A	N6-threonylcarbamoyladenosine	A37	cytoplasmic	De Crécy-Lagard et al., 2019
OSGEPL1	t^6A	N6-threonylcarbamoyladenosine	A37	mitochondrial	De Crécy-Lagard et al., 2019

Enzyme	Mod symbol	Mod name	Position	tRNA species	Reference
PUS1	Ψ	Pseudouridine	U27, U28	both	De Crécy-Lagard et al., 2019
PUS1	Ψ	Pseudouridine	U29, U67	mitochondrial	De Crécy-Lagard et al., 2019
PUS1	Ψ	Pseudouridine	U30	cytoplasmic	De Crécy-Lagard et al., 2019
PUS10	Ψ	Pseudouridine	U54	cytoplasmic	De Crécy-Lagard et al., 2019
PUS3	Ψ	Pseudouridine	U38, U39	both	De Crécy-Lagard et al., 2019
PUS7	Ψ	Pseudouridine	U13, U35	cytoplasmic	De Crécy-Lagard et al., 2019
PUS7L	Ψ	Pseudouridine	U13, U35	cytoplasmic	De Crécy-Lagard et al., 2019
PUSL1	Ψ	Pseudouridine		mitochondrial	
QTRT1	Q	Queuosine	34	both	De Crécy-Lagard et al., 2019
QTRT2	Q	Queuosine	34	both	De Crécy-Lagard et al., 2019
TARBP1	Gm	2'-O-methylguanosine	G18	cytoplasmic	De Crécy-Lagard et al., 2019
THADA	Um, Cm	2'-O-methylation	32	cytoplasmic	De Crécy-Lagard et al., 2019
THG1L	xG	unknown modified guanosine	0	cytoplasmic	De Crécy-Lagard et al., 2019De Crécy-Lagard et al., 2019
THUMPD1	ac^4C	N4-acetylcytidine	C12	cytoplasmic	De Crécy-Lagard et al., 2019
THUMPD3	m^2G	2-methylguanosine	G6, G7	cytoplasmic	Yang et al., 2021
TRDMT1	m^5C	5-methylcytidine	C38	cytoplasmic	De Crécy-Lagard et al., 2019
TRIT1	i^6A	N6-isopentenyladenosine	A37	both	De Crécy-Lagard et al., 2019
TRMO	m^6t^6A	N6-methyl-N6-threonylcarbamoyladenosine	A37	cytoplasmic	Kimura et al., 2014
TRMT1	$m^{2,2}G$	2,2-dimethylguanosine	G26	both	De Crécy-Lagard et al., 2019
TRMT9B	$mchm^5U$?	5-(carboxyhydroxymethyl)uridine methyl ester		cytoplasmic ?	De Crécy-Lagard et al., 2019
TRMT10A	m^1G	1-methylguanosine	G9	cytoplasmic	De Crécy-Lagard et al., 2019
TRMT10B	m^1A	1-methyladenosine	A9	cytoplasmic	Vilardo et al., 2020
TRMT10C	m^1A, m1G	1-methyladenosine, 1-methylguanosine	9	mitochondrial	De Crécy-Lagard et al., 2019
TRMT11	m^2G	2-methylguanosine	G10	both	De Crécy-Lagard et al., 2019
TRMT112	m^2G	2-methylguanosine	G6, G10	cytoplasmic, both	Yang et al., 2021
TRMT12	o^2yW	Peroxywybutosine	G37	cytoplasmic	De Crécy-Lagard et al., 2019
TRMT13	Nm	2'-O-methylation	4	cytoplasmic	De Crécy-Lagard et al., 2019
TRMT1L	$m^{2,2}G$	2,2-dimethylguanosine	G37	cytoplasmic	Jonkhout et al., 2021
TRMT2A	m^5U	5-methyluridine	U54	cytoplasmic	De Crécy-Lagard et al., 2019
TRMT2B	m^5U	5-methyluridine	U54	both	De Crécy-Lagard et al., 2019
TRMT44	Um	2'-O-methyluridine	U44	cytoplasmic	De Crécy-Lagard et al., 2019
TRMT5	m^1G	1-methylguanosine	G37	both	De Crécy-Lagard et al., 2019
TRMT6	m^1A	1-methyladenosine	A58	cytoplasmic	De Crécy-Lagard et al., 2019
TRMT61A	m^1A	1-methyladenosine	A58	cytoplasmic	De Crécy-Lagard et al., 2019
TRMT61B	m^1A	1-methyladenosine	A58	mitochondrial	De Crécy-Lagard et al., 2019
TRMU	tm^5s^2U	5-taurinomethyl-2-thiouridine	U34	mitochondrial	De Crécy-Lagard et al., 2019
TRUB1	Ψ	Pseudouridine	U55	cytoplasmic	De Crécy-Lagard et al., 2019
TRUB2	Ψ	Pseudouridine	U55	mitochondrial	De Crécy-Lagard et al., 2019
TYW1	yW	Wybutosine	G37	cytoplasmic	De Crécy-Lagard et al., 2019
TYW3	yW	Wybutosine	G37	cytoplasmic	De Crécy-Lagard et al., 2019
WDR4	m^7G	7-methylguanosine	G46	cytoplasmic	De Crécy-Lagard et al., 2019
WDR6	hm^5Cm	2'-O-methyl-5-hydroxymethylcytidine	34	cytoplasmic	De Crécy-Lagard et al., 2019
WDR6	Cm, Gm	2'-O-methylation	34	cytoplasmic	De Crécy-Lagard et al., 2019
WDR6	f^5Cm	5-formyl-2'-O-methylcytidine	34	cytoplasmic	De Crécy-Lagard et al., 2019
YRDC	t^6A	N6-threonylcarbamoyladenosine	A37	both	De Crécy-Lagard et al., 2019

5.2 List of Abbreviations

Abbreviation	Description
A	adenine
A site	aminoacyl site
aaRS	aminoacyl tRNA synthetase
aRG	apical radial glial cell
Asn	asparagine
Asp	aspartate
ATP	adenosine triphosphate
C	cytosine
CP	cranial placode
CREs	cis regulatory elements
DNA	deoxyribonucleic acid
E site	exit site
eIF	eukaryotic translation intitiation factor
ETC	electron transport chain
G	guanine
Gly	glycine
hESC	human embryonic stem cell
hetADAT	heterodimeric adenosine deaminase acting on tRNA
hPSC	human pluripotent stem cell
ID	Intellectual Disability
Ile	isoleucine
IP	intermediate progenitor
iPSC	induced pluripotent stem cell
IRES	internal ribosome entry site
lncRNA	long noncoding RNA
mESC	mouse embryonic stem cell
Met	methionine
METTL	methyltransferase
miRNA	micro RNA
mRNA	messenger RNA
mt-	mitochondrial
NC	neural crest
NE	neuroectoderm
NEC	neuroepithelial cell
NES	neuroepithelial stem cell
NNE	non-neural ectoderm
NSC	neural stem cell
NSUN	NOP/Sun RNA methyltransferase
OP-puro	O-propargyl-puromycin

Abbreviation	Description
oRG	outer radial glial cell
OXPHOS	oxidative phosphorylation
P site	peptidyl site
Phe	phenylalanine
pre-	precursor
PUS	pseudouridine synthase
RNA	ribonucleic acid
ROS	reactive oxygen species
rRNA	ribosomal RNA
RTD	tRNA decay pathway
Sec	selenocysteine
SVZ	subventricular zone
T	thymine
TCA cycle	citric acid cycle
TFAM	mitochondrial transcription factor A
tRFs	tRNA derived fragments
tRNA	transfer RNA
Trp	tryptophan
TSEN	tRNA splicing endonuclease
U	uracil
uORFs	upstream open reading frames
UTR	untranslated region
Val	valine
VZ	ventricular zone

References

Abbasi-Moheb, L., Mertel, S., Gonsior, M., Nouri-Vahid, L., Kahrizi, K., Cirak, S., Wieczorek, D., Motazacker, M. M., Esmaeeli-Nieh, S., Cremer, K., Weißmann, R., Tzschach, A., Garshasbi, M., Abedini, S. S., Najmabadi, H., Ropers, H. H., Sigrist, S. J., & Kuss, A. W. (2012). Mutations in NSUN2 cause Autosomal-Recessive Intellectual Disability. *American Journal of Human Genetics*, *90*(5), 847–855. https://doi.org/10.1016/j.ajhg.2012.03.021

Ackerman, S. (1992). *Discovering the Brain*. https://doi.org/10.17226/1785

Adkison, L. R. (2012). *Elsevier's Integrated Review Genetics* (Second Edi).

Agris, P. F., Vendeix, F. A., & Graham, W. D. (2007). tRNA's Wobble Decoding of the Genome: 40 Years of Modification. *Journal of Molecular Biology*, *366*(1), 1–13. https://doi.org/10.1016/j.jmb.2006.11.046

Alazami, A. M., Hijazi, H., Al-Dosari, M. S., Shaheen, R., Hashem, A., Aldahmesh, M. A., Mohamed, J. Y., Kentab, A., Salih, M. A., Awaji, A., Masoodi, T. A., & Alkuraya, F. S. (2013). Mutation in ADAT3, encoding adenosine deaminase acting on transfer RNA, causes intellectual disability and strabismus. *Journal of medical genetics*, *50*(7), 425–430. https://doi.org/10.1136/jmedgenet-2012-101378

Alberts, B., Johnson, A., Lewis, J., Raff, M., Roberts, K., & Walter, P. (2014). *Molecular Biology of the Cell* (6th).

Alexandrov, A., Chernyakov, I., Gu, W., Hiley, S. L., Hughes, T. R., Grayhack, E. J., & Phizicky, E. M. (2006). Rapid tRNA decay can result from lack of nonessential modifications. *Molecular cell*, *21*(1), 87–96. https://doi.org/10.1016/j.molcel.2005.10.036

Amos, H., & Korn, M. (1958). 5-Methyl cytosine in the RNA of Escherichia coli. *Biochimica et biophysica acta*, *29*(2), 444–445. https://doi.org/10.1016/0006-3002(58)90214-2

Amunts, A., Brown, A., Toots, J., Scheres, S. H. W., & Ramakrishnan, V. (2015). Ribosome. The structure of the human mitochondrial ribosome. *Science (New York, N.Y.)*, *348*(6230), 95–98. https://doi.org/10.1126/science.aaa1193

Arrondel, C., Missoury, S., Snoek, R., Patat, J., Menara, G., Collinet, B., Liger, D., Durand, D., Gribouval, O., Boyer, O., Buscara, L., Martin, G., Machuca, E., Nevo, F., Lescop, E., Braun, D. A., Boschat, A.-C., Sanquer, S., Guerrera, I. C., ... Mollet, G. (2019). Defects in t(6)A tRNA modification due to GON7 and YRDC mutations lead to Galloway-Mowat syndrome. *Nature communications*, *10*(1), 3967. https://doi.org/10.1038/s41467-019-11951-x

Baker, C. V., & Bronner-Fraser, M. (2001). Vertebrate cranial placodes I. Embryonic induction. *Developmental biology*, *232*(1), 1–61. https://doi.org/10.1006/dbio.2001.0156

Bannister, A. J., & Kouzarides, T. (2011). Regulation of chromatin by histone modifications. *Cell Research*, *21*(3), 381–395. https://doi.org/10.1038/cr.2011.22

Baser, A., Skabkin, M., & Martin-Villalba, A. (2017). Neural Stem Cell Activation and the Role of Protein Synthesis. *Brain plasticity (Amsterdam, Netherlands)*, *3*(1), 27–41. https://doi.org/10.3233/BPL-160038

Behrens, A., Rodschinka, G., & Nedialkova, D. D. (2021). High-resolution quantitative profiling of tRNA abundance and modification status in eukaryotes by mim-tRNAseq. *Molecular Cell*, *81*(8), 1802–1815. https://doi.org/10.1016/j.molcel.2021.01.028

Bento-Abreu, A., Jager, G., Swinnen, B., Rue, L., Hendrickx, S., Jones, A., Staats, K. A., Taes, I., Eykens, C., Nonneman, A., Nuyts, R., Timmers, M., Silva, L., Chariot, A., Nguyen, L., Ravits, J., Lemmens, R., Cabooter, D., Van Den Bosch, L., ... Robberecht, W. (2018). Elongator subunit 3 (ELP3) modifies ALS through tRNA modification. *Human molecular genetics*, *27*(7), 1276–1289. https://doi.org/10.1093/hmg/ddy043

Berg, J. M., Tymoczko, J. L., & Stryer, L. (2013). *Stryer Biochemie* (7th).

Bhattacharya, D., Azambuja, A. P., & Simoes-Costa, M. (2020). Metabolic Reprogramming Promotes Neural Crest Migration via Yap/Tead Signaling. *Developmental cell*, *53*(2), 199–211. https://doi.org/10.1016/j.devcel.2020.03.005

Bhattacharya, D., Khan, B., & Simoes-Costa, M. (2021). Neural crest metabolism: At the crossroads of development and disease. *Developmental Biology*, *475*(February), 245–255. https://doi.org/10.1016/j.ydbio.2021.01.018

Bigarella, C. L., Liang, R., & Ghaffari, S. (2014). Stem cells and the impact of ROS signaling. *Development (Cambridge, England)*, *141*(22), 4206–4218. https://doi.org/10.1242/dev.107086

Björk, G. R., Wikström, P. M., & Byström, A. S. (1989). Prevention of translational frameshifting by the modified nucleoside 1-methylguanosine. *Science (New York, N.Y.)*, *244*(4907), 986–989. https://doi.org/10.1126/science.2471265

Blaesius, K., Abbasi, A. A., Tahir, T. H., Tietze, A., Picker-Minh, S., Ali, G., Farooq, S., Hu, H., Latif, Z., Khan, M. N., & Kaindl, A. (2018). Mutations in the tRNA methyltransferase 1 gene TRMT1 cause congenital microcephaly, isolated inferior vermian hypoplasia and cystic leukomalacia in addition to intellectual disability. *American journal of medical genetics. Part A*, *176*(11), 2517–2521. https://doi.org/10.1002/ajmg.a.38631

Blanco, S., Dietmann, S., Flores, J. V., Hussain, S., Kutter, C., Humphreys, P., Lukk, M., Lombard, P., Treps, L., Popis, M., Kellner, S., Hölter, S. M., Garrett, L., Wurst, W., Becker, L., Klopstock, T., Fuchs, H., Gailus-Durner, V., Hrabě de Angelis, M., ... Frye, M. (2014). Aberrant methylation of tRNAs links cellular stress to neurodevelopmental disorders. *The EMBO Journal*, *33*(18), 2020 LP –2039. http://emboj.embopress.org/content/33/18/2020.abstract

Blanco, S., Kurowski, A., Nichols, J., Watt, F. M., Benitah, S. A., & Frye, M. (2011). The RNA-methyltransferase Misu (NSun2) poises epidermal stem cells to differentiate. *PLoS genetics*, *7*(12), e1002403. https://doi.org/10.1371/journal.pgen.1002403

Boccaletto, P., Stefaniak, F., Ray, A., Cappannini, A., Mukherjee, S., Purta, E., Kurkowska, M., Shirvanizadeh, N., Destefanis, E., Groza, P., Avşar, G., Romitelli, A., Pir, P., Dassi, E., Conticello, S. G., Aguilo, F., & Bujnicki, J. M. (2022). MODOMICS: a database of RNA modification pathways. 2021 update. *Nucleic acids research*, *50*(D1), D231–D235. https://doi.org/10.1093/nar/gkab1083

Bornelöv, S., Selmi, T., Flad, S., Dietmann, S., & Frye, M. (2019). Codon usage optimization in pluripotent embryonic stem cells. *Genome Biology*, 1–16.

Brazane, M., Dimitrova, D. G., Pigeon, J., Paolantoni, C., Ye, T., Marchand, V., Da Silva, B., Schaefer, E., Angelova, M. T., Stark, Z., Delatycki, M., Dudding-Byth, T., Gecz, J., Plaçais, P.-Y., Teysset, L., Préat, T., Piton, A., Hassan, B. A., Roignant, J.-Y., ... Carré, C. (2023). The ribose methylation enzyme FTSJ1 has a conserved role in neuron morphology and learning performance. *Life science alliance*, *6*(4). https://doi.org/10.26508/lsa.202201877

Brenner, S., Barnett, L., Katz, E. R., & Crick, F. H. C. (1967). UGA: A Third Nonsense Triplet in the Genetic Code. *Nature*, *213*(5075), 449–450. https://doi.org/10.1038/213449a0

Broly, M., Polevoda, B. V., Awayda, K. M., Tong, N., Lentini, J., Besnard, T., Deb, W., O'Rourke, D., Baptista, J., Ellard, S., Almannai, M., Hashem, M., Abdulwahab, F., Shamseldin, H., Al-Tala, S., Alkuraya, F. S., Leon, A., van Loon, R. L. E., Ferlini, A., … O'Connell, M. R. (2022). THUMPD1 bi-allelic variants cause loss of tRNA acetylation and a syndromic neurodevelopmental disorder. *American journal of human genetics*, *109*(4), 587–600. https://doi.org/10.1016/j.ajhg.2022.02.001

Bronner, M. E., & Simões-Costa, M. (2016). The Neural Crest Migrating into the Twenty-First Century. *Current topics in developmental biology*, *116*, 115–134. https://doi.org/10.1016/bs.ctdb.2015.12.003

Brons, I. G. M., Smithers, L. E., Trotter, M. W. B., Rugg-Gunn, P., Sun, B., Chuva de Sousa Lopes, S. M., Howlett, S. K., Clarkson, A., Ahrlund-Richter, L., Pedersen, R. A., & Vallier, L. (2007). Derivation of pluripotent epiblast stem cells from mammalian embryos. *Nature*, *448*(7150), 191–195. https://doi.org/10.1038/nature05950

Brown, T. A., Tkachuk, A. N., Shtengel, G., Kopek, B. G., Bogenhagen, D. F., Hess, H. F., & Clayton, D. A. (2011). Superresolution fluorescence imaging of mitochondrial nucleoids reveals their spatial range, limits, and membrane interaction. *Molecular and cellular biology*, *31*(24), 4994–5010. https://doi.org/10.1128/MCB.05694-11

Brzezicha, B., Schmidt, M., Makalowska, I., Jarmolowski, A., Pienkowska, J., & Szweykowska-Kulinska, Z. (2006). Identification of human tRNA:m5C methyltransferase catalysing intron-dependent m5C formation in the first position of the anticodon of the pre-tRNA Leu (CAA). *Nucleic acids research*, *34*(20), 6034–6043. https://doi.org/10.1093/nar/gkl765

Buszczak, M., Signer, R. A. J., & Morrison, S. J. (2014). Cellular differences in protein synthesis regulate tissue homeostasis. *Cell*, *159*(2), 242–251. https://doi.org/10.1016/j.cell.2014.09.016

Buttgereit, F., & Brand, M. D. (1995). A hierarchy of ATP-consuming processes in mammalian cells. *The Biochemical journal*, *312 (Pt 1*(Pt 1), 163–167. https://doi.org/10.1042/bj3120163

Bykhovskaya, Y., Casas, K., Mengesha, E., Inbal, A., & Fischel-Ghodsian, N. (2004). Missense mutation in pseudouridine synthase 1 (PUS1) causes mitochondrial myopathy and sideroblastic anemia (MLASA). *American journal of human genetics*, *74*(6), 1303–1308. https://doi.org/10.1086/421530

Chan, D. C. (2006). Mitochondrial fusion and fission in mammals. *Annual review of cell and developmental biology*, *22*, 79–99. https://doi.org/10.1146/annurev.cellbio.22.010305.104638

Chan, P. P., & Lowe, T. M. (2016). GtRNAdb 2.0: an expanded database of transfer RNA genes identified in complete and draft genomes. *Nucleic acids research*, *44*(D1), 184–9. https://doi.org/10.1093/nar/gkv1309

Chang, Y.-H., Nishimura, S., Oishi, H., Kelly, V. P., Kuno, A., & Takahashi, S. (2019). TRMT2A is a novel cell cycle regulator that suppresses cell proliferation. *Biochemical and biophysical research communications*, *508*(2), 410–415. https://doi.org/10.1016/j.bbrc.2018.11.104

Charif, M., Titah, S. M. C., Roubertie, A., Desquiret-Dumas, V., Gueguen, N., Meunier, I., Leid, J., Massal, F., Zanlonghi, X., Mercier, J., Raynaud de Mauverger, E.,

Procaccio, V., Mousson de Camaret, B., Lenaers, G., & Hamel, C. P. (2015). Optic neuropathy, cardiomyopathy, cognitive disability in patients with a homozygous mutation in the nuclear MTO1 and a mitochondrial MT-TF variant. *American journal of medical genetics. Part A*, *167A*(10), 2366–2374. https://doi.org/10.1002/ajmg.a.37188

Chau, K. F., Shannon, M. L., Fame, R. M., Fonseca, E., Mullan, H., Johnson, M. B., Sendamarai, A. K., Springel, M. W., Laurent, B., & Lehtinen, M. K. (2018). Downregulation of ribosome biogenesis during early forebrain development. *eLIFE*, 1–26.

Chen, M., & Manley, J. L. (2009). Mechanisms of alternative splicing regulation: insights from molecular and genomics approaches. *Nature reviews. Molecular cell biology*, *10*(11), 741–754. https://doi.org/10.1038/nrm2777

Chen, X., Li, A., Sun, B.-F., Yang, Y., Han, Y.-N., Yuan, X., Chen, R.-X., Wei, W.-S., Liu, Y., Gao, C.-C., Chen, Y.-S., Zhang, M., Ma, X.-D., Liu, Z.-W., Luo, J.-H., Lyu, C., Wang, H.-L., Ma, J., Zhao, Y.-L., … Yang, Y.-G. (2019). 5-methylcytosine promotes pathogenesis of bladder cancer through stabilizing mRNAs. *Nature cell biology*, *21*(8), 978–990. https://doi.org/10.1038/s41556-019-0361-y

Chen, Z., Qi, M., Shen, B., Luo, G., Wu, Y., Li, J., Lu, Z., Zheng, Z., Dai, Q., & Wang, H. (2019). Transfer RNA demethylase ALKBH3 promotes cancer progression via induction of tRNA-derived small RNAs. *Nucleic acids research*, *47*(5), 2533–2545. https://doi.org/10.1093/nar/gky1250

Choe, B. K., & Taylor, M. W. (1972). Kinetics of synthesis and characterization of transferRNA precursors in mammalian cells. *Biochimica et Biophysica Acta*, *272*, 275–287.

Cohn, W. E. (1960). Pseudouridine, a carbon-carbon linked ribonucleoside in ribonucleic acids: isolation, structure, and chemical characteristics. *The Journal of biological chemistry*, *235*, 1488–1498.

Crick, F. H. C. (1966). Codon—anticodon pairing: The wobble hypothesis. *Journal of Molecular Biology*, *19*(2), 548–555. https://doi.org/https://doi.org/10.1016/S0022-2836(66)80022-0

Cui, Q., Yin, K., Zhang, X., Ye, P., Chen, X., Chao, J., Meng, H., Wei, J., Roeth, D., Li, L., Qin, Y., Sun, G., Zhang, M., Klein, J., Huynhle, M., Wang, C., Zhang, L., Badie, B., Kalkum, M., … Shi, Y. (2021). Targeting PUS7 suppresses tRNA pseudouridylation and glioblastoma tumorigenesis. *Nature cancer*, *2*(9), 932–949. https://doi.org/10.1038/s43018-021-00238-0

Dai, Z., Liu, H., Liao, J., Huang, C., Ren, X., Zhu, W., Zhu, S., Peng, B., Li, S., Lai, J., Liang, L., Xu, L., Peng, S., Lin, S., & Kuang, M. (2021). N(7)-Methylguanosine tRNA modification enhances oncogenic mRNA translation and promotes intrahepatic cholangiocarcinoma progression. *Molecular cell*, *81*(16), 3339–3355. https://doi.org/10.1016/j.molcel.2021.07.003

Danzer, E., Rintoul, N. E., & Adzick, N. S. (2017). 171 - Pathophysiology of Neural Tube Defects. In R. A. Polin, S. H. Abman, D. H. Rowitch, W. E. Benitz, & W. W. Fox (Eds.), *Fetal and neonatal physiology (fifth edition)* (Fifth Edit, pp. 1712–1723). Elsevier. https://doi.org/https://doi.org/10.1016/B978-0-323-35214-7.00171-2

Daoud, H., Zhang, D., McMurray, F., Yu, A., Luco, S. M., Vanstone, J., Jarinova, O., Carson, N., Wickens, J., Shishodia, S., Choi, H., McDonough, M. A., Schofield, C. J., Harper, M.-E., Dyment, D. A., & Armour, C. M. (2016). Identification of a pathogenic FTO mutation by next-generation sequencing in a newborn with

growth retardation and developmental delay. *Journal of medical genetics*, *53*(3), 200–207. https://doi.org/10.1136/jmedgenet-2015-103399

De Crécy-Lagard, V., Boccaletto, P., Mangleburg, C. G., Sharma, P., Lowe, T. M., Leidel, S. A., & Bujnicki, J. M. (2019). Survey and summary: Matching tRNA modifications in humans to their known and predicted enzymes. *Nucleic Acids Research*, *47*(5), 2143–2159. https://doi.org/10.1093/nar/gkz011

de Almeida, A. J. P. O., de Oliveira, J. C. P. L., da Silva Pontes, L. V., de Souza Júnior, J. F., Gonçalves, T. A. F., Dantas, S. H., de Almeida Feitosa, M. S., Silva, A. O., & de Medeiros, I. A. (2022). ROS: Basic Concepts, Sources, Cellular Signaling, and its Implications in Aging Pathways. *Oxidative medicine and cellular longevity*, *2022*, 1225578. https://doi.org/10.1155/2022/1225578

Delaunay, S., Helm, M., & Frye, M. (2024). RNA modifications in physiology and disease: towards clinical applications. *Nature Reviews Genetics*, *25*(2), 104–122. https://doi.org/10.1038/s41576-023-00645-2

Delaunay, S., Pascual, G., Feng, B., Klann, K., Behm, M., Hotz-Wagenblatt, A., Richter, K., Zaoui, K., Herpel, E., Münch, C., Dietmann, S., Hess, J., Benitah, S. A., & Frye, M. (2022). Mitochondrial RNA modifications shape metabolic plasticity in metastasis. *Nature*, *607*(7919), 593–603. https://doi.org/10.1038/s41586-022-04898-5

Delaunay, S., Rapino, F., Tharun, L., Zhou, Z., Heukamp, L., Termathe, M., Shostak, K., Klevernic, I., Florin, A., Desmecht, H., Desmet, C. J., Nguyen, L., Leidel, S. A., Willis, A. E., Büttner, R., Chariot, A., & Close, P. (2016). Elp3 links tRNA modification to IRES-dependent translation of LEF1 to sustain metastasis in breast cancer. *The Journal of experimental medicine*, *213*(11), 2503–2523. https://doi.org/10.1084/jem.20160397

Deutscher, M. P. (1984). Processing of tRNA in prokaryotes and eukaryotes. *CRC critical reviews in biochemistry*, *17*(1), 45–71. https://doi.org/10.3109/10409238409110269

Dever, T. E., Dinman, J. D., & Green, R. (2018). Translation Elongation and Recoding in Eukaryotes. *Cold Spring Harbor perspectives in biology*, *10*(8). https://doi.org/10.1101/cshperspect.a032649

Dhara, S. K., & Stice, S. L. (2008). Neural differentiation of human embryonic stem cells. *Journal of Cellular Biochemistry*, *438*(July), 19–30. https://doi.org/10.1007/978-1-59745-133-8{_}3

Djumagulov, M., Demeshkina, N., Jenner, L., Rozov, A., Yusupov, M., & Yusupova, G. (2021). Accuracy mechanism of eukaryotic ribosome translocation. *Nature*, *600*(7889), 543–546. https://doi.org/10.1038/s41586-021-04131-9

Duchen, M. R. (2000). Mitochondria and calcium: from cell signalling to cell death. *The Journal of physiology*, *529 Pt 1*(Pt 1), 57–68. https://doi.org/10.1111/j.1469-7793.2000.00057.x

Eden, E., Lipson, D., Yogev, S., & Yakhini, Z. (2007). Discovering motifs in ranked lists of DNA sequences. *PLoS computational biology*, *3*(3), e39. https://doi.org/10.1371/journal.pcbi.0030039

Eden, E., Navon, R., Steinfeld, I., Lipson, D., & Yakhini, Z. (2009). GOrilla: a tool for discovery and visualization of enriched GO terms in ranked gene lists. *BMC bioinformatics*, *10*, 48. https://doi.org/10.1186/1471-2105-10-48

Falk, A., Koch, P., Kesavan, J., Takashima, Y., Ladewig, J., Alexander, M., Wiskow, O., Tailor, J., Trotter, M., Pollard, S., Smith, A., & Brüstle, O. (2012). Capture of neuroepithelial-like stem cells from pluripotent stem cells provides a versatile

system for in vitro production of human neurons. *PLoS ONE*, *7*(1), 1–13. https://doi.org/10.1371/journal.pone.0029597

Fame, R. M., Shannon, M. L., Chau, K. F., Head, J. P., & Lehtinen, M. K. (2019). A concerted metabolic shift in early forebrain alters the CSF proteome and depends on MYC downregulation for mitochondrial maturation. *The Company of Biologists*. https://doi.org/10.1242/dev.182857

Fang, D., Yan, S., Yu, Q., Chen, D., & Yan, S. S. (2016). Mfn2 is Required for Mitochondrial Development and Synapse Formation in Human Induced Pluripotent Stem Cells/hiPSC Derived Cortical Neurons. *Scientific reports*, *6*, 31462. https://doi.org/10.1038/srep31462

Fattal, O., Budur, K., Vaughan, A. J., & Franco, K. (2006). Review of the literature on major mental disorders in adult patients with mitochondrial diseases. *Psychosomatics*, *47*(1), 1–7. https://doi.org/10.1176/appi.psy.47.1.1

Filipowicz, W., Bhattacharyya, S. N., & Sonenberg, N. (2008). Mechanisms of post-transcriptional regulation by microRNAs: are the answers in sight? *Nature reviews. Genetics*, *9*(2), 102–114. https://doi.org/10.1038/nrg2290

Flores, J. V., Cordero-Espinoza, L., Oeztuerk-Winder, F., Andersson-Rolf, A., Selmi, T., Blanco, S., Tailor, J., Dietmann, S., & Frye, M. (2017). Cytosine-5 RNA Methylation Regulates Neural Stem Cell Differentiation and Motility. *Stem Cell Reports*, *8*, 112–124. https://doi.org/10.1016/j.stemcr.2016.11.014

Fonseca, T. B., Sánchez-Guerrero, Á., Milosevic, I., & Raimundo, N. (2019, June). Mitochondrial fission requires DRP1 but not dynamins. https://doi.org/10.1038/s41586-019-1296-y

Freude, K., Hoffmann, K., Jensen, L.-R., Delatycki, M. B., des Portes, V., Moser, B., Hamel, B., van Bokhoven, H., Moraine, C., Fryns, J.-P., Chelly, J., Gecz, J., Lenzner, S., Kalscheuer, V. M., & Ropers, H.-H. (2004). Mutations in the FTSJ1 gene coding for a novel S-adenosylmethionine-binding protein cause nonsyndromic X-linked mental retardation. *American journal of human genetics*, *75*(2), 305–309. https://doi.org/10.1086/422507

Frye, M., Harada, B. T., Behm, M., & He, C. (2018). RNA modifications modulate gene expression during development. *Science*, *1349*(October), 1346–1349.

Gallie, D. R. (1991). The cap and poly(A) tail function synergistically to regulate mRNA translational efficiency. *Genes & development*, *5*(11), 2108–2116. https://doi.org/10.1101/gad.5.11.2108

Gao, L., Behrens, A., Rodschinka, G., Forcelloni, S., Wani, S., Strasser, K., & Nedialkova, D. D. (2024). *Selective gene expression maintains human tRNA anticodon pools during differentiation* (Vol. 26). Springer US. https://doi.org/10.1038/s41556-023-01317-3

Garalde, D. R., Snell, E. A., Jachimowicz, D., Sipos, B., Lloyd, J. H., Bruce, M., Pantic, N., Admassu, T., James, P., Warland, A., Jordan, M., Ciccone, J., Serra, S., Keenan, J., Martin, S., Mcneill, L., Wallace, E. J., Jayasinghe, L., Wright, C., … Turner, D. J. (2018). Highly parallel direct RNA sequencing on an array of nanopores. *Nature Methods*. https://doi.org/10.1038/nmeth.4577

Ghimire, S., Mantziou, V., Moris, N., & Martinez Arias, A. (2021). Human gastrulation: The embryo and its models. *Developmental Biology*, *474*, 100–108. https://doi.org/https://doi.org/10.1016/j.ydbio.2021.01.006

Giegé, R. (2008). Toward a more complete view of tRNA biology. *Nature Structural and Molecular Biology*, *15*(10), 1007–1014. https://doi.org/10.1038/nsmb.1498

Gingold, H., Tehler, D., Christoffersen, N. R., Nielsen, M. M., Asmar, F., Kooistra, S. M., Christophersen, N. S., Christensen, L. L., Borre, M., Sørensen, K. D., Andersen, L. D., Andersen, C. L., Hulleman, E., Wurdinger, T., Ralfkiær, E., Helin, K., Grønbæk, K., Orntoft, T., Waszak, S. M., ... Pilpel, Y. (2014). A dual program for translation regulation in cellular proliferation and differentiation. *Cell*, *158*(6), 1281–92. https://doi.org/10.1016/j.cell.2014.08.011

Gonzalez, D. L., Giannerini, S., & Rosa, R. (2012). On the origin of the mitochondrial genetic code: Towards a unified mathematical framework for the management of genetic information. *Nature Precedings*. https://doi.org/10.1038/npre.2012.7136.1

Greber, B. J., Bieri, P., Leibundgut, M., Leitner, A., Aebersold, R., Boehringer, D., & Ban, N. (2015). Ribosome. The complete structure of the 55S mammalian mitochondrial ribosome. *Science (New York, N.Y.)*, *348*(6232), 303–308. https://doi.org/10.1126/science.aaa3872

Gu, W., Gaeta, X., Sahakyan, A., Chan, A. B., Hong, C. S., Kim, R., Braas, D., Plath, K., Lowry, W. E., & Christofk, H. R. (2016). Glycolytic Metabolism Plays a Functional Role in Regulating Human Pluripotent Stem Cell State. *Cell stem cell*, *19*(4), 476–490. https://doi.org/10.1016/j.stem.2016.08.008

Guy, M. P., Young, D. L., Payea, M. J., Zhang, X., Kon, Y., Dean, K. M., Grayhack, E. J., Mathews, D. H., Fields, S., & Phizicky, E. M. (2014). Identification of the determinants of tRNA function and susceptibility to rapid tRNA decay by high-throughput in vivo analysis. *Genes & development*, *28*(15), 1721–1732. https://doi.org/10.1101/gad.245936.114

Haldipur, P., Aldinger, K. A., Bernardo, S., Deng, M., Timms, A. E., Overman, L. M., Winter, C., Lisgo, S. N., Razavi, F., Silvestri, E., Manganaro, L., Adle-Biassette, H., Guimiot, F., Russo, R., Kidron, D., Hof, P. R., Gerrelli, D., Lindsay, S. J., Dobyns, W. B., ... Millen, K. J. (2019). Spatiotemporal expansion of primary progenitor zones in the developing human cerebellum. *Science (New York, N.Y.)*, *366*(6464), 454–460. https://doi.org/10.1126/science.aax7526

Han, L., & Phizicky, E. M. (2018). A rationale for tRNA modification circuits in the anticodon loop. *RNA (New York, N.Y.)*, *24*(10), 1277–1284. https://doi.org/10.1261/rna.067736.118

Han, S. T., Kim, A. C., Garcia, K., Schimmenti, L. A., Macnamara, E., Network, U. D., Gahl, W. A., Malicdan, M. C., & Tifft, C. J. (2022). PUS7 deficiency in human patients causes profound neurodevelopmental phenotype by dysregulating protein translation. *Molecular genetics and metabolism*, *135*(3), 221–229. https://doi.org/10.1016/j.ymgme.2022.01.103

Harnett, D., Ambrozkiewicz, M. C., Zinnall, U., Rusanova, A., Borisova, E., Drescher, A. N., Couce-Iglesias, M., Villamil, G., Dannenberg, R., Imami, K., Münster-Wandowski, A., Fauler, B., Mielke, T., Selbach, M., Landthaler, M., Spahn, C. M., Tarabykin, V., Ohler, U., & Kraushar, M. L. (2022). A critical period of translational control during brain development at codon resolution. *Nature Structural and Molecular Biology*, *29*(12), 1277–1290. https://doi.org/10.1038/s41594-022-00882-9

Haskins, N., Bhuvanendran, S., Anselmi, C., Gams, A., Kanholm, T., Kocher, K. M., LoTempio, J., Krohmaly, K. I., Sohai, D., Stearrett, N., Bonner, E., Tuchman, M., Morizono, H., Jaiswal, J. K., & Caldovic, L. (2020). Mitochondrial Enzymes of the Urea Cycle Cluster at the Inner Mitochondrial Membrane. *Frontiers in physiology*, *11*, 542950. https://doi.org/10.3389/fphys.2020.542950

Hoffmann, A., Erber, L., Betat, H., Stadler, P. F., Mörl, M., & Fallmann, J. (2021). Changes of the tRNA Modification Pattern during the Development of Dictyostelium discoideum. *Non-coding RNA*, *7*(2). https://doi.org/10.3390/ncrna7020032

Hogan, C. A., Gratz, S. J., Dumouchel, J. L., Thakur, R. S., Delgado, A., Lentini, J. M., Madhwani, K. R., Fu, D., & O'Connor-Giles, K. M. (2023). Expanded tRNA methyltransferase family member TRMT9B regulates synaptic growth and function. *EMBO reports*, *24*(10), 1–17. https://doi.org/10.15252/embr.202356808

Holliday, R., & Pugh, J. E. (1975). DNA modification mechanisms and gene activity during development. *Science (New York, N.Y.)*, *187*(4173), 226–232.

Ibba, M., & Soll, D. (2000). Aminoacyl-tRNA synthesis. *Annual review of biochemistry*, *69*, 617–650. https://doi.org/10.1146/annurev.biochem.69.1.617

Ingolia, N. T., Lareau, L. F., & Weissman, J. S. (2011). Ribosome Profiling of Mouse Embryonic Stem Cells Reveals the Complexity and Dynamics of Mammalian Proteomes. *Cell*, *147*(4), 789–802. https://doi.org/10.1016/j.cell.2011.10.002

International Human Genome Sequencing Consortium. (2004). Finishing the euchromatic sequence of the human genome. *Nature*, *431*(7011), 931–945. https://doi.org/10.1038/nature03001

Ivanov, P., Emara, M. M., Villen, J., Gygi, S. P., & Anderson, P. (2011). Angiogenin-induced tRNA fragments inhibit translation initiation. *Molecular cell*, *43*(4), 613–623. https://doi.org/10.1016/j.molcel.2011.06.022

James A. Thomson, S. S. S., Joseph Itskovitz-Eldor, Michelle A. Waknitz, V. S. M., Jennifer J. Swiergiel, & Jones, J. M. (1998). Embryonic Stem Cell Lines Derived from Human Blastocysts. *Science*, *282*(5391), 1145–1147. https://doi.org/10.1126/science.282.5391.1145

Jarrous, N., Mani, D., & Ramanathan, A. (2022). Coordination of transcription and processing of tRNA. *The FEBS journal*, *289*(13), 3630–3641. https://doi.org/10.1111/febs.15904

Jonkhout, N., Cruciani, S., Santos Vieira, H. G., Tran, J., Liu, H., Liu, G., Pickford, R., Kaczorowski, D., Franco, G. R., Vauti, F., Camacho, N., Abedini, S. S., Najmabadi, H., Ribas de Pouplana, L., Christ, D., Schonrock, N., Mattick, J. S., & Novoa, E. M. (2021). Subcellular relocalization and nuclear redistribution of the RNA methyltransferases TRMT1 and TRMT1L upon neuronal activation. *RNA biology*, *18*(11), 1905–1919. https://doi.org/10.1080/15476286.2021.1881291

Kartsounis, L. D., Troung, D. D., Morgan-Hughes, J. A., & Harding, A. E. (1992). The neuropsychological features of mitochondrial myopathies and encephalomyopathies. *Archives of neurology*, *49*(2), 158–160. https://doi.org/10.1001/archneur.1992.00530260058020

Kewu, P., Zhe, H., Lee, J. T., & Wong, C.-M. (2015). Current perspectives on the role of TRAMP in nuclear RNA surveillance and quality control. *Research and Reports in Biochemistry*, 111. https://doi.org/10.2147/rrbc.s58509

Khacho, M., Clark, A., Svoboda, D. S., Azzi, J., MacLaurin, J. G., Meghaizel, C., Sesaki, H., Lagace, D. C., Germain, M., Harper, M. E., Park, D. S., & Slack, R. S. (2016). Mitochondrial Dynamics Impacts Stem Cell Identity and Fate Decisions by Regulating a Nuclear Transcriptional Program. *Cell Stem Cell*, *19*(2), 232–247. https://doi.org/10.1016/j.stem.2016.04.015

Khacho, M., Harris, R., & Slack, R. S. (2019). Mitochondria as central regulators of neural stem cell fate and cognitive function. *Nature Reviews Neuroscience*, *20*(1), 34–48. https://doi.org/10.1038/s41583-018-0091-3

Kim, Y. E., Hipp, M. S., Bracher, A., Hayer-Hartl, M., & Hartl, F. U. (2013). Molecular chaperone functions in protein folding and proteostasis. *Annual review of biochemistry*, *82*, 323–355. https://doi.org/10.1146/annurev-biochem-060208-092442

Kimmel, R. A., Turnbull, D. H., Blanquet, V., Wurst, W., Loomis, C. A., & Joyner, A. L. (2000). Two lineage boundaries coordinate vertebrate apical ectodermal ridge formation. *Genes & development*, *14*(11), 1377–1389.

Kimura, S., Miyauchi, K., Ikeuchi, Y., Thiaville, P. C., Crécy-Lagard, V. d., & Suzuki, T. (2014). Discovery of the β-barrel-type RNA methyltransferase responsible for N6-methylation of N6-threonylcarbamoyladenosine in tRNAs. *Nucleic acids research*, *42*(14), 9350–9365. https://doi.org/10.1093/nar/gku618

Kirchner, S., & Ignatova, Z. (2015). Emerging roles of tRNA in adaptive translation, signalling dynamics and disease. *Nature Reviews Genetics*, *16*(2), 98–112. https://doi.org/10.1038/nrg3861

Kleiber, N., Lemus-Diaz, N., Stiller, C., Heinrichs, M., Mai, M. M.-Q., Hackert, P., Richter-Dennerlein, R., Höbartner, C., Bohnsack, K. E., & Bohnsack, M. T. (2022). The RNA methyltransferase METTL8 installs m(3)C(32) in mitochondrial tRNAs(Thr/Ser(UCN)) to optimise tRNA structure and mitochondrial translation. *Nature communications*, *13*(1), 209. https://doi.org/10.1038/s41467-021-27905-1

Kleinjan, D. A., & van Heyningen, V. (2005). Long-range control of gene expression: emerging mechanisms and disruption in disease. *American journal of human genetics*, *76*(1), 8–32. https://doi.org/10.1086/426833

Koh, C. S., & Sarin, L. P. (2018). Transfer RNA modification and infection - Implications for pathogenicity and host responses. *Biochimica et biophysica acta. Gene regulatory mechanisms*, *1861*(4), 419–432. https://doi.org/10.1016/j.bbagrm.2018.01.015

Kojima, Y., Kaufman-Francis, K., Studdert, J. B., Steiner, K. A., Power, M. D., Loebel, D. A. F., Jones, V., Hor, A., de Alencastro, G., Logan, G. J., Teber, E. T., Tam, O. H., Stutz, M. D., Alexander, I. E., Pickett, H. A., & Tam, P. P. L. (2014). The transcriptional and functional properties of mouse epiblast stem cells resemble the anterior primitive streak. *Cell stem cell*, *14*(1), 107–120. https://doi.org/10.1016/j.stem.2013.09.014

Kolitz, S. E., & Lorsch, J. R. (2010). Eukaryotic initiator tRNA: finely tuned and ready for action. *FEBS letters*, *584*(2), 396–404. https://doi.org/10.1016/j.febslet.2009.11.047

Koonin, E. V., & Novozhilov, A. S. (2009). Origin and evolution of the genetic code: the universal enigma. *IUBMB life*, *61*(2), 99–111. https://doi.org/10.1002/iub.146

Kopajtich, R., Nicholls, T. J., Rorbach, J., Metodiev, M. D., Freisinger, P., Mandel, H., Vanlander, A., Ghezzi, D., Carrozzo, R., Taylor, R. W., Marquard, K., Murayama, K., Wieland, T., Schwarzmayr, T., Mayr, J. A., Pearce, S. F., Powell, C. A., Saada, A., Ohtake, A., ... Prokisch, H. (2014). Mutations in GTPBP3 cause a mitochondrial translation defect associated with hypertrophic cardiomyopathy, lactic acidosis, and encephalopathy. *American journal of human genetics*, *95*(6), 708–720. https://doi.org/10.1016/j.ajhg.2014.10.017

Kristen, M., Lander, M., Vogt, L.-m., Gleue, L., Jörg, M., Bregeon, D., Marchand, V., Motorin, Y., Friedland, K., & Helm, M. (0). High-throughput quantification of femtomolar tRNA pools by combination of cDNA hybridization and Deep Sequencing.

Kühlbrandt, W. (2015). Structure and function of mitochondrial membrane protein complexes. *BMC biology*, *13*, 89. https://doi.org/10.1186/s12915-015-0201-x

Lazarou, M., Sliter, D. A., Kane, L. A., Sarraf, S. A., Wang, C., Burman, J. L., Sideris, D. P., Fogel, A. I., & Youle, R. J. (2015). The ubiquitin kinase PINK1 recruits autophagy receptors to induce mitophagy. *Nature*, *524*(7565), 309–314. https://doi.org/10.1038/nature14893

Le Lièvre, C. S., & Le Douarin, N. M. (1975). Mesenchymal derivatives of the neural crest: analysis of chimaeric quail and chick embryos. *Journal of embryology and experimental morphology*, *34*(1), 125–154.

Lee, J.-H., Wang, R., Xiong, F., Krakowiak, J., Liao, Z., Nguyen, P. T., Moroz-Omori, E. V., Shao, J., Zhu, X., Bolt, M. J., Wu, H., Singh, P. K., Bi, M., Shi, C. J., Jamal, N., Li, G., Mistry, R., Jung, S. Y., Tsai, K.-L., ... Li, W. (2021). Enhancer RNA m6A methylation facilitates transcriptional condensate formation and gene activation. *Molecular Cell*, *81*(16), 3368–3385. https://doi.org/https://doi.org/10.1016/j.molcel.2021.07.024

Lee, K., Cascella, M., & Marwaha, R. (2024, January). Intellectual Disability.

Lee, T. I., & Young, R. A. (2013). Transcriptional regulation and its misregulation in disease. *Cell*, *152*(6), 1237–1251. https://doi.org/10.1016/j.cell.2013.02.014

Lees, J. G., Gardner, D. K., & Harvey, A. J. (2018). Mitochondrial and glycolytic remodeling during nascent neural differentiation of human pluripotent stem cells. *Development (Cambridge)*, *145*(20). https://doi.org/10.1242/dev.168997

Li, J., Wang, Y.-N., Xu, B.-S., Liu, Y.-P., Zhou, M., Long, T., Li, H., Dong, H., Nie, Y., Chen, P. R., Wang, E.-D., & Liu, R.-J. (2020). Intellectual disability-associated gene ftsj1 is responsible for 2'-O-methylation of specific tRNAs. *EMBO reports*, *21*(8), e50095. https://doi.org/10.15252/embr.202050095

Liao, J., Yi, Y., Yue, X., Wu, X., Zhu, M., Chen, Y., Peng, S., Kuang, M., Lin, S., & Peng, Z. (2023). Methyltransferase 1 is required for nonhomologous end-joining repair and renders hepatocellular carcinoma resistant to radiotherapy. *Hepatology (Baltimore, Md.)*, *77*(6), 1896–1910. https://doi.org/10.1002/hep.32615

Lin, S., Liu, Q., Jiang, Y.-Z., & Gregory, R. I. (2019). Nucleotide resolution profiling of m7G tRNA modification by TRAC-Seq. *Nature Protocols*, *14*(11), 3220–3242. https://doi.org/10.1038/s41596-019-0226-7

Lin, S., Liu, Q., Lelyveld, V. S., Choe, J., Szostak, J. W., & Gregory, R. I. (2018). Mettl1/Wdr4-Mediated m7G tRNA Methylome Is Required for Normal mRNA Translation and Embryonic Stem Cell Self-Renewal and Differentiation. *Molecular Cell*, *71*(2), 244–255. https://doi.org/10.1016/j.molcel.2018.06.001

Liu, F., Clark, W., Luo, G., Wang, X., Fu, Y., Wei, J., Wang, X., Hao, Z., Dai, Q., Zheng, G., Ma, H., Han, D., Evans, M., Klungland, A., Pan, T., & He, C. (2016). ALKBH1-Mediated tRNA Demethylation Regulates Translation. *Cell*, *167*(3), 816–828. https://doi.org/10.1016/j.cell.2016.09.038

Liu, S., Zhang, H., & Duan, E. (2013). Epidermal development in mammals: key regulators, signals from beneath, and stem cells. *International journal of molecular sciences*, *14*(6), 10869–10895. https://doi.org/10.3390/ijms140610869

Lloyd, A. J., Gilbey, A. M., Blewett, A. M., De Pascale, G., El Zoeiby, A., Levesque, R. C., Catherwood, A. C., Tomasz, A., Bugg, T. D. H., Roper, D. I., & Dowson, C. G. (2008). Characterization of tRNA-dependent peptide bond formation by MurM in the synthesis of Streptococcus pneumoniae peptidoglycan. *The Journal of biological chemistry*, *283*(10), 6402–6417. https://doi.org/10.1074/jbc.M708105200

Lucas, M. C., Pryszcz, L. P., Medina, R., Milenkovic, I., Camacho, N., Marchand, V., Motorin, Y., Ribas de Pouplana, L., & Novoa, E. M. (2024). Quantitative analysis

of tRNA abundance and modifications by nanopore RNA sequencing. *Nature Biotechnology*, *42*(1), 72–86. https://doi.org/10.1038/s41587-023-01743-6

Lui, J. H., Hansen, D. V., & Kriegstein, A. R. (2011). Development and evolution of the human neocortex. *Cell*, *146*(1), 18–36. https://doi.org/10.1016/j.cell.2011.06.030

Luo, S., Valencia, C. A., Zhang, J., Lee, N.-C., Slone, J., Gui, B., Wang, X., Li, Z., Dell, S., Brown, J., Chen, S. M., Chien, Y.-H., Hwu, W.-L., Fan, P.-C., Wong, L.-J., Atwal, P. S., & Huang, T. (2018). Biparental Inheritance of Mitochondrial DNA in Humans. *Proceedings of the National Academy of Sciences of the United States of America*, *115*(51), 13039–13044. https://doi.org/10.1073/pnas.1810946115

Mann, M., & Jensen, O. N. (2003). Proteomic analysis of post-translational modifications. *Nature biotechnology*, *21*(3), 255–261. https://doi.org/10.1038/nbt0303-255

Martinez, F. J., Lee, J. H., Lee, J. E., Blanco, S., Nickerson, E., Gabriel, S., Frye, M., Al-Gazali, L., & Gleeson, J. G. (2012). Whole exome sequencing identifies a splicing mutation in NSUN2 as a cause of a Dubowitz-like syndrome. *Journal of Medical Genetics*, *49*(6), 380–385. https://doi.org/10.1136/jmedgenet-2011-100686

Martinez, N. M., Su, A., Burns, M. C., Nussbacher, J. K., Schaening, C., Sathe, S., Yeo, G. W., & Gilbert, W. V. (2022). Pseudouridine synthases modify human pre-mRNA co-transcriptionally and affect pre-mRNA processing. *Molecular Cell*, *82*(3), 645–659. https://doi.org/https://doi.org/10.1016/j.molcel.2021.12.023

Mauer, J., Luo, X., Blanjoie, A., Jiao, X., Grozhik, A. V., Patil, D. P., Linder, B., Pickering, B. F., Vasseur, J.-J., Chen, Q., Gross, S. S., Elemento, O., Debart, F., Kiledjian, M., & Jaffrey, S. R. (2017). Reversible methylation of m(6)A(m) in the 5' cap controls mRNA stability. *Nature*, *541*(7637), 371–375. https://doi.org/10.1038/nature21022

Mayr, C. (2019). What Are 3' UTRs Doing? *Cold Spring Harbor perspectives in biology*, *11*(10). https://doi.org/10.1101/cshperspect.a034728

Mei, Y., Yong, J., Liu, H., Shi, Y., Meinkoth, J., Dreyfuss, G., & Yang, X. (2010). tRNA binds to cytochrome c and inhibits caspase activation. *Molecular cell*, *37*(5), 668–678. https://doi.org/10.1016/j.molcel.2010.01.023

Metsalu, T., & Vilo, J. (2015). ClustVis: a web tool for visualizing clustering of multivariate data using Principal Component Analysis and heatmap. *Nucleic acids research*, *43*(W1), 566–70. https://doi.org/10.1093/nar/gkv468

Mikkola, M. L. (2007). Genetic basis of skin appendage development. *Seminars in cell & developmental biology*, *18*(2), 225–236. https://doi.org/10.1016/j.semcdb.2007.01.007

Milicevic, N., Jenner, L., Myasnikov, A., Yusupov, M., & Yusupova, G. (2024). mRNA reading frame maintenance during eukaryotic ribosome translocation. *Nature*, *625*(7994), 393–400. https://doi.org/10.1038/s41586-023-06780-4

MITCHELL, P. (1961). Coupling of Phosphorylation to Electron and Hydrogen Transfer by a Chemi-Osmotic type of Mechanism. *Nature*, *191*(4784), 144–148. https://doi.org/10.1038/191144a0

Molina, A. J. A., Wikstrom, J. D., Stiles, L., Las, G., Mohamed, H., Elorza, A., Walzer, G., Twig, G., Katz, S., Corkey, B. E., & Shirihai, O. S. (2009). Mitochondrial networking protects beta-cells from nutrient-induced apoptosis. *Diabetes*, *58*(10), 2303–2315. https://doi.org/10.2337/db07-1781

Monies, D., Vågbø, C. B., Al-Owain, M., Alhomaidi, S., & Alkuraya, F. S. (2019). Recessive Truncating Mutations in ALKBH8 Cause Intellectual Disability and

Severe Impairment of Wobble Uridine Modification. *American journal of human genetics*, *104*(6), 1202–1209. https://doi.org/10.1016/j.ajhg.2019.03.026

Nagayoshi, Y., Chujo, T., Hirata, S., Nakatsuka, H., Chen, C.-W., Takakura, M., Miyauchi, K., Ikeuchi, Y., Carlyle, B. C., Kitchen, R. R., Suzuki, T., Katsuoka, F., Yamamoto, M., Goto, Y., Tanaka, M., Natsume, K., Nairn, A. C., Suzuki, T., Tomizawa, K., & Wei, F.-Y. (2021). Loss of Ftsj1 perturbs codon-specific translation efficiency in the brain and is associated with X-linked intellectual disability. *Science advances*, *7*(13). https://doi.org/10.1126/sciadv.abf3072

Nakamura, Y., Ito, K., & Isaksson, L. A. (1996). Emerging understanding of translation termination. *Cell*, *87*(2), 147–150. https://doi.org/10.1016/s0092-8674(00)81331-8

Nedialkova, D. D., & Leidel, S. A. (2015). Optimization of Codon Translation Rates via tRNA Modifications Maintains Proteome Integrity. *Cell*, *161*(7), 1606–1618. https://doi.org/10.1016/j.cell.2015.05.022

Nishikura, K. (2016). A-to-I editing of coding and non-coding RNAs by ADARs. *Nat Rev Mol Cell Biol*, *17*(2), 83–96. http://dx.doi.org/10.1038/nrm.2015.4%2010.1038/nrm.2015.4

Noden, D. M. (1983). The role of the neural crest in patterning of avian cranial skeletal, connective, and muscle tissues. *Developmental biology*, *96*(1), 144–165. https://doi.org/10.1016/0012-1606(83)90318-4

Novoa, E. M., & Ribas de Pouplana, L. (2012). Speeding with control: Codon usage, tRNAs, and ribosomes. *Trends in Genetics*, *28*(11), 574–581. https://doi.org/10.1016/j.tig.2012.07.006

Oberbauer, V., & Schaefer, M. R. (2018). tRNA-Derived Small RNAs: Biogenesis, Modification, Function and Potential Impact on Human Disease Development. *Genes*, *9*(12). https://doi.org/10.3390/genes9120607

Ojala, D., Montoya, J., & Attardi, G. (1981). tRNA punctuation model of RNA processing in human mitochondria. *Nature*, *290*(5806), 470–474. https://doi.org/10.1038/290470a0

Ong, C.-T., & Corces, V. G. (2011). Enhancer function: new insights into the regulation of tissue-specific gene expression. *Nature reviews. Genetics*, *12*(4), 283–293. https://doi.org/10.1038/nrg2957

Osumi, N., Shinohara, H., Numayama-Tsuruta, K., & Maekawa, M. (2008). Concise review: Pax6 transcription factor contributes to both embryonic and adult neurogenesis as a multifunctional regulator. *Stem cells (Dayton, Ohio)*, *26*(7), 1663–1672. https://doi.org/10.1634/stemcells.2007-0884

Palma, F. R., Gantner, B. N., Sakiyama, M. J., Kayzuka, C., Shukla, S., Lacchini, R., Cunniff, B., & Bonini, M. G. (2024). ROS production by mitochondria: function or dysfunction? *Oncogene*, *43*(5), 295–303. https://doi.org/10.1038/s41388-023-02907-z

Paridaen, J. T. M. L., & Huttner, W. B. (2014). Neurogenesis during development of the vertebrate central nervous system. *EMBO reports*, *15*(4), 351–364. https://doi.org/10.1002/embr.201438447

Passmore, L. A., & Coller, J. (2022). Roles of mRNA poly(A) tails in regulation of eukaryotic gene expression. *Nature reviews. Molecular cell biology*, *23*(2), 93–106. https://doi.org/10.1038/s41580-021-00417-y

Piel, R. B. 3., Dailey, H. A. J., & Medlock, A. E. (2019). The mitochondrial heme metabolon: Insights into the complex(ity) of heme synthesis and distribution.

Molecular genetics and metabolism, *128*(3), 198–203. https://doi.org/10.1016/j.ymgme.2019.01.006

Polikanov, Y. S., Melnikov, S. V., Söll, D., & Steitz, T. A. (2015). Structural insights into the role of rRNA modifications in protein synthesis and ribosome assembly. *Nature Structural & Molecular Biology*, *22*(4), 342–344. https://doi.org/10.1038/nsmb.2992

Rackham, O., & Filipovska, A. (2022). Organization and expression of the mammalian mitochondrial genome. *Nature Reviews Genetics*, *23*(10), 606–623. https://doi.org/10.1038/s41576-022-00480-x

Rak, R., Polonsky, M., Eizenberg-Magar, I., Mo, Y., Sakaguchi, Y., Mizrahi, O., Nachshon, A., Reich-Zeliger, S., Stern-Ginossar, N., Dahan, O., Suzuki, T., Friedman, N., & Pilpel, Y. (2021). Dynamic changes in tRNA modifications and abundance during T cell activation. *Proceedings of the National Academy of Sciences of the United States of America*, *118*(42). https://doi.org/10.1073/pnas.2106556118

Ramanathan, A., Robb, G. B., & Chan, S.-H. (2016). mRNA capping: biological functions and applications. *Nucleic acids research*, *44*(16), 7511–7526. https://doi.org/10.1093/nar/gkw551

Rappol, T., Waldl, M., Chugunova, A., Ivo, L., Pauli, A., & Vilardo, E. (2024). tRNA expression and modification landscapes , and their dynamics during zebrafish embryo development. *Nucleic Acids Research*, 1–43. https://doi.org/10.1093/nar/gkae595

Rath, S., Sharma, R., Gupta, R., Ast, T., Chan, C., Durham, T. J., Goodman, R. P., Grabarek, Z., Haas, M. E., Hung, W. H. W., Joshi, P. R., Jourdain, A. A., Kim, S. H., Kotrys, A. V., Lam, S. S., McCoy, J. G., Meisel, J. D., Miranda, M., Panda, A., … Mootha, V. K. (2021). MitoCarta3.0: an updated mitochondrial proteome now with sub-organelle localization and pathway annotations. *Nucleic acids research*, *49*(D1), D1541–D1547. https://doi.org/10.1093/nar/gkaa1011

Reinhardt, P., Glatza, M., Hemmer, K., Tsytsyura, Y., Thiel, C. S., Höing, S., Moritz, S., Parga, J. A., Wagner, L., Bruder, J. M., Wu, G., Schmid, B., Röpke, A., Klingauf, J., Schwamborn, J. C., Gasser, T., Schöler, H. R., & Sterneckert, J. (2013). Derivation and expansion using only small molecules of human neural progenitors for neurodegenerative disease modeling. *PloS one*, *8*(3), e59252. https://doi.org/10.1371/journal.pone.0059252

Renault, T. T., & Chipuk, J. E. (2014). Death upon a kiss: mitochondrial outer membrane composition and organelle communication govern sensitivity to BAK/BAX-dependent apoptosis. *Chemistry & biology*, *21*(1), 114–123. https://doi.org/10.1016/j.chembiol.2013.10.009

Rodnina, M. V., Fischer, N., Maracci, C., & Stark, H. (2017). Ribosome dynamics during decoding. *Philosophical transactions of the Royal Society of London. Series B, Biological sciences*, *372*(1716). https://doi.org/10.1098/rstb.2016.0182

Roeder, R. G., & Rutter, W. J. (1969). Multiple forms of DNA-dependent RNA polymerase in eukaryotic organisms. *Nature*, *224*(5216), 234–237. https://doi.org/10.1038/224234a0

Roeder, R. G., & Rutter, W. J. (1970). Specific nucleolar and nucleoplasmic RNA polymerases. *Proceedings of the National Academy of Sciences of the United States of America*, *65*(3), 675–682. https://doi.org/10.1073/pnas.65.3.675

Rossant, J., & Tam, P. P. L. (2017). New Insights into Early Human Development: Lessons for Stem Cell Derivation and Differentiation. *Cell stem cell*, *20*(1), 18–28. https://doi.org/10.1016/j.stem.2016.12.004

Roundtree, I. A., Evans, M. E., Pan, T., & He, C. (2017). Dynamic RNA Modifications in Gene Expression Regulation. *Cell*, *169*(7), 1187–1200. https://doi.org/10.1016/j.cell.2017.05.045

Rozov, A., Demeshkina, N., Westhof, E., Yusupov, M., & Yusupova, G. (2015). Structural insights into the translational infidelity mechanism. *Nature communications*, *6*, 7251. https://doi.org/10.1038/ncomms8251

Ryczek, N., Łyś, A., & Makałowska, I. (2023). The Functional Meaning of 5'UTR in Protein-Coding Genes. *International journal of molecular sciences*, *24*(3). https://doi.org/10.3390/ijms24032976

Saikia, M., Jobava, R., Parisien, M., Putnam, A., Krokowski, D., Gao, X.-H., Guan, B.-J., Yuan, Y., Jankowsky, E., Feng, Z., Hu, G.-f., Pusztai-Carey, M., Gorla, M., Sepuri, N. B. V., Pan, T., & Hatzoglou, M. (2014). Angiogenin-cleaved tRNA halves interact with cytochrome c, protecting cells from apoptosis during osmotic stress. *Molecular and cellular biology*, *34*(13), 2450–2463. https://doi.org/10.1128/MCB.00136-14

Saka, Y., & Smith, J. C. (2001). Spatial and temporal patterns of cell division during early Xenopus embryogenesis. *Developmental biology*, *229*(2), 307–318. https://doi.org/10.1006/dbio.2000.0101

Sampath, P., Pritchard, D. K., Pabon, L., Reinecke, H., Schwartz, S. M., Morris, D. R., & Murry, C. E. (2008). A Hierarchical Network Controls Protein Translation during Murine Embryonic Stem Cell Self-Renewal and Differentiation. https://doi.org/10.1016/j.stem.2008.03.013

Savva, Y. A., Rieder, L. E., & Reenan, R. A. (2012). The ADAR protein family (2013/01/01). *Genome Biol*, *13*(12), 252. https://doi.org/10.1186/gb-2012-13-12-252

Schaefer, M., Pollex, T., Hanna, K., & Lyko, F. (2009). RNA cytosine methylation analysis by bisulfite sequencing. *Nucleic acids research*, *37*(2), e12. https://doi.org/10.1093/nar/gkn954

Schlosser, G. (2006). Induction and specification of cranial placodes. *Developmental Biology*, *294*(2), 303–351. https://doi.org/https://doi.org/10.1016/j.ydbio.2006.03.009

Schulz, W. A., Steinhoff, C., & Florl, A. R. (2006). Methylation of endogenous human retroelements in health and disease. *Current topics in microbiology and immunology*, *310*, 211–250. https://doi.org/10.1007/3-540-31181-5{_}11

Shaheen, R., Abdel-Salam, G. M. H., Guy, M. P., Alomar, R., Abdel-Hamid, M. S., Afifi, H. H., Ismail, S. I., Emam, B. A., Phizicky, E. M., & Alkuraya, F. S. (2015). Mutation in WDR4 impairs tRNA m7G46 methylation and causes a distinct form of microcephalic primordial dwarfism. *Genome Biology*, *16*(1), 210. https://doi.org/10.1186/s13059-015-0779-x

Shaheen, R., Al-Salam, Z., El-Hattab, A. W., & Alkuraya, F. S. (2016). The syndrome dysmorphic facies, renal agenesis, ambiguous genitalia, microcephaly, polydactyly and lissencephaly (DREAM-PL): Report of two additional patients. *American journal of medical genetics. Part A*, *170*(12), 3222–3226. https://doi.org/10.1002/ajmg.a.37877

Simpson, C. L., Lemmens, R., Miskiewicz, K., Broom, W. J., Hansen, V. K., van Vught, P. W. J., Landers, J. E., Sapp, P., Van Den Bosch, L., Knight, J., Neale, B. M., Turner, M. R., Veldink, J. H., Ophoff, R. A., Tripathi, V. B., Beleza, A., Shah, M. N., Proitsi, P., Van Hoecke, A., ... Al-Chalabi, A. (2009). Variants of the

elongator protein 3 (ELP3) gene are associated with motor neuron degeneration. *Human molecular genetics*, *18*(3), 472–481. https://doi.org/10.1093/hmg/ddn375

Slaugenhaupt, S. A., Blumenfeld, A., Gill, S. P., Leyne, M., Mull, J., Cuajungco, M. P., Liebert, C. B., Chadwick, B., Idelson, M., Reznik, L., Robbins, C., Makalowska, I., Brownstein, M., Krappmann, D., Scheidereit, C., Maayan, C., Axelrod, F. B., & Gusella, J. F. (2001). Tissue-specific expression of a splicing mutation in the IKBKAP gene causes familial dysautonomia. *American journal of human genetics*, *68*(3), 598–605. https://doi.org/10.1086/318810

Soheilypour, M., & Mofrad, M. R. K. (2018). Quality control of mRNAs at the entry of the nuclear pore: Cooperation in a complex molecular system. *Nucleus (Austin, Tex.)*, *9*(1), 202–211. https://doi.org/10.1080/19491034.2018.1439304

Spiegel, R., Saada, A., Flannery, P. J., Burté, F., Soiferman, D., Khayat, M., Eisner, V., Vladovski, E., Taylor, R. W., Bindoff, L. A., Shaag, A., Mandel, H., Schuler-Furman, O., Shalev, S. A., Elpeleg, O., & Yu-Wai-Man, P. (2016). Fatal infantile mitochondrial encephalomyopathy, hypertrophic cardiomyopathy and optic atrophy associated with a homozygous OPA1 mutation. *Journal of medical genetics*, *53*(2), 127–131. https://doi.org/10.1136/jmedgenet-2015-103361

Srinivasan, M., Mehta, P., Yu, Y., Prugar, E., Koonin, E. V., Karzai, A. W., & Sternglanz, R. (2011). The highly conserved KEOPS/EKC complex is essential for a universal tRNA modification, t6A. *The EMBO journal*, *30*(5), 873–881. https://doi.org/10.1038/emboj.2010.343

Strug, L. J., Clarke, T., Chiang, T., Chien, M., Baskurt, Z., Li, W., Dorfman, R., Bali, B., Wirrell, E., Kugler, S. L., Mandelbaum, D. E., Wolf, S. M., McGoldrick, P., Hardison, H., Novotny, E. J., Ju, J., Greenberg, D. A., Russo, J. J., & Pal, D. K. (2009). Centrotemporal sharp wave EEG trait in rolandic epilepsy maps to Elongator Protein Complex 4 (ELP4). *European journal of human genetics : EJHG*, *17*(9), 1171–1181. https://doi.org/10.1038/ejhg.2008.267

Suzuki, T., Yashiro, Y., Kikuchi, I., Ishigami, Y., Saito, H., Matsuzawa, I., Okada, S., Mito, M., Iwasaki, S., Ma, D., Zhao, X., Asano, K., Lin, H., Kirino, Y., Sakaguchi, Y., & Suzuki, T. (2020). Complete chemical structures of human mitochondrial tRNAs. *Nature Communications*, *11*(1), 4269. https://doi.org/10.1038/s41467-020-18068-6

Suzuki, T. (2021). The expanding world of tRNA modifications and their disease relevance. *Nature Reviews Molecular Cell Biology*, *22*(6), 375–392. https://doi.org/10.1038/s41580-021-00342-0

Tailor, J., Kittappa, R., Leto, K., Gates, M., Borel, M., Paulsen, O., Spitzer, S., Thora Karadottir, R., Rossi, F., Falk, A., & Smith, A. (2013). Stem cells expanded from the human embryonic hindbrain stably retain regional specification and high neurogenic potency. *Journal of Neuroscience*, *33*(30), 12407–12422. https://doi.org/10.1523/JNEUROSCI.0130-13.2013

Takahashi, K., & Yamanaka, S. (2006). Induction of pluripotent stem cells from mouse embryonic and adult fibroblast cultures by defined factors. *Cell*, *126*(4), 663–676. https://doi.org/10.1016/j.cell.2006.07.024

Takemoto, C., Spremulli, L. L., Benkowski, L. A., Ueda, T., Yokogawa, T., & Watanabe, K. (2009). Unconventional decoding of the AUA codon as methionine by mitochondrial tRNAMet with the anticodon f5CAU as revealed with a mitochondrial in vitro translation system. *Nucleic acids research*, *37*(5), 1616–1627. https://doi.org/10.1093/nar/gkp001

Tchieu, J., Zimmer, B., Fattahi, F., Amin, S., Zeltner, N., Chen, S., & Studer, L. (2017). A Modular Platform for Differentiation of Human PSCs into All Major Ectodermal Lineages. *Cell Stem Cell*, *21*(3), 399–410. https://doi.org/10.1016/j.stem.2017.08.015

Thiaville, P. C., Iwata-Reuyl, D., & de Crécy-Lagard, V. (2014). Diversity of the biosynthesis pathway for threonylcarbamoyladenosine (t(6)A), a universal modification of tRNA. *RNA biology*, *11*(12), 1529–1539. https://doi.org/10.4161/15476286.2014.992277

Thompson, D. M., Lu, C., Green, P. J., & Parker, R. (2008). tRNA cleavage is a conserved response to oxidative stress in eukaryotes. *RNA (New York, N.Y.)*, *14*(10), 2095–2103. https://doi.org/10.1261/rna.1232808

Tomita, K., & Liu, Y. (2018). Human BCDIN3D Is a Cytoplasmic tRNA(His)-Specific 5'-Monophosphate Methyltransferase. *Frontiers in genetics*, *9*, 305. https://doi.org/10.3389/fgene.2018.00305

Torres, A. G., Batlle, E., & Ribas de Pouplana, L. (2014). Role of tRNA modifications in human diseases. *Trends in Molecular Medicine*, *20*(6), 306–314. https://doi.org/10.1016/j.molmed.2014.01.008

Torres, A. G., Pineyro, D., Rodriguez-Escriba, M., Camacho, N., Reina, O., Saint-Leger, A., Filonava, L., Batlle, E., & Ribas De Pouplana, L. (2015). Inosine modifications in human tRNAs are incorporated at the precursor tRNA level. *Nucleic Acids Research*, *43*(10), 5145–5157. https://doi.org/10.1093/nar/gkv277

Tuorto, F., Herbst, F., Alerasool, N., Bender, S., Popp, O., Federico, G., Reitter, S., Liebers, R., Stoecklin, G., Grone, H.-J., Dittmar, G., Glimm, H., & Lyko, F. (2015). The tRNA methyltransferase Dnmt2 is required for accurate polypeptide synthesis during haematopoiesis. *The EMBO journal*, *34*(18), 2350–2362. https://doi.org/10.15252/embj.201591382

Tuorto, F., Liebers, R., Musch, T., Schaefer, M., Hofmann, S., Kellner, S., Frye, M., Helm, M., Stoecklin, G., & Lyko, F. (2012). RNA cytosine methylation by Dnmt2 and NSun2 promotes tRNA stability and protein synthesis. *Nature Structural and Molecular Biology*, *19*(9), 900–905. https://doi.org/10.1038/nsmb.2357

Turconi, A. C., Benti, R., Castelli, E., Pochintesta, S., Felisari, G., Comi, G., Gagliardi, C., Del Piccolo, L., & Bresolin, N. (1999). Focal cognitive impairment in mitochondrial encephalomyopathies: a neuropsychological and neuroimaging study. *Journal of the neurological sciences*, *170*(1), 57–63. https://doi.org/10.1016/s0022-510x(99)00199-9

Van Haute, L., Dietmann, S., Kremer, L., Hussain, S., Pearce, S. F., Powell, C. A., Rorbach, J., Lantaff, R., Blanco, S., Sauer, S., Kotzaeridou, U., Hoffmann, G. F., Memari, Y., Kolb-Kokocinski, A., Durbin, R., Mayr, J. A., Frye, M., Prokisch, H., & Minczuk, M. (2016). Deficient methylation and formylation of mt-tRNAMet wobble cytosine in a patient carrying mutations in NSUN3. *Nature Communications*, *7*, 12039. http://dx.doi.org/10.1038/ncomms12039%2010.1038/ncomms12039%20http://www.nature.com/articles/ncomms12039#supplementary-information

Vangaveti, S., Ranganathan, S. V., & Agris, P. F. (2022). Physical Chemistry of a Single tRNA-Modified Nucleoside Regulates Decoding of the Synonymous Lysine Wobble Codon and Affects Type 2 Diabetes. *The journal of physical chemistry. B*, *126*(6), 1168–1177. https://doi.org/10.1021/acs.jpcb.1c09053

Vilardo, E., Amman, F., Toth, U., Kotter, A., Helm, M., & Rossmanith, W. (2020). Functional characterization of the human tRNA methyltransferases TRMT10A

and TRMT10B. *Nucleic acids research*, *48*(11), 6157–6169. https://doi.org/10.1093/nar/gkaa353

Wang, L., & Lin, S. (2023). Emerging functions of tRNA modifications in mRNA translation and diseases. *Journal of Genetics and Genomics*, *50*(4), 223–232. https://doi.org/10.1016/j.jgg.2022.10.002

Wang, Z., Zang, C., Rosenfeld, J. A., Schones, D. E., Barski, A., Cuddapah, S., Cui, K., Roh, T.-Y., Peng, W., Zhang, M. Q., & Zhao, K. (2008). Combinatorial patterns of histone acetylations and methylations in the human genome. *Nature genetics*, *40*(7), 897–903. https://doi.org/10.1038/ng.154

Waterham, H. R., Koster, J., van Roermund, C. W. T., Mooyer, P. A. W., Wanders, R. J. A., & Leonard, J. V. (2007). A lethal defect of mitochondrial and peroxisomal fission. *The New England journal of medicine*, *356*(17), 1736–1741. https://doi.org/10.1056/NEJMoa064436

Watson, J. D., & Crick, F. H. C. (1953). Molecular Structure of Nucleic Acids: A Structure for Deoxyribose Nucleic Acid. *Nature*, *171*(4356), 737–738. https://doi.org/10.1038/171737a0

Wek, S. A., Zhu, S., & Wek, R. C. (1995). The histidyl-tRNA synthetase-related sequence in the eIF-2 alpha protein kinase GCN2 interacts with tRNA and is required for activation in response to starvation for different amino acids. *Molecular and cellular biology*, *15*(8), 4497–4506.

White, B. N., Tener, G. M., Holden, J., & Suzuki, D. T. (1973). Analysis of tRNAs during the development of Drosophila. *Developmental Biology*, *33*(1), 185–195. https://doi.org/https://doi.org/10.1016/0012-1606(73)90173-5

Wu, P.-R., Chiang, S.-Y., Midence, R., Kao, W.-C., Lai, C.-L., Cheng, I.-C., Chou, S.-J., Chen, C.-C., Huang, C.-Y., & Chen, R.-H. (2023). Wdr4 promotes cerebellar development and locomotion through Arhgap17-mediated Rac1 activation. *Cell Death & Disease*, *14*(1), 52. https://doi.org/10.1038/s41419-022-05442-z

Xu, Y., & Chou, K.-C. (2016). Recent Progress in Predicting Posttranslational Modification Sites in Proteins. *Current topics in medicinal chemistry*, *16*(6), 591–603. https://doi.org/10.2174/1568026615666150819110421

Yang, W.-Q., Xiong, Q.-P., Ge, J.-Y., Li, H., Zhu, W.-Y., Nie, Y., Lin, X., Lv, D., Li, J., Lin, H., & Liu, R.-J. (2021). THUMPD3-TRMT112 is a m2G methyltransferase working on a broad range of tRNA substrates. *Nucleic acids research*, *49*(20), 11900–11919. https://doi.org/10.1093/nar/gkab927

Yao, C.-H., Wang, R., Wang, Y., Kung, C.-P., Weber, J. D., & Patti, G. J. (2019). Mitochondrial fusion supports increased oxidative phosphorylation during cell proliferation. *eLife*, *8*. https://doi.org/10.7554/eLife.41351

Yew, T. W., McCreight, L., Colclough, K., Ellard, S., & Pearson, E. R. (2016, September). tRNA methyltransferase homologue gene TRMT10A mutation in young adult-onset diabetes with intellectual disability, microcephaly and epilepsy. https://doi.org/10.1111/dme.13024

Yoluç, Y., van de Logt, E., & Kellner-Kaiser, S. (2021). The Stress-Dependent Dynamics of Saccharomyces cerevisiae tRNA and rRNA Modification Profiles. *Genes*, *12*(9). https://doi.org/10.3390/genes12091344

Youle, R. J., & van der Bliek, A. M. (2012). Mitochondrial fission, fusion, and stress. *Science (New York, N.Y.)*, *337*(6098), 1062–1065. https://doi.org/10.1126/science.1219855

Zhang, H., Ryu, D., Wu, Y., Gariani, K., Wang, X., Luan, P., D'Amico, D., Ropelle, E. R., Lutolf, M. P., Aebersold, R., Schoonjans, K., Menzies, K. J., & Auwerx, J. (2016).

NAD repletion improves mitochondrial and stem cell function and enhances life span in mice. *Science (New York, N.Y.)*, *352*(6292), 1436–1443. https://doi.org/10.1126/science.aaf2693

Zhang, J., Khvorostov, I., Hong, J. S., Oktay, Y., Vergnes, L., Nuebel, E., Wahjudi, P. N., Setoguchi, K., Wang, G., Do, A., Jung, H.-J., McCaffery, J. M., Kurland, I. J., Reue, K., Lee, W.-N. P., Koehler, C. M., & Teitell, M. A. (2011). UCP2 regulates energy metabolism and differentiation potential of human pluripotent stem cells. *The EMBO journal*, *30*(24), 4860–4873. https://doi.org/10.1038/emboj.2011.401

Zorova, L. D., Popkov, V. A., Plotnikov, E. Y., Silachev, D. N., Pevzner, I. B., Jankauskas, S. S., Babenko, V. A., Zorov, S. D., Balakireva, A. V., Juhaszova, M., Sollott, S. J., & Zorov, D. B. (2018). Mitochondrial membrane potential. *Analytical biochemistry*, *552*, 50–59. https://doi.org/10.1016/j.ab.2017.07.009